3.0 Laboratory Analyses

3.1 Overview

Figure 3.1-1 shows the sample analysis process flow for filter samples. Table 3.1-1 specifies the number of source samples submitted to chemical analysis. The analytical detection limits for all reported chemical species are provided in Table 3.1-2.

The procedures for substrate handling and chemical analysis are briefly described here. The reader is referred to the Quality Assurance Plan for this project (Appendix F) for additional details.

3.2 Acceptance Testing and Chain-of-Custody

The sampling media consist of: (1) Gelman (Ann Arbor, MI) polymethyl pentane ringed, 2.0μ pore size, 47-mm-diameter PTFE Teflon membrane filters (#R2PJ047); and (2) Pallflex (Puttman, CT) 47-mm-diameter quartz fiber filters (#2500 QAOT-UP). The manufacturers and identification numbers are important specifications since only these have been found to acceptably meet the requirements for blank levels and artifact formation on quartz filters. Both filter media specified here have been acceptance tested. All filters and 47-mm disks used are compatible with the Nucleopore filter holders used in the PISD, DSS, and modified Method 5G-type samplers. Nucleopore drain disks are used as flow homogenizers under the Teflon filters.

Filters are procured from the vendors cited above and are assigned DRI batch numbers in sets of 100. At least one filter from each batch is analyzed for all species which will ultimately be quantified on it to verify that pre-established specifications have been met. Lots are rejected if they do not pass this test. Each filter is individually examined prior to labeling for discoloration, pinholes, creases, or other defects. Testing of sample media continues throughout the course of the project. In addition to 5% laboratory blanks, field blank samples are distributed and analyzed at a rate of 10% of the total number of samples.

These filter substrates require treatment and representative chemical analyses before they can be used. Discoveries of excessive blank levels and filter interferences in several previous monitoring programs which have not included these measures have severely compromised the results of those studies. Substrate pre-treatments are:

- Pre-firing of Quartz Fiber Filters. Quartz fiber filters absorb organic vapors with time. Blank quartz fiber filters are heated for at least three hours at 900°C. A sample of each batch of 100 pre-fired filters is tested for carbon blank levels prior to sampling, and sets of filters with carbon levels

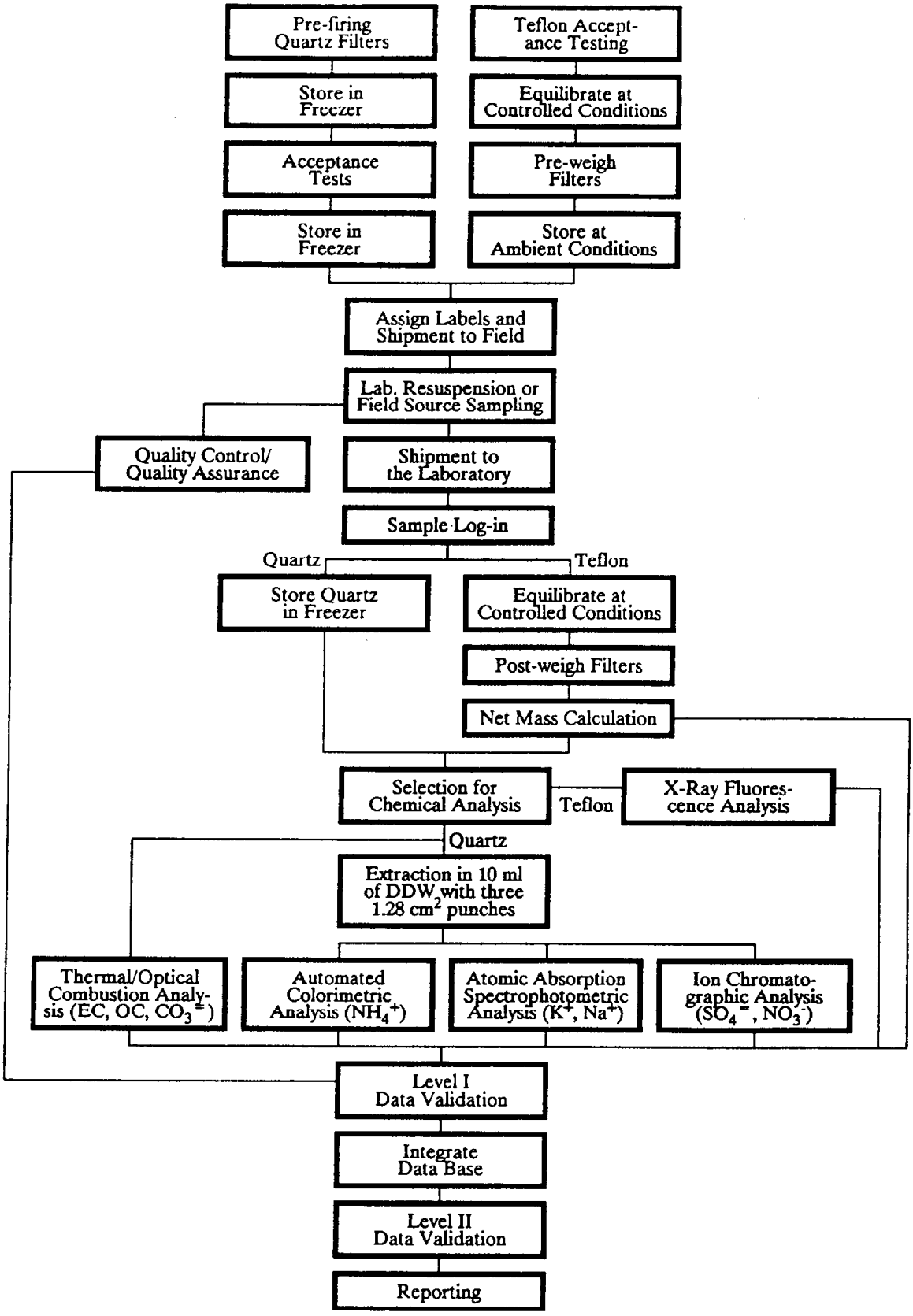

Figure 3.1-1. Flow diagram for source sampling and analysis activities.

Table 3.1-1
Number of Chemical Analyses for Source Samples[a]

Measurement	Geological Material[b]	Construc-tion Dust	Dairy Dust	Residential Wood Combustion	Diesel Truck Emissions	Diesel Bus Emissions	Crude Oil Boiler Emissions	Agricultural Burning Emissions	Labor-atory Blanks	Total Number of Samples
Resuspension Sampling on Teflon and Quartz Filters	78	0	0	0	0	0	0	0	0	78
Gravimetric Analysis (mass) on Teflon Filters	312	12	12	84	32	12	36	56	37	593
XRF[c] Analysis (Elements) on Teflon Filters	312	12	12	84	32	12	36	56	37	593
IC[d] Analysis ($SO_4^=$, NO_3^-) on Quartz Extracts	312	12	12	84	32	12	36	56	37	593
Atomic Absorption Analysis (K^+, Na^+) on Quartz Extracts	312	12	12	84	32	12	36	56	37	593
Automated Colorimetry Analysis (NH_4^+) on Quartz Extracts	312	12	12	84	32	12	36	56	37	593
Thermal/Optical Reflectance Carbon Analysis (OC, EC, CO_3, TC) on Quartz Filters	312	12	12	84	32	12	36	56	37	593

a. Includes field blanks.
b. Resuspension sampling of geological material for PM_1, $PM_{2.5}$, PM_{10}, and PM_{30} on both Teflon and Quartz.
c. XRF: X-ray Fluorescence analysis.
d. IC: Ion Chromatograph analysis.

Table 3.1-2
Analytical Detection Limits

Species	Analysis Method	Minimum Detectable Limit ($\mu g/m^3$)[a,c]	Lower Quantifiable Limit ($\mu g/m^3$)[b,c]
Mass	Gravimetric	1.00	1.07
Cl^-	Anion Chromatography	0.01	0.03
NO_3^-	Anion Chromatography	0.01	0.42
$SO_4^=$	Anion Chromatography	0.01	0.04
NH_4^+	Automated Colorimetry	0.01	0.05
EC	Thermal/Optical Reflectance	0.04	0.08
OC	Thermal/Optical Reflectance	0.04	0.08
CC	Thermal/Optical Reflectance	0.09	0.10
Na^+	Atomic Absorption Spectrophotometry	0.01	0.02
K^+	Atomic Absorption Spectrophotometry	0.01	0.02
Al	Energy Dispersive X-Ray Fluorescence	0.0031	0.053
Si	Energy Dispersive X-Ray Fluorescence	0.0018	0.083
P	Energy Dispersive X-Ray Fluorescence	0.0009	0.0011
S	Energy Dispersive X-Ray Fluorescence	0.0007	0.012
Cl	Energy Dispersive X-Ray Fluorescence	0.0020	0.0046
K	Energy Dispersive X-Ray Fluorescence	0.0009	0.0080
Ca	Energy Dispersive X-Ray Fluorescence	0.0009	0.016
Ti	Energy Dispersive X-Ray Fluorescence	0.0006	0.0023
V	Energy Dispersive X-Ray Fluorescence	0.0004	0.00047
Cr	Energy Dispersive X-Ray Fluorescence	0.0004	0.00065
Mn	Energy Dispersive X-Ray Fluorescence	0.0004	0.00080
Fe	Energy Dispersive X-Ray Fluorescence	0.0002	0.017
Co	Energy Dispersive X-Ray Fluorescence	0.0002	0.00019
Ni	Energy Dispersive X-Ray Fluorescence	0.0002	0.0026
Cu	Energy Dispersive X-Ray Fluorescence	0.0002	0.016
Zn	Energy Dispersive X-Ray Fluorescence	0.0004	0.010
Ga	Energy Dispersive X-Ray Fluorescence	0.0006	0.0010
As	Energy Dispersive X-Ray Fluorescence	0.0004	0.00071
Se	Energy Dispersive X-Ray Fluorescence	0.0004	0.00042
Br	Energy Dispersive X-Ray Fluorescence	0.0002	0.00024
Rb	Energy Dispersive X-Ray Fluorescence	0.0002	0.00020
Sr	Energy Dispersive X-Ray Fluorescence	0.0004	0.00029
Y	Energy Dispersive X-Ray Fluorescence	0.0004	0.00037
Zr	Energy Dispersive X-Ray Fluorescence	0.0006	0.00038
Mo	Energy Dispersive X-Ray Fluorescence	0.0009	0.0016
Pd	Energy Dispersive X-Ray Fluorescence	0.0020	0.0017
Ag	Energy Dispersive X-Ray Fluorescence	0.0022	0.0028
Cd	Energy Dispersive X-Ray Fluorescence	0.0022	0.0024
In	Energy Dispersive X-Ray Fluorescence	0.0028	0.0031
Sn	Energy Dispersive X-Ray Fluorescence	0.0037	0.0036
Sb	Energy Dispersive X-Ray Fluorescence	0.0044	0.0064
Ba	Energy Dispersive X-Ray Fluorescence	0.0153	0.011
La	Energy Dispersive X-Ray Fluorescence	0.0175	0.013
Hg	Energy Dispersive X-Ray Fluorescence	0.0011	0.0012
Pb	Energy Dispersive X-Ray Fluorescence	0.0009	0.0015

a. Minimum Detectable Limit (MDL) is the concentration at which instrument response equals three times the standard deviation of the response to a known concentration of zero.
b. Lower Quantifiable Limit (LQL) equals three times the standard deviation of dynamic field blanks as determined from the sampling program.
c. Calculation is based on 9.3 cm^2 of exposed filter area with a nominal 50.4 m^3 sample volume.

exceeding $2\mu g/cm^2$ are re-fired or rejected. The quartz filters are also acceptance tested for Cl^-, NO_3^-, and SO_4^{2-} by ion chromatography, for NH_4^+ by colorimetry, and for Na and K by atomic absorption spectrometry. Filter lots with levels greater than $1\mu g$ per filter for any of these species are rejected. All pre-fired filters are stored in a freezer prior to preparation for field sampling.

- Equilibrating Teflon Membrane Filters. On several occasions over the past ten years, batches of Gelman ringed Teflon filters have yielded variable (by up to $100\mu g$/filter over a few days) blank masses. As the time from manufacture increases, this variability decreases. Since Gelman has minimized its long-term inventory of these filters, and is manufacturing them on an as-ordered basis, this variability is being observed with greater frequency. A one-month equilibration in the weighing environment is currently being applied to these filters at DRI, and this appears to have reduced the variability to acceptable levels (within $\pm 15\mu g$/filter for re-weights of 47-mm-diameter filters). Experiments with equilibration in a vacuum oven are being conducted at DRI in an attempt to reduce this time. Sets of Teflon membrane filters which exceed $1\mu g$/filter for nitrate, $0.5\mu g$/filter for sulfate, and twice XRF detection limits for elements are rejected.

The results of all filter treatments, chemical analyses, and visual inspections are recorded in a data base with the lot numbers. A set of filter IDs is assigned to each lot so that a record of acceptance testing can be associated with each sample.

After the acceptance testing, Teflon membrane filters are labeled and weighed in a temperature- and humidity-controlled environment. Pre-fired quartz fiber filters are stored under low temperature before being labeled and shipped to the field. The pre-weighed Teflon and pre-fired quartz filters are stored in separate Petri slides prior to loading into filter holders.

Nucleopore filter holders are washed in a dishwasher, then rinsed in distilled water. Filters are loaded into the holders by gloved hands in a clean environment. Gummed ID labels are attached to each filter holder and the IDs are recorded on a data sheet.

Each filter holder is covered and inserted into a transport container. One out of ten filter sets serves as a laboratory control or dynamic blank.

After field sampling, the samples are taken to a clean area and unloaded into Petri slides. These filters are kept under refrigeration and shipped to DRI in ice chests with the sampling data sheets. Upon receipt at DRI, samples are logged in and placed in a refrigerator prior to chemical analysis. A log book is maintained in which the condition of each sample is recorded along with the following information: (1) date and time of

sample arrival; (2) site location, sample type, and corresponding sample number; and (3) physical appearance of the filter samples.

Teflon filters are equilibrated in a temperature- and relative-humidity-controlled environment for 24 hours. They are then weighed prior to selection for x-ray fluorescence analysis. Other filters are stored at low temperature prior to analysis.

3.3 Dust Resuspension

When bulk dust samples are submitted to the laboratory for analyses, they must undergo a series of preparatory steps. These include drying, sieving, and resuspension. The detailed procedures followed are provided in Appendix D.

The resuspension chamber used by DRI to suspend sieved soils consists of two PISD samplers configured for $<30\mu$ (TSP), $<10\mu$, $<2.5\mu$, and $<1.0\mu$ size cuts. Four quartz and four Teflon filters are exposed simultaneously. A special table supports the eight inlet tubes and vacuum gauges, replacing the round tripod-supported platforms used in the field. A large, specially-designed cardboard chamber encloses the inlet tubes and ensures a uniform distribution of the resuspended sample. In operation, filters are loaded at the bottom of the sample inlet tubes, the chamber is placed over the inlets, a glass fiber filter which filters make-up air for the chamber is replaced, the two PISD pumps are turned on, and a small amount of sample is blown into the chamber from a glass flask using a small bellows pump. After four minutes the PISD pumps are turned off and the filters are checked on an analytical balance for a sufficient amount of deposit. Based on XRF considerations, optimum loading is between 1 and 3 mg. Filters which are sufficiently loaded are sent to the weighing room for equilibration and final weighing. Filters with insufficient deposits are returned to the chamber and additional sample is resuspended.

Because of the predominance of the coarse fraction in crustal materials, the $<30\mu$ (TSP) and $<10\mu$ filters load much more quickly than the $<2.5\mu$ and $<1.0\mu$ filters. When the $<30\mu$ and $<10\mu$ filters are optimally loaded, they are replaced with Teflon-coated glass fiber filters and the resuspension process continues until the fine fraction filters are sufficiently loaded. These replacement filters are not analyzed chemically, but they are weighed to allow the relationship between the four size fractions to be determined.

Data sheets are completed for each resuspended sample which include sample times, filter IDs, sample type, and vacuum checks. Flows through the critical orifices are checked after every ten samples with a calibrated rotameter. The system is also checked for leaks every ten samples. The chamber, table, and inlets are thoroughly cleaned with methanol between samples, and the impactor plates are re-greased.

Additional information concerning the operation of the PISD samplers may be obtained from the Parallel Impactor Sampling Device (PISD) Standard Operating Procedure (Appendix B).

3.4 Gravimetric Analysis

Unexposed and exposed Teflon membrane filters are equilibrated at 20 ±5°C temperature and 30 ±5% relative humidity for a minimum of 24 hours prior to weighing. Weighing is performed on a Cahn 31 electromicrobalance with ±0.001 mg sensitivity. The charge on each filter is neutralized by a polonium source for thirty seconds prior to being placed on the balance pan.

The balance is calibrated with a 20 mg Class M weight and the tare is set prior to weighing each batch of fifty filters. After every ten filters are weighed, the calibration and tare are re-checked. If the results of these performance tests deviate from specifications by more than 5μg, the balance is re-calibrated. If the difference exceeds 15μg, the previous ten samples are re-weighed. At least ten percent of all weights are checked by an independent technician and samples are re-weighed if these check weights do not agree with the original weights within ±0.010 mg. Pre- and post-weights, check weights, and re-weights (if applied) are recorded on data sheets for later entry into the data base management system.

3.5 X-Ray Fluorescence Analysis

X-ray fluorescence (XRF) analysis is performed on Teflon membrane filters for Al, Si, P, S, Cl, K, Ca, Ti, V, Cr, Mn, Fe, Co, Ni, Cu, Zn, Ga, As, Se, Br, Rb, Sr, Y, Zr, Mo, Pd, Ag, Cd, In, Sn, Sb, Ba, La, Hg, and Pb with an energy-dispersive x-ray fluorescence (EDXRF) analyzer.

In XRF, inner shell electrons are removed from the atoms of the aerosol deposit. An x-ray photon with a wavelength characteristic of each element is emitted when an outer shell electron occupies the vacant inner shell. The number of these photons is proportional to the number of atoms present. The characteristic x-ray peaks for each element are defined by 200 eV wide windows in an energy spectrum ranging from 1 to 50 KeV.

XRF analyses are performed on a Kevex Corporation Model 700/8000 energy-dispersive x-ray fluorescence (EDXRF) analyzer using a side-window, liquid-cooled, 60-kV, 3.3-milliamp rhodium anode x-ray tube and secondary fluorescers. The system is schematically illustrated in Figure 3.5-1. The x-ray output stability is within 0.25 percent for any eight-hour period within a 24-hour duration. The silicon detector has an active area of 30 mm^2, with system resolution better than 165 eV. The analysis is controlled, spectra are acquired,

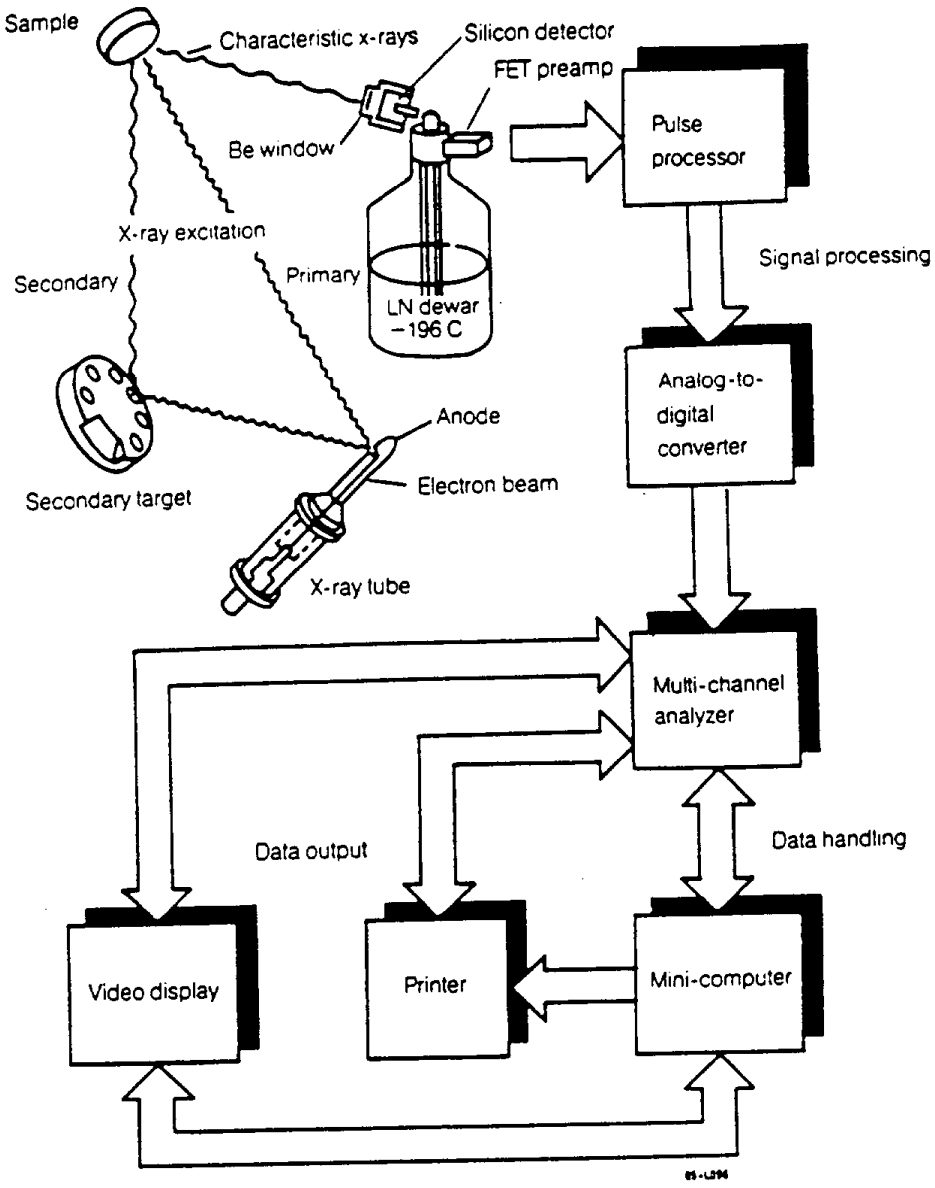

Figure 3.5-1. Major components of Kevex 700/8000 XRF system.

and elemental concentrations are calculated by software implemented on an LSI 11/23 microcomputer which is interfaced to the analyzer.

Five separate XRF analyses are conducted on each sample to optimize detection limits for the specified elements. These conditions are summarized in Table 3.5-1 with the elements which are measured with greatest sensitivity by each condition. Figure 3.5-2 shows an example spectrum from one of these excitation conditions.

Three types of XRF standards are used for calibration, performance testing, and auditing: (1) vacuum-deposited thin-film elements and compounds (micromatter); (2) polymer films (Dzubay et al., 1981); and (3) NBS thin-glass films. The vacuum deposits cover the largest number of elements and are used as calibration standards. The polymer film and NBS standards are used as quality control standards. NBS standards are the definitive standard reference material, but these are only available for the species Al, Ca, Co, Cu, Mn, and Si (SRM 1832), and Fe, Pb, K, Si, Ti, and Zn (SRM 1833).

A separate micromatter thin-film standard is used to calibrate the system for each element. Sensitivity factors (number of x-ray counts per $\mu g/cm^2$ of the element) are determined for each excitation condition. These factors are then adjusted for absorption of the incident and emitted radiation in the thin film. These sensitivity factors are plotted as a function of atomic number and a smooth curve is fitted to the experimental values. The calibration sensitivities are then read from these curves for the atomic numbers of each element in each excitation condition. The polymer film and NBS standards are analyzed on a periodic basis using these sensitivity factors to verify both the standards and the stability of the instrument response. When deviations from specified values are greater than ±5%, the system is re-calibrated.

The sensitivity factors are multiplied by the net peak intensities yielded by ambient samples to obtain the $\mu g/cm^2$ deposit for each element. The net peak intensity is obtained by: (1) subtracting background radiation; (2) subtracting spectral interferences; and (3) adjusting for x-ray absorption.

The elemental x-ray peaks reside on a background of radiation scattered from the sampling substrate. A model background is formed by averaging spectra obtained from ten filters of the same type used in ambient sampling. This model background has the same shape and features of the sample spectra (minus the elemental peaks) if the deposit mass is small relative to the substrate mass (Russ, 1977). This model background is normalized to an excitation radiation scatter peak in each sample spectrum to account for the difference in scatter intensity due to different masses. Experience has shown that use of a scatter peak for blank normalization from too low an energy region (e.g., the Ti secondary target scatter peak from Condition 2) can lead to unreliable background estimation. Therefore, the Mo scatter peak is used for Conditions 1 and 2, and the Ge scatter peak is used for Conditions 3, 4, and 5.

Table 3.5-1
Excitation Conditions of Kevex/DRI X-Ray Fluorescence Analyzer

Parameter	Condition Number				
	1	2	3	4	5
Tube Voltage	60 kV	30 kV	30 kV	30 kV	8 kV
Tube Current	1.5 mA	3.3 mA	3.3 mA	3.3 mA	1.0 mA
Excitation Filter Thickness	Mo 0.2 mm	Mo 0.2 mm	None None	None None	Whatman 41 3 layers
Secondary Target Filter Thickness	None None None	None None None	Ge Whatman 41 1 layer	Ti Mylar 3.8 μ	None None None
Analysis Time	100 sec	400 sec	400 sec	100 sec	100 sec
Energy Range	0-40 keV	0-20 keV	0-10 keV	0-10 keV	0-10 keV
Elements	Ag, Cd, Sn, Sb, Ba, Cs	Fe, Co, Ni, Cu, Zn, Ga, As, Se, Br, Rb, Sn, Y, Zr, Hg, Sr, Ge, Pb	K, Ca, Ti, V, Cr, Mn, Fe, Co, Ni, Cu, Zn	Al, Si, P, S, Cl, K, Ca	Al, Si, P, S

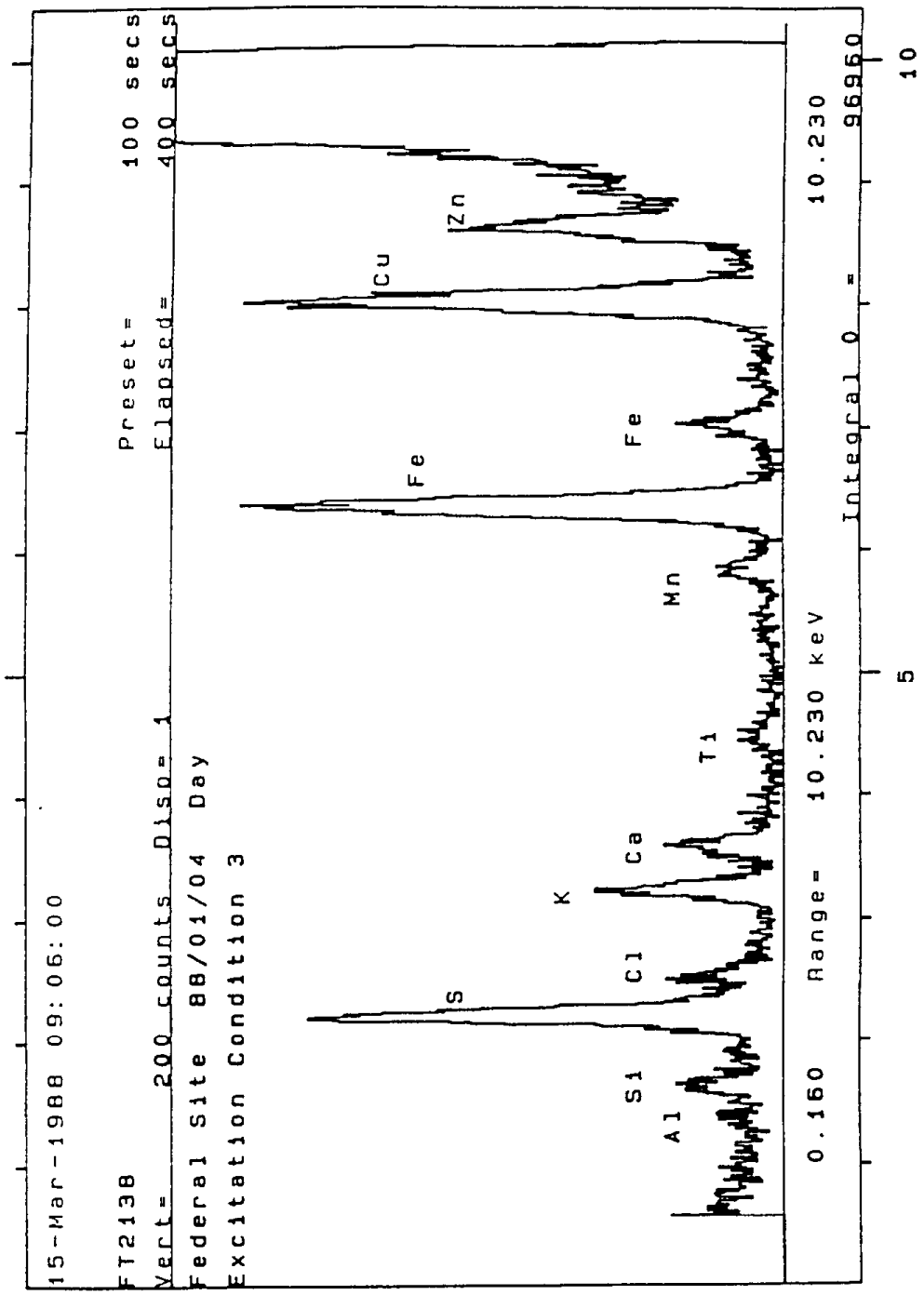

Figure 3.5-2. Typical XRF Spectrum

The number and spacing of the characteristic x-ray lines relative to detector resolution are such that the peaks from one element can interfere with a peak from another element (Dzubay, 1986). A variety of methods have been used to subtract these peak overlaps (Arinc et al., 1977; Parkes et al., 1979; Drane et al., 1983), including least squares fitting to library spectra, fitting to Gaussian and other mathematical functions, and the use of peak overlap coefficients. Peak overlap coefficients are applied to aerosol deposits. The most important of these overlaps are the K_β to K_α overlaps of elements from potassium (K) to zirconium (Zr), the lead (Pb) Lα to arsenic (As) K_α interference, and the lead (Pb) M line to sulfur (S) K line interference. The ratios of overlap peaks to the primary peak are determined from the thin-film standards for each element for the spectral regions of the remaining elements. These ratios are multiplied by the net peak intensity of the primary peak and subtracted from the spectral regions of other elements.

The ability of an x-ray to penetrate matter depends on the energy of the x-ray and the composition and thickness of the material. In general, lower energy x-rays, characteristic of light elements, are absorbed in matter to a much greater degree than higher energy rays. Larger particles collected during aerosol sampling have sufficient size to cause absorption of x-rays within the particles. Attenuation factors for fine particles (particles with aerodynamic diameter less than 2.5μ) are generally negligible (Criss, 1976), even for the lightest elements, but these attenuations can be significant for coarse fraction particles (particles with aerodynamic diameter from 2.5μ to 10μ or 2.5μ to 15μ).

X-ray fluorescence calibration is performed using thin-film standards. Results for particulate matter samples must be corrected for the absorption of x-rays within discrete particles in the deposit. The magnitude of the correction depends on the excitation and fluorescent x-ray energies and their angles, and the size, composition, and density of the particles. Correction factors were calculated using a computer program written by Tom Dzubay (personal communication, 1988), based on the method described by Dzubay and Nelson (1975) for coarse particle corrections. Parameters defining the deposit characteristics, including particle size distribution, the sampler inlet cut-point and efficiency, average deposit composition, and density, were varied over multiple program runs to determine the appropriate particle size correction factors and associated variabilities.

Particle size distribution was estimated by the method of Hinds (1982) using log-probability graphs. For each sample, the data was plotted as percent of total mass versus the particle size cut-point for each of the $<1.0\mu$, $<2.5\mu$, and $<10\mu$ size fractions, with the $<30\mu$ size fraction used as total mass. For a log-normal distribution, a straight line fits the data, with the distribution peak defined as the particle size at the 50 percent mass point. The distribution standard deviation is related to the slope of the line, and is calculated by

Geometric Standard Deviation $= \left[\frac{d_{84}}{d_{16}} \right]^{1/2}$

Where d_{84} = particle diameter at 84% and

d_{16} = particle diameter at 16%.

Each sample was assigned to one of three particle size distribution categories based on particle size distribution peak and geometric standard deviation. Group 0 includes the agricultural field burn, woodstove, diesel motor emission, and oil-fired steam generator sources, which all have particle size distribution peaks of 1.0μ or less. No particle size corrections are necessary for these sources. Group 1 samples include all the resuspended soils, the Fresno construction dust, and the dairy dust samples except for Visalia urban unpaved road dust, Taft unpaved road dust, Owens Valley desert dust, and Mammoth cinder dust samples, which are categorized as Group 2. The particle size distribution peak for Group 1 ranged from 7.6μ to 8.7μ with a weighted average of 7.8μ. The geometric standard deviation ranged from 1.77 to 1.89, with a weighted average of 1.82. For Group 2 samples, the particle size distribution peak ranged from 5.6 to 6.6μ, with a weighted average of 6.3μ. The geometric standard deviation ranged from 2.62 to 2.70 with a weighted average of 2.66.

Tables 3.5-2 and 3.5-3 summarize the particle size distributions for resuspension and non-resuspension source samples, respectively. It should be noted that for most of combustion-dominated sources for which the size distribution data are presented in Table 3.5-3, he majority of the particulate mass is in the less-than-one-micron size range. The calculated percentage of particles in that size range even exceeded 100% for several sources. The uncertainties around the values which exceeded 100%, combined with the data for the other combustion sources, simply illustrate that the percentages of particulate mass made up of particles less than one micron from typical combustion sources are in the 80 and 90 percentile levels. Because the majority of particulate mass is less than one micron, the percentages of particulate mass for some of the size categories (e.g., >1.0 but $<2.5\mu$)) were negative. Mathematically, this is caused by the fact that there is little difference in mass captured by the two sizes of filters (<1.0 and $<2.5\mu$ in this example) used to calculate the size category, and the uncertainties around the measured values can cause the calculated value to be negative. An intuitive explanation of this example is that nearly all the mass of particulate material is in the less-than-one-micron range, and very little of the overall particulate mass is from particles between 1.0μ and 2.5μ.

Particulate density for samples in Groups 1 and 2 was estimated to range from 2.5 to 2.9 g/cm^3 based on values listed in the Handbook for Chemistry and Physics (Chemical Rubber Company, 1978) for common minerals expected to be present in the samples. Average composition was determined from the Group 1 and 2 samples, and the range of compositions was taken from the highest iron and highest calcium samples.

Table 3.5-2
Soil and Road Dust Resuspensions
Size Distributions by Percent Mass of TSP

Sample Mnemonic	Percent of TSP					
	$< 1.0\ \mu$	$> 1.0, < 2.5\ \mu$	$< 2.5\ \mu$	$> 2.5, < 10\ \mu$	$< 10\ \mu$	$> 10, < 30\ \mu$
SOIL01	3.6 ± 0.5	7.2 ± 1.2	10.8 ± 0.7	44.7 ± 4.1	55.5 ± 4.6	44.5 ± 4.6
SOIL03	3.2 ± 0.8	5.9 ± 0.7	9.2 ± 0.2	38.4 ± 3.8	47.5 ± 3.6	52.5 ± 3.6
SOIL04	6.6 ± 1.2	8.9 ± 1.1	15.5 ± 2.3	51.1 ± 3.9	66.6 ± 1.7	33.4 ± 1.7
SOIL05	5.5 ± 0.4	8.4 ± 1.4	13.9 ± 1.8	41.1 ± 3.5	55.1 ± 3.9	44.9 ± 3.9
SOIL06	4.7 ± 1.6	9.3 ± 5.8	14.0 ± 7.3	20.5 ± 8.4	34.5 ± 2.7	65.5 ± 2.7
SOIL07	6.3 ± 1.3	7.2 ± 0.9	13.5 ± 0.6	51.4 ± 0.7	64.9 ± 0.7	35.1 ± 0.7
SOIL08	2.1 ± 0.5	3.4 ± 0.2	5.4 ± 0.6	36.7 ± 2.5	42.2 ± 3.2	57.8 ± 3.2
SOIL09	4.3 ± 0.7	7.0 ± 0.7	11.3 ± 1.4	37.0 ± 4.7	48.3 ± 6.0	51.7 ± 6.0
SOIL10	2.1 ± 0.9	4.6 ± 0.9	6.6 ± 1.5	21.6 ± 3.1	28.2 ± 4.4	71.8 ± 4.4
SOIL11	3.1 ± 0.2	5.8 ± 0.5	8.8 ± 0.7	46.5 ± 0.6	55.3 ± 1.1	44.7 ± 1.1
SOIL12	4.2 ± 2.8	1.4 ± 5.7	5.6 ± 3.0	43.5 ± 1.0	49.1 ± 3.1	50.9 ± 3.1
SOIL13	6.5 ± 0.8	6.5 ± 0.7	13.0 ± 0.7	36.7 ± 6.0	49.7 ± 5.3	50.3 ± 5.3
SOIL14	2.5 ± 1.0	9.3 ± 8.5	11.8 ± 8.8	27.7 ± 14.9	39.5 ± 10.3	60.5 ± 10.3
SOIL15	1.3 ± 0.5	3.5 ± 1.3	4.8 ± 1.2	34.0 ± 4.5	38.8 ± 5.7	61.2 ± 5.7
SOIL16	4.5 ± 1.1	8.7 ± 1.5	13.3 ± 0.9	46.9 ± 2.7	60.2 ± 3.5	39.8 ± 3.5
SOIL17	6.5 ± 1.9	10.5 ± 1.9	17.0 ± 3.8	53.. ± 12.5	70.5 ± 13.1	29.5 ± 13.1
SOIL18	4.1 ± 0.5	6.5 ± 0.6	10.6 ± 1.0	45.5 ± 4.5	56.1 ± 5.5	43.9 ± 5.5
SOIL19	2.7 ± 0.5	7.0 ± 0.8	9.7 ± 1.4	34.1 ± 1.5	43.8 ± 0.9	56.2 ± 0.9
SOIL20	3.7 ± 0.3	5.8 ± 1.0	9.4 ± 1.3	38.7 ± 4.5	48.1 ± 5.3	51.9 ± 5.3
SOIL21	2.3 ± 0.4	2.9 ± 0.4	5.1 ± 0.0	27.5 ± 3.8	32.6 ± 3.8	67.4 ± 3.8
SOIL22	5.9 ± 1.3	7.0 ± 0.3	12.8 ± 1.0	44.6 ± 6.2	57.4 ± 7.2	42.6 ± 7.2
SOIL23	6.9 ± 4.6	6.3 ± 5.0	13.2 ± 5.9	38.1 ± 11.5	51.3 ± 17.4	48.7 ± 17.4
SOIL24	2.8 ± 1.3	5.3 ± 2.5	8.1 ± 2.1	49.7 ± 10.9	57.8 ± 12.8	42.2 ± 12.8
SOIL25	5.6 ± 0.0	7.7 ± 0.2	13.2 ± 0.3	62.7 ± 5.3	76.0 ± 5.1	24.0 ± 5.1
SOIL26	13.9 ± 9.9	0.6 ± 13.8	14.5 ± 3.9	70.9 ± 25.4	85.4 ± 21.5	14.6 ± 21.5
SOIL27	2.4 ± 0.4	4.8 ± 0.5	7.1 ± 0.2	37.2 ± 4.2	44.3 ± 4.4	55.7 ± 4.4

Table 3.5-3
CARB Non-Resuspension Sources
Size Distributions by Percent Mass of TSP

Sample Mnemonic	Percent of TSP					
	$< 1.0\ \mu$	$> 1.0, < 2.5\ \mu$	$< 2.5\ \mu$	$> 2.5, < 10\ \mu$	$< 10\ \mu$	$> 10, < 30\ \mu$
BAAGBC	67.5 ± 22.0	−1.1 ± 4.1	66.4 ± 19.1	12.7 ± 2.5	79.1 ± 20.1	20.9 ± 20.1
BAMAJC	90.9 ± 12.8	−0.1 ± 12.6	90.8 ± 25.3	3.3 ± 21.3	94.1 ± 24.5	5.9 ± 24.5
CHCRUC	88.4 ± 3.9	10.0 ± 2.9	98.4 ± 4.7	0.5 ± 2.5	98.9 ± 5.2	1.1 ± 5.2
ELAGBC	83.7 ± 12.2	2.8 ± 11.5	86.6 ± 7.9	−1.0 ± 4.5	85.6 ± 3.6	14.4 ± 3.6
FRCONC	4.6 ± 3.0	1.3 ± 1.0	5.8 ± 3.9	29.1 ± 0.5	34.9 ± 3.4	65.1 ± 3.4
MADIEC	103.3 ± 17.9	−8.8 ± 11.4	89.8 ± 33.7	−5.5 ± 32.2	81.0 ± 5.3	19.0 ± 5.3
MAFISC	78.8 ± 5.3	9.2 ± 0.5	88.0 ± 4.7	4.6 ± 6.4	93.8 ± 2.7	6.2 ± 2.7
MAMAJC	107.5 ± 16.0	−7.2 ± 23.2	100.4 ± 10.4	−1.0 ± 14.6	99.4 ± 5.2	0.6 ± 5.2
SFCRUC	86.4 ± 4.6	12.3 ± 38.3	96.5 ± 4.5	2.4 ± 4.8	99.6 ± 1.2	0.4 ± 1.2
STAGBC	64.7 ± 9.7	5.9 ± 1.9	70.6 ± 11.5	14.8 ± 5.9	85.4 ± 6.2	14.6 ± 6.2
VIAGBC	114.9 ± 45.2	−12.2 ± 13.1	102.7 ± 32.1	18.4 ± 24.5	121.1 ± 56.6	−21.1 ± 56.6
VIDAIC	5.2 ± 1.9	0.9 ± 0.9	6.1 ± 2.8	42.5 ± 3.7	48.6 ± 2.1	51.4 ± 2.1
WHDIEC	91.8 ± 6.8	0.4 ± 1.7	92.3 ± 5.5	3.9 ± 5.9	96.2 ± 2.6	3.8 ± 2.6

Particle size corrections were calculated for Al, Si, P, S, Cl, K, Ca, Ti, V, Cr, Mn, and Fe in the $<2.5\mu$, $<10\mu$, and $<30\mu$ size fractions of Group 1 and 2 samples using the average values for the parameters particle size distribution peak, particle size distribution width, density, and elemental composition. Correction factor uncertainty was determined by varying the above parameters over their allowable range and calculating maximum and minimum particle size correction factors. Results are shown in Tables 3.5-4 and 3.5-5. Corrected concentration was calculated as raw concentration divided by the appropriate correction factor. A minimum correction factor uncertainty of ten percent was used in all cases.

During XRF analysis, filters are removed from their Petri slides and placed with their deposit sides downward into polycarbonate filter cassettes. A polycarbonate retainer ring keeps the filter flat against the bottom of the cassette. These cassettes are loaded into a carousel in the x-ray chamber which contains sixteen openings. The filter IDs are recorded on a data sheet to correspond to numbered positions in the carousel. The sample chamber is evacuated to 10^{-3} torr and a computer program controls the positioning of the samples and the excitation conditions. Complete analysis of sixteen samples under five excitation conditions requires approximately seven hours. The vacuum in the x-ray chamber and the heat induced by the absorption of x-rays can cause certain materials to volatize. For this reason, labile species such as nitrate and organic carbon are measured on the quartz fiber, rather than the Teflon membrane filter.

A quality control standard and a replicate from a previous batch are analyzed with each set of fourteen samples. If the quality control values differ from specifications by more than ±15% or if the replicate concentrations differ from the original values (assuming they at least exceed ten times detection limits) by more than ±10%, the samples are re-analyzed. If further tests of standards show that the system calibration has changed significantly, the instrument is re-calibrated as described above.

3.6 Filter Extraction

Water-soluble sulfate, nitrate, potassium, and ammonium are obtained by extracting portions of the quartz fiber particle filter in deionized distilled water.

Three punches of 1.28 cm^2 are placed in Falcon (#2045) 16 × 150 mm polystyrene extraction vials which are labeled with the filter ID. The extraction tubes are placed in tube racks, and 10 ml deionized distilled water (DDW) are added.

Table 3.5-4
X-Ray Fluorescence Particle Size Correction Factors
for Group 1 Source Samples

Element	2.5 μ	10 μ	30 μ
Al	0.665 ± 0.036	0.536 ± 0.037	0.461 ± 0.037
Si	0.712 ± 0.033	0.590 ± 0.035	0.515 ± 0.036
P	0.712 ± 0.033	0.590 ± 0.035	0.515 ± 0.035
S	0.759 ± 0.030	0.647 ± 0.032	0.574 ± 0.034
Cl	0.851 ± 0.020	0.769 ± 0.024	0.709 ± 0.027
K	0.899 ± 0.015	0.838 ± 0.018	0.789 ± 0.021
Ca	0.909 ± 0.013	0.854 ± 0.017	0.809 ± 0.020
Ti	0.951 ± 0.008	0.918 ± 0.010	0.889 ± 0.012
V	0.960 ± 0.008	0.933 ± 0.008	0.909 ± 0.010
Cr	0.967 ± 0.005	0.944 ± 0.007	0.923 ± 0.009
Mn	0.972 ± 0.004	0.953 ± 0.006	0.935 ± 0.008
Fe	0.976 ± 0.004	0.959 ± 0.005	0.944 ± 0.006

Table 3.5-5
X-Ray Fluorescence Particle Size Correction Factors
for Group 2 Source Samples

Element	2.5 μ	10 μ	30 μ
Al	0.697 ± 0.025	0.574 ± 0.031	0.506 ± 0.034
Si	0.741 ± 0.022	0.627 ± 0.028	0.591 ± 0.032
P	0.741 ± 0.023	0.627 ± 0.028	0.559 ± 0.032
S	0.785 ± 0.019	0.681 ± 0.026	0.616 ± 0.030
Cl	0.868 ± 0.013	0.794 ± 0.019	0.741 ± 0.024
K	0.911 ± 0.009	0.857 ± 0.013	0.815 ± 0.018
Ca	0.921 ± 0.008	0.871 ± 0.013	0.832 ± 0.017
Ti	0.957 ± 0.005	0.928 ± 0.008	0.904 ± 0.010
V	0.965 ± 0.004	0.941 ± 0.006	0.921 ± 0.009
Cr	0.971 ± 0.003	0.951 ± 0.005	0.933 ± 0.008
Mn	0.976 ± 0.002	0.959 ± 0.004	0.944 ± 0.006
Fe	0.979 ± 0.003	0.965 ± 0.003	0.952 ± 0.005

The extraction vials are capped and sonicated for 30 minutes. The bath water is continually replaced to prevent temperature increases from the dissipation of ultrasonic energy in the water. After extraction, these solutions are stored under refrigeration prior to analysis. The unused filter is placed back to the original Petri slide and archived.

3.7 Ion Chromatographic Analyses

Anion chromatography for sulfate and nitrate is performed with a Dionex 4000i (Sunnyvale, CA) ion chromatograph. In IC, an ion-exchange column separates the sample ions in time for individual quantification by a conductivity detector. Prior to detection, the column effluent enters a suppressor column where the chemical composition of one element is altered, resulting in a matrix of low conductivity. The ions are identified by their elution/retention times and are quantitated by the conductivity peak area.

Approximately two milliliters (ml) of each extract are manually injected into the eluent which flows at 1.5 ml/min. The anion analysis system contains an anion separator column (AS4-A column Cat No 38019) with a strong basic anion exchange resin, and an anion micro membrane suppressor column (250 × 6 mm ID) with a strong acid ion exchange resin. The anion eluent consists of 17% 0.01 M $NaHCO_3$, 18% 0.01 M Na_2CO_3, and 65% DDW. This DDW is verified to have a resistance in excess of 18 Mohm prior to preparation of the eluent.

Standard solutions of $NaNO_3$ and K_2SO_4 are prepared monthly with reagent grade salts which are dehydrated in a desiccator several hours prior to weighing. These anhydrous salts are weighed to the nearest 0.010 mg on a regularly-calibrated analytical balance under controlled temperature (~20°C) and relative humidity (less than 40%) conditions. The salts are diluted in 1000 ml of distilled deionized water to provide a working standard. Calibration standards are created daily by diluting portions of this working standard to 0.2, 1, 5, 10, and 20μg/ml levels. These transfer standards are also traceable to NBS weights and volumes via the mass and volume measurements from which the standardized values were derived.

Solutions are analyzed in batches. The first two samples are distilled water blanks which are used to establish a baseline. The next six samples are the five calibration standards and a distilled water blank. These are followed by sets of ten ambient filter extracts, a replicate of a previous batch of analyses, and one of the calibration standards. Calibration is performed before the sample run. The ions are identified by matching the retention times of each peak in the unknown sample with each peak in the chromatogram of the standard. Peak identification, calibration, and data acquisition is performed on an IBM/AT microcomputer with Dionex

Autoion 400 Data Software. A continuous printout includes the concentrations of sulfate and nitrate, operating parameters, and the sample spectrum for each sample.

After analysis, the printout for each sample in the batch is reviewed for: (1) proper operational settings; (2) correct peak shapes and integration windows; (3) peak overlaps; (4) correct background substraction; and (5) quality control sample comparisons. When values for replicates differ by more than ±10% or values for standards differ by more than ±5%, all samples before and after these quality control checks are designated for re-analysis in a subsequent batch. Individual samples with unusual peak shapes, background subtraction, or operating parameters are also designated for re-analysis.

3.8 Atomic Absorption Spectrophotometric Analyses

A Perkin Elmer Model 2380 Double Beam Atomic Absorption Spectrometer is used to analyze quartz filter extracts for soluble potassium and sodium. A dual hollow cathode lamp emits wavelengths appropriate for potassium and sodium analyses. For potassium the monochrometer is set at 766.5 nm with a 2.0 nm bandpass; for sodium the monochrometer is set at 589.0 with a 0.7 nm bandpass.

Approximately one to two milliliters of the extract are aspirated into an air/acetylene flame at approximately 0.5 ml/min. The output of the photomultiplier is recorded on an IBM/XT at a rate of two readings per second. These are averaged over a 30-second interval and compared with standards using a Lotus 1-2-3 worksheet.

For routine analysis, fifty sample vials containing 5 ml of solution are loaded into the autosampler. The first six vials contain standards and a distilled deionized water blank. Four sets of eleven vials follow which contain nine ambient extracts, one standard, and one replicate from a previous batch. Samples are re-analyzed when quality control standards differ from specifications by more than ±5% or when replicates (at levels exceeding ten times detection limits) differ by more than ±10%.

Fisher certified atomic absorption standard solutions are used as stock standard solutions for sodium (#SO-S-139, Sodium Chloride Solution) and potassium (#SO-P-351, Potassium Chloride Solution). Dilutions of these 1000 ppm solutions yield 0.025, 0.050, 0.100, 0.250, 0.500, 1.000, and 1.500μg/ml calibration standards. Ionization interference is eliminated by addition of cesium chloride (CsCl) to the samples and standard solutions.

3.9 Automated Colorimetric Analysis

The Technicon (Tarrytown, NY) TRAACS 800 Automated Colorimetric System is used to measure ammonium concentrations by the indophenol method. Ammonium in the extract is reacted with alkaline phenol and sodium hypochlorite to produce indophenol, a blue dye. The reaction is catalyzed by the addition of sodium nitroprusside. The absorbance of the solution is measured at 630 nm.

Approximately two milliliters of extract are placed in an autosampler which is controlled by a computer. Seven standard concentrations (0.05, 0.1, 0.3, 0.5, 1.0, 2.0, and 3.0μg/ml) are prepared of ACS reagent-grade $(NH_4)_2SO_4$, following the same procedure as that for IC standards. Each set of samples consists of two distilled water blanks to establish a baseline, seven calibration standards and a blank, then sets of ten samples followed by analysis of one of the standards and a replicate from a previous batch. The computer control allows additional analysis of any filter extract to be repeated without the necessity of loading the extract into more than one vial. Analyzer performance is checked using two dilutions of NBS traceable ion chromatography ammonium standard solution (Fisher #SC349-100, 1000μg/ml ammonium) and NBS rainwater standard (#2694-II, 1.0μg/ml).

The system determines carry-over by analysis of a high standard followed by two blanks. The percent carry-over is then automatically calculated and can be applied to the samples analyzed during the run. Technicon software operating on an IBM/XT microcomputer controls the sample throughput, calculates concentrations, and records data.

Formaldehyde has been found to interfere when present in an amount which exceeds 20% of the ammonium content and hydrogen sulfide interferes in concentrations which exceed 1 mg/ml. Nitrate and sulfate are also potential interferents when present at levels which exceed 100 times the ammonium concentration. These levels are rarely exceeded in source samples. The precipitation of hydroxides of heavy metals such as calcium and magnesium is prevented by the addition of disodium ethylenediamine-tetracetate (EDTA) to the sample stream (Chow, 1981).

3.10 Thermal/Optical Reflectance Carbon Analysis

Much confusion has developed in recent years since a large variety of carbon analysis approaches have been applied which differ with respect to temperatures, oxidizing atmospheres, calibration, sample acidification, and classification into organic and elemental carbon categories. The thermal/optical reflectance method applied here has the advantage that the carbon evolving under different temperature and oxidation conditions is determined separately and summed to obtain the light-absorbing and non-light-absorbing fractions. These

fractions are useful for comparison with other methods which are specific to a single definition for elemental and organic carbon.

The thermal/optical reflectance carbon analyzer consists of a thermal system and an optical system which are diagrammed in Figure 3.10-1. The thermal system consists of a quartz tube placed inside a coiled heater. The current through the heater is controlled to attain and maintain pre-set temperatures for given time periods. A portion of a quartz filter is placed in the heating zone and heated to different temperatures under non-oxidizing and oxidizing atmospheres. The optical system consists of an He-Ne laser, a fiber optic transmitter and receiver, and a photocell. The filter deposit faces a quartz light tube so that the intensity of the reflected laser beam can be monitored throughout the analysis.

As the temperature increases to 550°C, organic compounds are volatilized from the filter in a non-oxidizing (He) atmosphere while elemental carbon is not oxidized. When oxygen is added to the helium at temperatures greater than 550°C, the elemental carbon burns and enters the sample stream. The evolved gases pass through an oxidizing bed of heated manganese dioxide where they reduce the carbon dioxide, then across a heated nickel catalyst which reduces the carbon dioxide to methane. The methane is then quantified with a flame ionization detector (FID).

The principal function of the laser reflectance system is to continuously monitor the filter reflectance throughout an analysis cycle. The negative change in reflectance is proportional to the degree of pyrolytic conversion from organic to elemental carbon which takes place during organic carbon analysis. After oxygen is introduced, the reflectance increases rapidly as the light-absorbing carbon is burned off the filter. The carbon measured after the reflectance attains the value which it had at the beginning of the analysis cycle is classified as elemental carbon. This adjustment for pyrolysis in the analysis is significant, as high as 25% of organic or elemental carbon, and it cannot be ignored. Johnson et al. (1981) reported that an average of 22% of the organic carbon in the samples he analyzed was pyrolytically converted to elemental carbon as evidenced by reflectance corrections. The precision of the pyrolytic conversion has been found to be ±10% in both organic and elemental carbon (Johnson et al., 1981).

Carbonate carbon is determined by treating the sample with 0.4 M hydrochloric acid solution. The acid causes carbonate compounds to evolve as carbon dioxide, which is detected by the FID after reduction to methane. Any carbonate compound must be removed before the thermal analysis step to avoid interference with high-temperature elemental carbon. In addition, measurement of carbonate carbon provides an additional chemical species to further characterize a given sample.

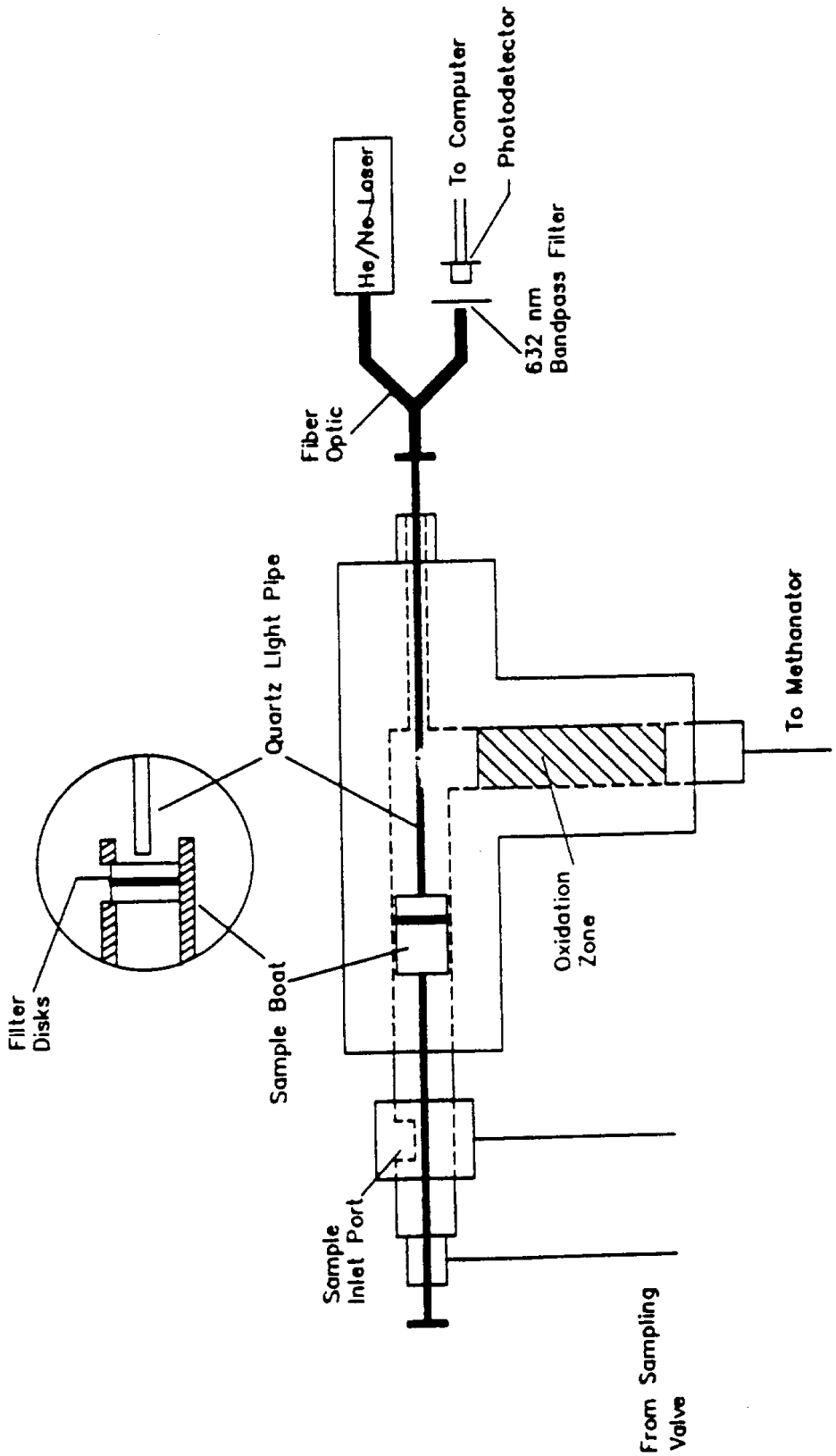

Figure 3.10-1. Carbon analyzer combustion oven.

A typical thermal/optical reflectance output from analysis of an ARB sample is shown in Figure 3.10-2. This figure identifies the different temperatures and oxidizing conditions which are achieved during the analysis. The fractions of carbonaceous material which evolve at the different temperatures are shown, as is the fraction which represents the organic carbon pyrolized during the analysis. The rapid increase in reflectance after oxygen is added demonstrates that this method classifies most of the light-absorbing material as elemental carbon.

For routine analysis, a 0.5 cm^2 circular punch is removed from a quartz fiber filter. This punch is placed vertically into a quartz boat which is positioned under an acid injection port. After the analyzer is thoroughly flushed with helium, 15μl of the 0.4 M hydrochloride acid solution is placed on the punch and the FID output is integrated and recorded by the microcomputer. After the punch has dried, the boat is pushed into the oven area with a thermocouple pushrod. The temperature ramps from ambient temperature to 250°C, to 450°C, and to 550°C; the FID output is recorded every two seconds on a microcomputer data acquisition system. A 2% oxygen (O_2) in helium (He) atmosphere is introduced at 550°C, followed by temperature increases to 700°C, then 800°C. The microcomputer controls the time intervals; monitors the temperatures, FID output, and reflectance; and integrates the FID response over the pre-specified temperature, oxidation, and reflectance intervals. The fractions in the intervals corresponding to reflectances less than or equal to the initial value are summed to yield organic carbon, and fractions in the intervals with reflectances greater than the initial value in the oxidizing atmosphere are summed to yield elemental carbon.

The system is calibrated by analyzing samples of unknown amounts of methane, carbon dioxide, and potassium hydrogen phthalate (KHP). The FID response is ratioed to a reference level of methane injected at the end of each sample analysis. Performance tests of instrument calibration are conducted at the beginning and end of daily operation, as well as at the end of each sample run. All intervening samples are re-analyzed if calibration changes of more than ±10 percent are found.

Known amounts of American Chemical Society (ACS) certified reagent grade crystal sucrose and potassium hydrogen phthalate (KHP) are combusted as a verification of the organic carbon fractions. A total of 15 different standards are used for each calibration. Widely accepted primary standards for elemental and/or organic carbon are still lacking. Establishment of such standards is in progress.

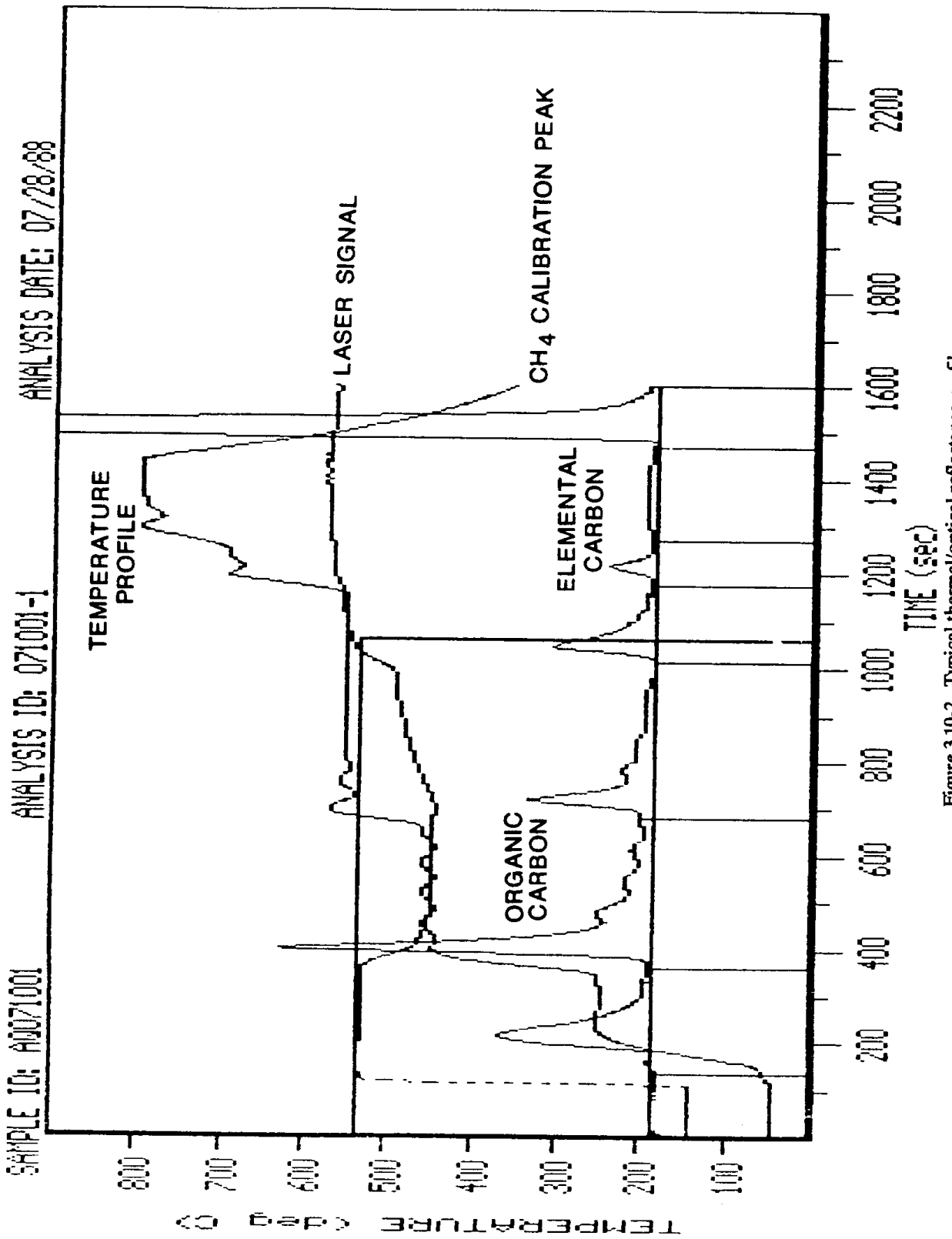

Figure 3.10-2. Typical thermal/optical reflectance profile.

3.11 Interlaboratory Comparison of Carbon Analyses

Organic and elemental carbon are important constituents of atmospheric particulate material. Unfortunately, no standard method exists for measuring their concentration in particulate samples. Interlaboratory comparisons (Countess, 1987; Groblicki et al., 1983) have shown that distinguishing between elemental carbon and organic carbon is the most problematic part of the analysis. Because of the unusual nature of the source samples collected for this study, twenty filters were blindly submitted to two other laboratories for comparison purposes. These laboratories were Sunset Laboratory (SL) and ENSR Consulting and Engineering (ENSR). For uniformity, and because fine particles generally contain the highest percent carbon content, all filters selected for analysis except one were in the $<2.5\mu$ size fraction. The $<2.5\mu$ size fraction was selected over the $<1\mu$ size fraction even though they are both "fine" size categories since the $<2.5\mu$ size category is more commonly reported in the literature. One $<10\mu$ size fraction filter of road dust was also included in the round robin to determine if coarser particles influenced the comparability results. In some ambient/source samples carbonate carbon is above detection limits. For that reason carbonate carbon results from DRI and SL were also included as part of the comparison.

Table 3.11-1 gives a description of the samples used in the comparison, and the physical and chemical data determined by DRI. Tables 3.11-2 though 3.11-4 give the organic carbon, elemental carbon, and carbonate carbon results, respectively, from these laboratories.

Table 3.11-5 lists the linear regression parameters for the comparison data. Figures 3.11-1 through 3.11-4 are plots of organic carbon, elemental carbon, total carbon, and carbonate carbon, respectively, between data from ENSR and DRI and between data from SL and DRI.

As can be seen by reviewing Table 3.11-5 and Figures 3.11-1 through 3.11-3, the comparison data for organic carbon and elemental carbon are quite reasonable and the comparison data for total carbon is very good. The difficulty in distinguishing between elemental and organic carbon which has been noted in previous studies is apparent in this data and makes the elemental and organic carbon comparisons poorer than the total carbon comparisons. The total carbon values are simply the sum of the elemental and organic carbon values as well as the carbonate carbon values for the SL and DRI data. With the exception of several of the geological dust samples (most notably the Mammoth Lakes cinder sample), the carbonate carbon contribution to the total carbon content is relatively small. The comparison between the carbonate carbon data from SL and DRI is poor (Table 3.11-5 and Figure 3.11-4). However, even with the Mammoth Lakes cinder sample, the correlation in the total carbon values between the two laboratories is quite good. This correlation implies that distinguishing between carbonate carbon and carbon in recalcitrant organic compounds may be problematic in a fashion analogous to distinguishing between elemental carbon and organic carbon. There appeared to be no

Table 3.11-1
Interlaboratory Carbon Analyses Samples List with
DRI Analytical Results[a]

Filter ID	Sample Description	Size (μ)	Composite Mnemonic[b]	Total Mass (mg)	Organic Carbon ($\mu g/cm^2$)	Elemental Carbon ($\mu g/cm^2$)	Carbonate Carbon ($\mu g/cm^2$)
AQ070850	Blank filter	---	---	---	1.50	0.05	0.00
AQ070266	Stockton ag soil, "peat"	< 2.5	SOIL01	2.207	20.99	5.40	0.40
AQ070306	Fresno paved road dust	< 2.5	SOIL03	1.680	18.23	1.56	0.00
AQ070287	Fresno paved road dust	< 10	SOIL03	1.403	22.40	3.76	0.30
AQ070672	Sand and gravel	< 2.5	SOIL06	0.087	4.33	0.00	0.00
AQ070701	Bakersfield ag soil	< 2.5	SOIL10	1.348	3.89	0.12	0.29
AQ070474	Bakersfield paved road	< 2.5	SOIL12	1.376	20.02	1.51	0.43
AQ070527	El Centro ag soil	< 2.5	SOIL21	1.333	2.32	0.14	1.06
AQ070539	Owens Lake dust	< 2.5	SOIL24	0.980	2.93	0.00	1.93
AQ070551	Mammoth Lakes cinder	< 2.5	SOIL25	4.524	5.05	0.00	3.96
AQ070668	Mammoth Lakes paved road	< 2.5	SOIL27	2.316	25.58	5.19	0.22
AQ070084	Bakersfield fireplace	< 2.5	BMAJC	2.521	92.92	37.65	0.05
AQ070137	Mammoth Lakes woodstove	< 2.5	MAFISC	5.144	171.90	54.41	0.02
AQ070165	Mammoth Lakes diesel bus	< 2.5	MADIEC	1.819	114.48	2.95	0.00
AQ071003	Bakersfield ag burn	< 2.5	BAAGBC	0.690	25.14	2.72	0.00
AQ071007	El Centro ag burn	< 2.5	ELAGBC	1.751	39.87	14.68	0.00
AQ071068	Fresno construction dust	< 2.5	FRCONC	0.105	7.15	2.42	0.00
AQ071060	Visalia dairy dust	< 2.5	VIDAIC	0.406	8.63	2.17	0.00
AQ070977	Chevron crude oil emissions	< 2.5	CHCRUC	8.806	26.15	24.50	0.00
AQ070031	Wheeler diesel trucks	< 2.5	WHDIEC	0.484	24.07	17.82	0.00

a. See Table 4.3-1 for uncertainties.

b. The composite mnemonic is for identification purposes only. Individual filters were submitted for analysis.

Table 3.11-2
Interlaboratory Carbon Analyses—Organic Carbon Comparison

Filter ID	Sample Description	Size (μ)	Composite Mnemonic[a]	Total Mass (mg)	DRI[b] ($\mu g/cm^2$)	SL[b] ($\mu g/cm^2$)	ENSR[b] ($\mu g/cm^2$)	Mean[c] ($\mu g/cm^2$)	Std. Dev.[c] ($\mu g/cm^2$)
AQ070850	Blank filter	---	---	--	1.50	0.72	< 0.5	0.91	0.52
AQ070266	Stockton ag soil, "peat"	< 2.5	SOIL01	2.207	20.99	24.46	17.9	21.1	3.3
AQ070306	Fresno paved road dust	< 2.5	SOIL03	1.680	18.23	21.54	14.8	18.2	3.4
AQ070287	Fresno paved road dust	< 10	SOIL03	1.403	22.40	25.2	24.3	24.0	1.4
AQ070672	Sand and gravel	< 2.5	SOIL06	0.087	4.33	2.47	3.6	3.47	0.94
AQ070701	Bakersfield ag soil	< 2.5	SOIL10	1.348	3.89	4.39	3.3	3.86	0.54
AQ070474	Bakersfield paved road	< 2.5	SOIL12	1.376	20.02	21.9	17.9	19.94	2.0
AQ070527	El Centro ag soil	< 2.5	SOIL21	1.333	2.32	2.65	2.7	2.56	0.21
AQ070539	Owens Lake dust	< 2.5	SOIL24	0.980	2.93	2.55	2.8	2.76	0.19
AQ070551	Mammoth Lakes cinder	< 2.5	SOIL25	4.524	5.05	3.74	13.7	7.50	5.4
AQ070668	Mammoth Lakes paved road	< 2.5	SOIL27	2.316	25.58	26.79	21.9	24.8	2.6
AQ070084	Bakersfield fireplace	< 2.5	BMAJC	2.521	92.92	101.46	91.1	95.2	5.5
AQ070137[d]	Mammoth Lakes woodstove	< 2.5	MAFISC	5.144	171.90	245	283.3(243.3)[c]	226.7	48.4
AQ070165[d]	Mammoth Lakes diesel bus	< 2.5	MADIEC	1.819	114.48	138	107.7	120.1	15.9
AQ071003	Bakersfield ag burn	< 2.5	BAAGBC	0.690	25.14	29.05	21.2	25.1	3.9
AQ071007	El Centro ag burn	< 2.5	ELAGBC	1.751	39.87	47.93	38.5	42.1	5.1
AQ071068	Fresno construction dust	< 2.5	FRCONC	0.105	7.15	4.85	5.6	5.87	1.2
AQ071060	Visalia dairy dust	< 2.5	VIDAIC	0.406	8.63	9.66	8.7	9.00	0.58
AQ070977	Chevron crude oil emissions	< 2.5	CHCRUC	8.806	26.15	29.47	24.3	26.6	2.6
AQ070031	Wheeler diesel trucks	< 2.5	WHDIEC	0.484	24.07	29.95	23.2(22.9)[c]	25.7	3.7

a. The composite mnemonic is for identification purposes only. Individual filters were submitted for analysis.

b. DRI - Desert Research Institute — see Table 4.3-1 for uncertainties.
SL - Sunset Laboratory — reported uncertainties are ±5% plus 0.2 $\mu g/cm^2$ detection limit.
ENSR (formerly ERT) — estimated precision was ±0.3 $\mu g/cm^2$.

c. Duplicate runs.

d. Sunset Laboratory report notes that samples AQ070137 and AQ070165 were heavily loaded for the technique used for analysis and the organic carbon values were estimated.

e. "Less than" values were treated as absolute values for calculation of means and standard deviations. Replicate runs conducted by ENSR on Samples AQ070137 and AQ070031 were averaged before calculation of interlaboratory means and standard deviations.

Table 3.11-3
Interlaboratory Carbon Analyses—Elemental Carbon Comparison

Filter ID	Sample Description	Size (μ)	Composite Mnemonic[a]	Total Mass (mg)	DRI[b] ($\mu g/cm^2$)	SL[b] ($\mu g/cm^2$)	ENSR[b] ($\mu g/cm^2$)	Mean[c] ($\mu g/cm^2$)	Std. Dev.[c] ($\mu g/cm^2$)
AQ070850	Blank filter	---	---	--	0.05	<0.2	<0.5	0.25	0.23
AQ070266	Stockton ag soil, "peat"	<2.5	SOIL01	2.207	5.40	2.98	3.5	3.96	1.3
AQ070306	Fresno paved road dust	<2.5	SOIL03	1.680	1.56	1.27	3.5	2.11	1.2
AQ070287	Fresno paved road dust	<10	SOIL03	1.403	3.76	1.74	5.4	3.63	1.8
AQ070672	Sand and gravel	<2.5	SOIL06	0.087	0.00	<0.2	<0.5	0.23	0.25
AQ070701	Bakersfield ag soil	<2.5	SOIL10	1.348	0.12	<0.2	<0.5	0.27	0.20
AQ070474	Bakersfield paved road	<2.5	SOIL12	1.376	1.51	0.95	3.8	2.09	1.5
AQ070527	El Centro ag soil	<2.5	SOIL21	1.333	0.14	<0.2	<0.5	0.28	0.19
AQ070539	Owens Lake dust	<2.5	SOIL24	0.980	0.00	<0.2	<0.5	0.23	0.25
AQ070551	Mammoth Lakes cinder	<2.5	SOIL25	4.524	0.00	<0.2	1.0	0.40	0.53
AQ070668	Mammoth Lakes paved road	<2.5	SOIL27	2.316	5.19	2.29	4.6	4.03	1.5
AQ070084[d]	Bakersfield fireplace	<2.5	BMAJC	2.521	37.65	27.25	27.2	30.7	6.0
AQ070137[d]	Mammoth Lakes woodstove	<2.5	MAFISC	5.144	54.41	24.27	61.2(52.9)[c]	45.2	18.2
AQ070165	Mammoth Lakes diesel bus	<2.5	MADIEC	1.819	2.95	<0.2	5.8	2.98	2.8
AQ071003	Bakersfield ag burn	<2.5	BAAGBC	0.690	2.72	0.77	4.1	2.53	1.7
AQ071007	El Centro ag burn	<2.5	ELAGBC	1.751	14.68	6.1	6.8	9.19	4.8
AQ071068	Fresno construction dust	<2.5	FRCONC	0.105	2.42	1.76	2.3	2.16	0.35
AQ071060	Visalia dairy dust	<2.5	VIDAIC	0.406	2.17	0.9	2.2	1.76	0.74
AQ070977[d]	Chevron crude oil emissions	<2.5	CHCRUC	8.806	24.50	19.19	17.5	20.4	3.7
AQ070031	Wheeler diesel trucks	<2.5	WHDIEC	0.484	17.82	8.42	14.6(16.2)[c]	13.9	4.9

a. The composite mnemonic is for identification purposes only. Individual filters were submitted for analysis.

b. DRI - Desert Research Institute — see Table 4.3-1 for uncertainties.
SL - Sunset Laboratory — reported uncertainties are ±5% plus 0.2 $\mu g/cm^2$ detection limit.
ENSR (formerly ERT) — estimated precision was ±0.3 $\mu g/cm^2$.

c. Duplicate runs.

d. Sunset Laboratory report notes that samples AQ070137, AQ070084, and AQ070977 were very dark, which may cause the elemental carbon values to have a higher uncertainty.

e. "Less than" values were treated as absolute values for calculation of means and standard deviations. Replicate runs conducted by ENSR on Samples AQ070137 and AQ070031 were averaged before calculation of interlaboratory means and standard deviations.

Table 3.11-4
Interlaboratory Carbon Analyses— Carbonate Carbon Comparison

Filter ID	Sample Description	Size (μ)	Composite Mnemonic[a]	Total Mass (mg)	DRI[b] ($\mu g/cm^2$)	SL[b] ($\mu g/cm^2$)	Mean[c] ($\mu g/cm^2$)	Std. Dev.[c] ($\mu g/cm^2$)
AQ070850	Blank filter	---	---	--	0.00	< 0.2	0.10	0.10
AQ070266	Stockton ag soil, "peat"	< 2.5	SOIL01	2.207	0.40	< 0.2	0.30	0.10
AQ070306	Fresno paved road dust	< 2.5	SOIL03	1.680	0.00	0.3	0.15	0.15
AQ070287	Fresno paved road dust	< 10	SOIL03	1.403	0.30	0.3	0.30	0.0
AQ070672	Sand and gravel	< 2.5	SOIL06	0.087	0.00	< 0.2	0.10	0.10
AQ070701	Bakersfield ag soil	< 2.5	SOIL10	1.348	0.29	< 0.2	0.25	0.05
AQ070474	Bakersfield paved road	< 2.5	SOIL12	1.376	0.43	1.0	0.72	0.29
AQ070527	El Centro ag soil	< 2.5	SOIL21	1.333	1.06	1.5	1.28	0.22
AQ070539	Owens Lake dust	< 2.5	SOIL24	0.980	1.93	2.0	1.97	0.04
AQ070551	Mammoth Lakes cinder	< 2.5	SOIL25	4.524	3.96	11.1	7.53	3.6
AQ070668	Mammoth Lakes paved road	< 2.5	SOIL27	2.316	0.22	< 0.2	0.21	0.01
AQ070084	Bakersfield fireplace	< 2.5	BMAJC	2.521	0.05	< 0.2	0.13	0.08
AQ070137	Mammoth Lakes woodstove	< 2.5	MAFISC	5.144	0.02	< 0.2	0.11	0.09
AQ070165	Mammoth Lakes diesel bus	< 2.5	MADIEC	1.819	0.00	< 0.2	0.10	0.10
AQ071003	Bakersfield ag burn	< 2.5	BAAGBC	0.690	0.00	< 0.2	0.10	0.10
AQ071007	El Centro ag burn	< 2.5	ELAGBC	1.751	0.00	< 0.2	0.10	0.10
AQ071068	Fresno construction dust	< 2.5	FRCONC	0.105	0.00	< 0.2	0.10	0.10
AQ071060	Visalia dairy dust	< 2.5	VIDAIC	0.406	0.00	< 0.2	0.10	0.10
AQ070977	Chevron crude oil emissions	< 2.5	CHCRUC	8.806	0.00	1.0	0.50	0.50
AQ070031	Wheeler diesel trucks	< 2.5	WHDIEC	0.484	0.00	< 0.2	0.10	0.10

a. The composite mnemonic is for identification purposes only. Individual filters were submitted for analysis.

b. DRI - Desert Research Institute — see Table 4.3-1 for uncertainties.
SL - Sunset Laboratory — reported uncertainties are ±5% plus 0.2 $\mu g/cm^2$ detection limit.

c. "Less than" values were treated as absolute values for calculation of means and average deviations around means. The average deviation was calculated by the formula:

$$\frac{|x_1 - x_2|}{2}$$

Table 3.11-5
Linear Regression Parameters, Interlaboratory Carbon Analyses

Category	x	y	n	slope	intercept ($\mu g/cm^2$)	R^2
Organic Carbon	DRI	ENSR	20	1.3	-7.0	0.94
Organic Carbon	SL	DRI	20	0.73	3.5	0.99
Elemental Carbon	DRI	ENSR	20	0.90	0.071	0.94
Elemental Carbon	SL	DRI	20	1.6	0.75	0.91
Carbonate Carbon	DRI	ENSR	ND	ND	ND	ND
Carbonate Carbon	SL	DRI	20	0.36	0.12	0.89
Total Carbon	DRI	ENSR	20	1.3	-8.8	0.95
TC (less 137)[a]	DRI	ENSR	19	0.92	-0.17	0.99
Total Carbon	SL	DRI	20	0.86	3.06	0.99
TC (less 137)[a]	SL	DRI	19	0.93	1.22	0.98

a. Total carbon not including filter AQ070137, which had very heavy loading.

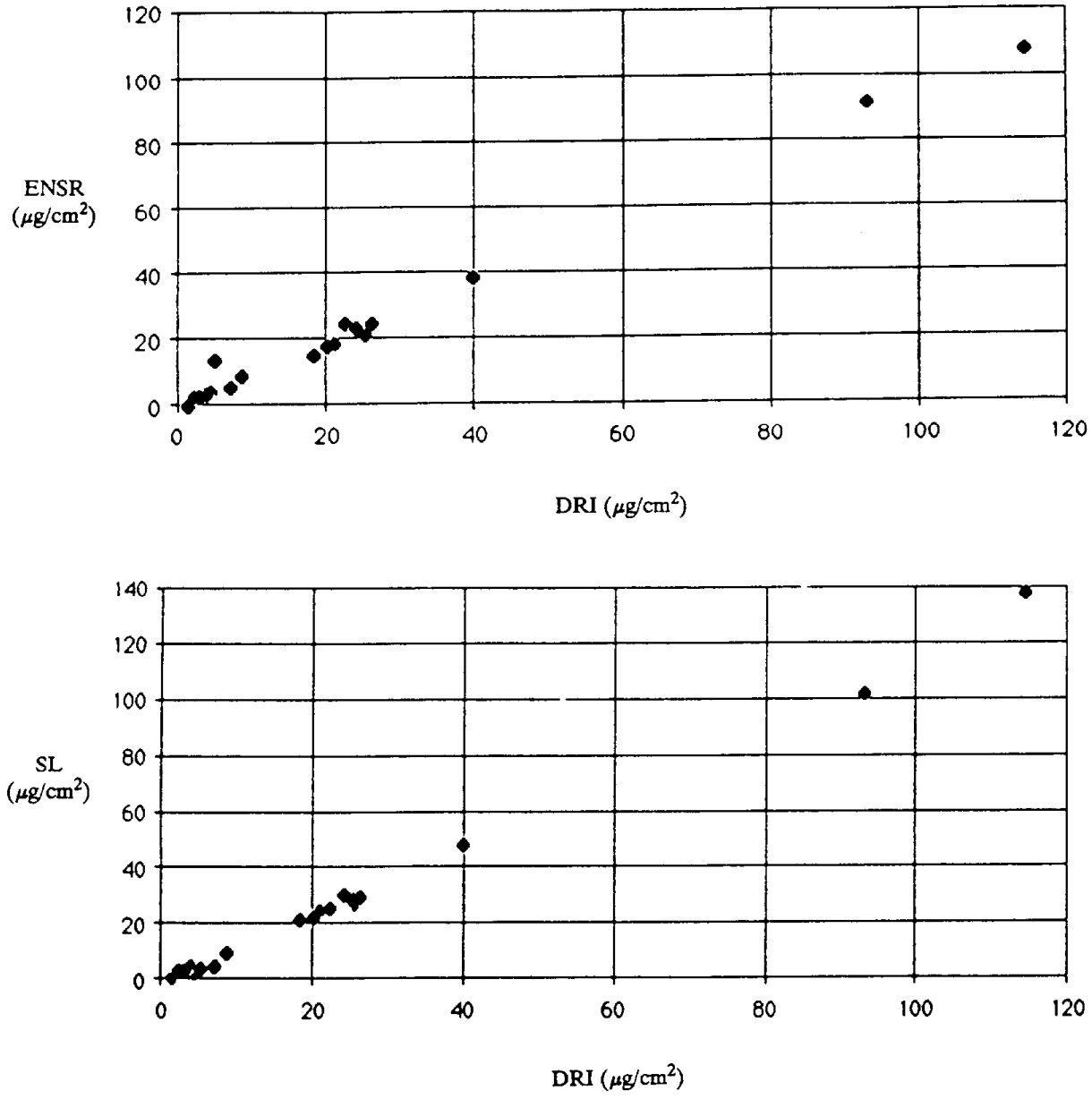

Figure 3.11-1. Organic carbon comparison plots. Top plot, ENSR data versus DRI data. Bottom plot, Sunset Laboratory (SL) data versus DRI data. Data for filter AQ070137 not included.

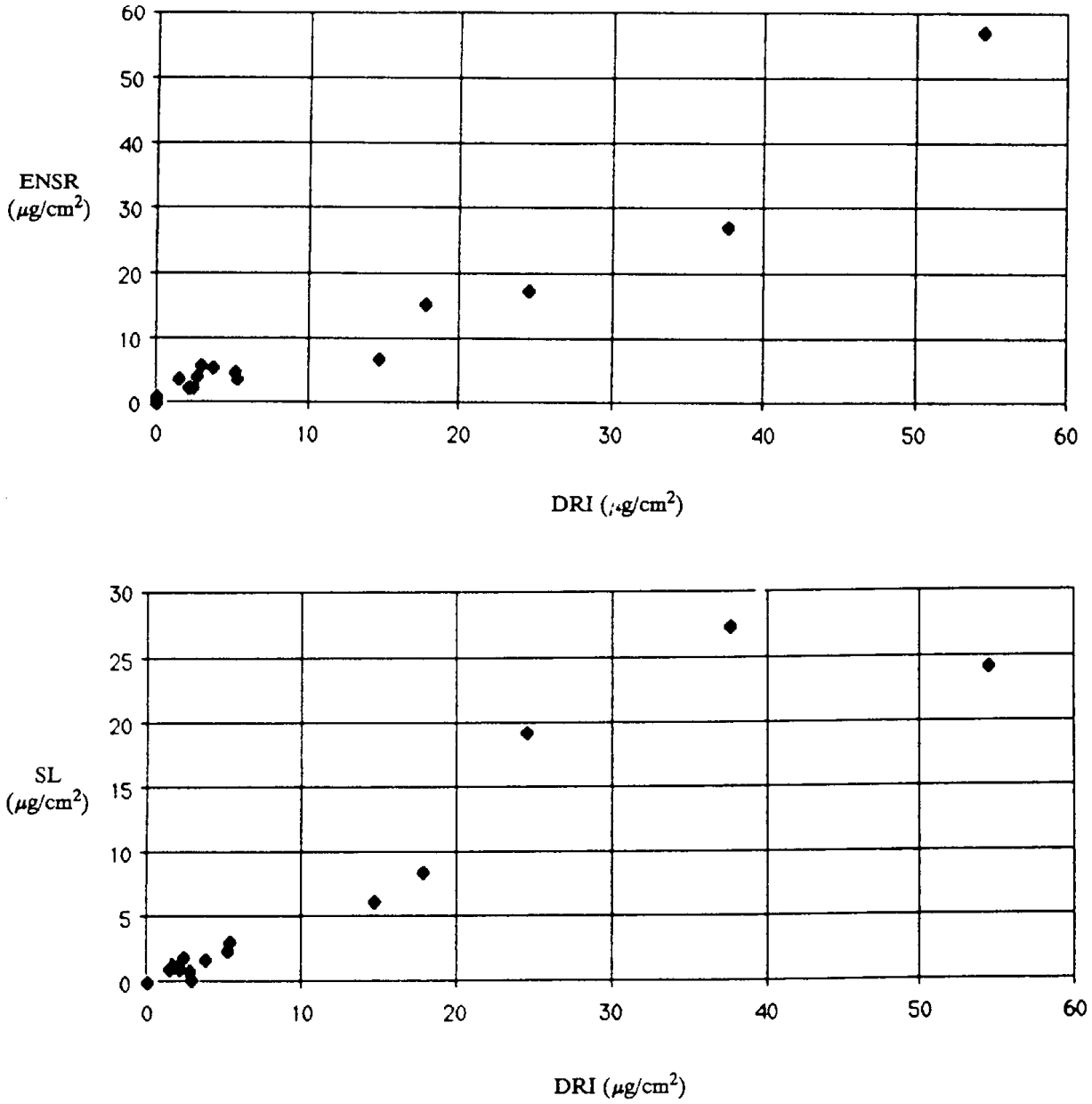

Figure 3.11-2. Elemental carbon comparison plots. Top plot, ENSR data versus DRI data. Bottom plot, Sunset Laboratory (SL) data versus DRI data.

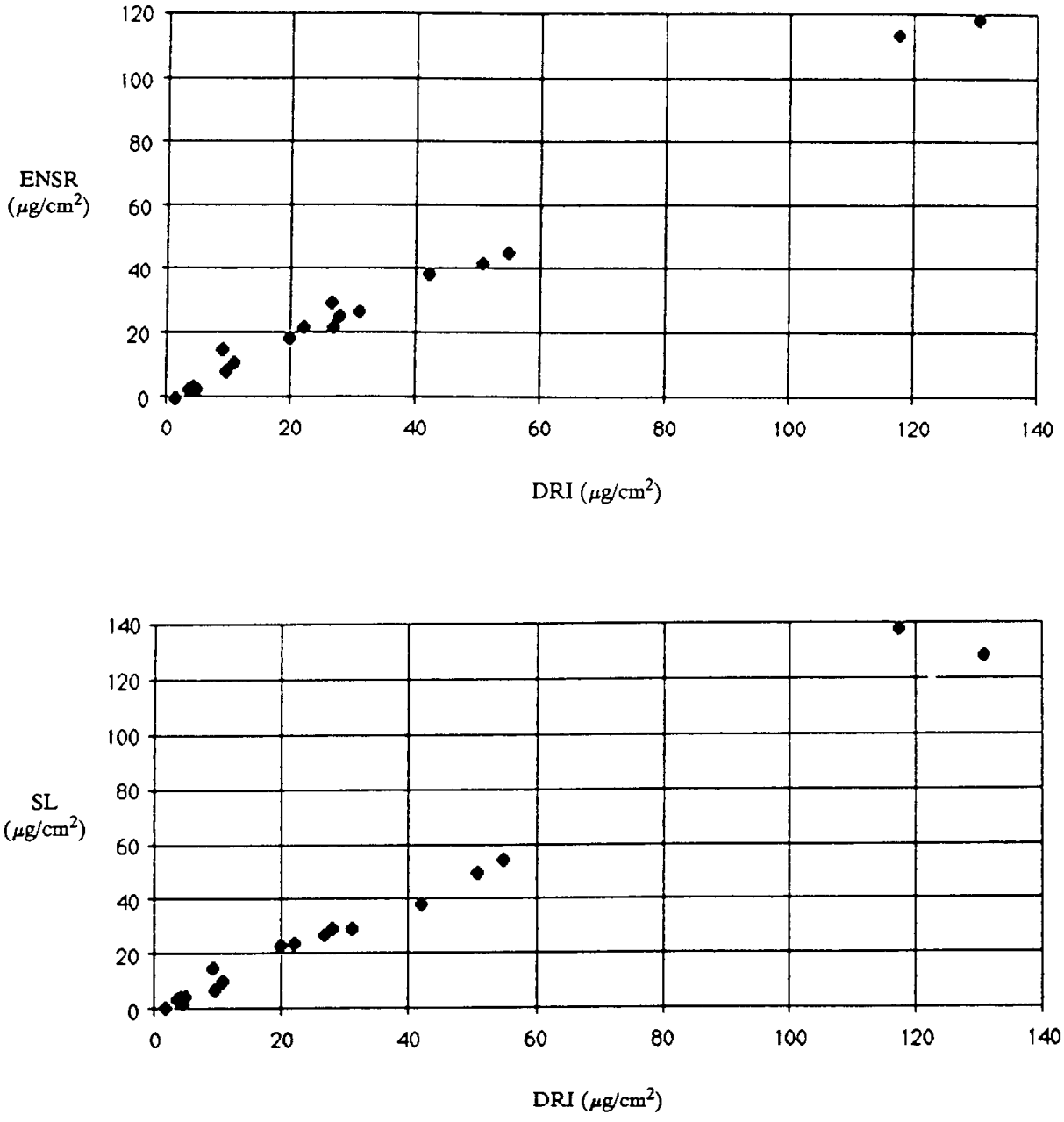

Figure 3.11-3. Total carbon comparison plots. Top plot, ENSR data versus DRI data. Bottom plot, Sunset laboratory (SL) data versus DRI data. Data for filter AQ070137 not included.

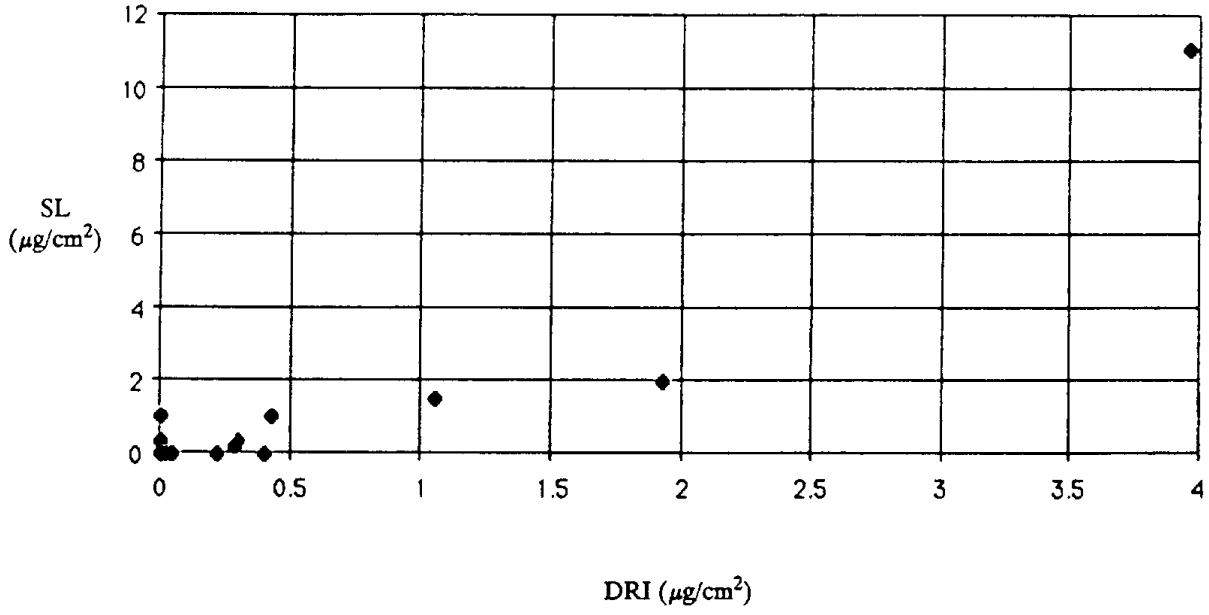

Figure 3.11-4. Carbonate carbon comparison plot.

obvious differences in terms of interlaboratory comparability results between the $<2.5\mu$ and $<10\mu$ road dust filters.

It is outside the scope of this study to do a detailed investigation into the relative merits of the analytical techniques used at the three laboratories. As discussed, the comparison data for organic carbon and elemental carbon are reasonable, the comparison data for carbon to carbonate are poor, and the comparison data for total carbon are good. It should be noted that carbonate carbon is not generally an important ambient aerosol constituent. Even with the reasonable comparisons for organic and elemental carbon, using organic and elemental carbon data interchangeably between laboratories would not be advisable. Two pragmatic recommendations can be made for use of carbon data in chemical mass balance (CMB) receptor modeling based on the interlaboratory comparison results. These are: (1) use total carbon only in the CMB model; or (2) ensure that the same laboratory conducts all the source and ambient carbon analyses for a given airshed.

4.0 Data Base Processing

4.1 Overview

The overall source profile data base management is illustrated in Figure 4.1-1.

Data processing consists of six general tasks:

- Recording. The relevant information contained at the time an operation is performed is registered on a data sheet, data logger, or other transfer medium.
- Input. The data are transferred from the recording medium into computer-accessible files.
- Merging. Data from various files pertaining to an individual sample are retrieved and related to each other.
- Calculations. Data items are combined in mathematical expressions to yield a desired result. These include concentrations, accuracies, and precisions.
- Validation. Data are verified against earlier or redundant recordings, with calibration and operating records, and with each other.
- Output. Data are arranged into desired formats for input to data interpretation and modeling software.

Since a single sample is submitted to many chemical analyses, data from the different chemical analyses must be unified as they become available.

The data base management system needs to fulfill the following requirements:

- Quantitative and descriptive information must be accommodated.
- Data from a number of sources must be merged in an efficient and cost-effective manner.
- Input data required by models should be easily accessible directly from the data base.

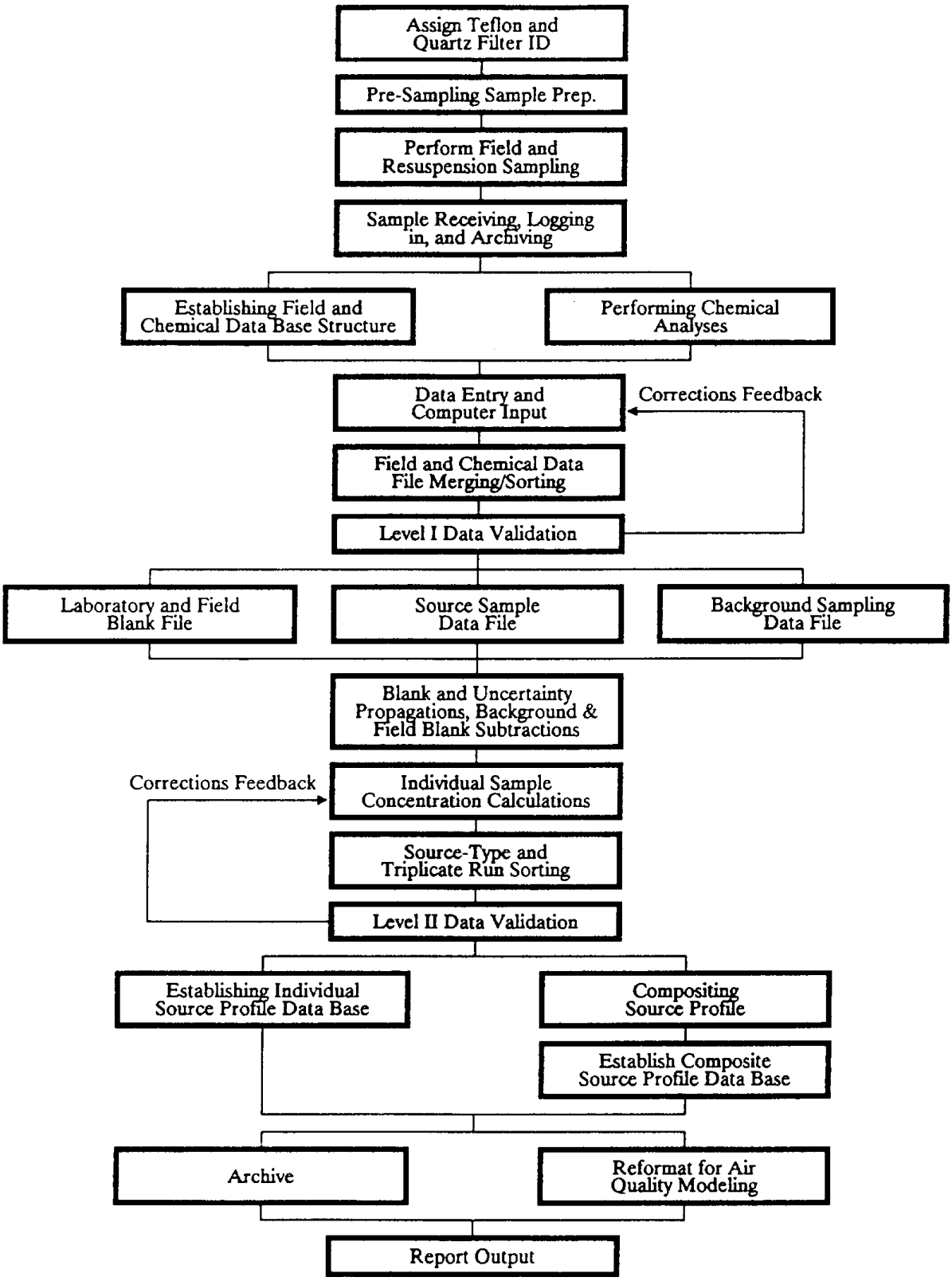

Figure 4.1-1. Source profile data base management flow diagram.

The dBase III Plus (Ashton-Tate, 1985) relational data base has been selected for this data base management task because:

- It is commonly available, reasonably priced, has good third-party documentation and support, and provides interfaces to many other software packages.

- Non-proprietary software is available to access dBase III Plus files directly without the need for the dBase III Plus software itself.

- dBase III Plus can handle 128 fields of 4000 characters per record and up to one billion records per file. A memo field is available which can be used to record data validation and ambient and source description data for each set of test results.

- Data entry, data validation, reformatting, and data reporting programs can be written.

Data validation is the most important function of data processing. Sample validation consists of procedures which identify deviations from measurement assumptions and procedures. Three levels (Mueller et al., 1983) of validation are applied which will result in the assignment of a rating for each measurement which is: (1) valid; (2) valid but suspect; or (3) invalid.

Level I sample validation takes place in the field or in the laboratory and consists of: (1) flagging samples when significant deviations from measurement assumptions have occurred; (2) verifying computer file entries against data sheets; (3) eliminating values for measurements which are known to be invalid because of instrument malfunctions; (4) replacing data from a backup data acquisition system in the event of failure of the primary system; and (5) adjusting measurement values of quantifiable calibration or interference biases.

Level II sample validation takes place after data from various measurement methods have been assembled in the master data base. Level II applies consistency tests based on known physical relationships between variables to the assembled data. Examples of these tests are: (1) the sum of all chemical species in a particulate matter sample should be less than or equal to the gravimetric mass of that sample; (2) size-segregated particle concentrations should be less than total particle concentrations; (3) the sum of all major species (with oxide forms included) should exceed 75 percent of the measured mass; and (4) analyses of the same species by different methods should yield compatible results (e.g., Al by XRF and INAA). (It should also be noted that there is no fixed rule regarding test 4, other than that if the differences are outside the uncertainties associated with each test, a careful investigation should be made to determine the source of the bias.) Samples are designated for re-analysis if they do not meet these criteria.

Data adjustments for quantifiable biases (e.g., large particle absorption corrections for aluminum) can be made in Level II validation if they are discovered after assembly of the master data base.

Level III sample validation is part of the data interpretation process. The first assumption upon finding a measurement which is inconsistent with physical expectations is that the unusual value is due to a measurement error. If, upon tracing the path of the measurement, nothing unusual is found, the value can be assumed to be a valid result of an environmental cause. Unusual values are identified during the data interpretation process as: (1) extreme values; (2) values which would otherwise normally track the values of other variables in a time series; and (3) values for observables which would normally follow a qualitatively predictable spatial or temporal pattern.

All data validation actions at each level are recorded in a data validation summary which accompanies the data base. Data base records contain flags to identify the level of validation which they have received at any point in their existence.

Every measurement consists of a value, a precision, an accuracy, and a validity (Mueller et al., 1979; Mueller and Watson, 1981; Hidy, 1985). Quality control (QC) and quality auditing establish the precision, accuracy, and validity of measured values (Watson et al., 1983). Quality assurance integrates quality control and quality auditing to determine these four attributes of each environmental measurement.

Quality assurance (QA) is a project management responsibility which integrates quality control, quality auditing, measurement method validation, and sample validation into the measurement process. The results of quality assurance are data values with specified precision, accuracy, and validity. Quality auditing is performed by personnel who are independent of those performing the procedures.

The QC activities include: (1) modification of standard operating procedures (SOPs) to be followed during source sampling, analysis, and data processing; (2) periodic calibrations and performance tests; (3) collocated sampling; (4) blank and replicate analyses; and (5) data validation.

The quality auditing function consists of two components: systems audits and performance audits. Systems audits start with a review of the operational and QC procedures to assess whether they are adequate to assure valid data which meet the specified levels of accuracy and precision. After reviewing the procedures, the auditor examines all phases of the measurement or data processing activity to determine that the procedures are being followed and that the operational people are properly trained. The systems audit is intended to be a cooperative assessment resulting in improved data, rather than a judgmental activity.

Performance audits establish whether the predetermined specifications are being achieved in practice. The performance audit challenges the measurement/analysis system with a known standard sample which is traceable to a primary standard. For data processing, the performance audit consists of independently processing sections of the data and comparing the results.

4.2 Standard Operating Procedures

Standard operating procedures (SOPs) codify the actions which are taken to implement a measurement process over a specified time period. State-of-the-art scientific information is incorporated into the SOP with each revision. SOPs include the following elements:

- A brief summary of the measurement method, its principles of operation, its expected accuracy and precision, and the assumptions which must be met for it to be valid.
- A list of materials, equipment, reagents, and suppliers. Specifications are given for each expendable item and its storage location is listed.
- Designation of an individual to be responsible for each part of the procedure.
- A general traceability path, the designation of primary standards or reference material, tolerances for transfer standards, and a schedule for transfer standard verification.
- Start-up, routine, and shut-down operating procedures and an abbreviated checklist.
- Copies of data forms with examples of filled-out forms.
- Routine maintenance schedules, maintenance procedures, and troubleshooting tips.
- Internal calibration and performance testing procedures and schedules.
- External performance auditing schedules.
- References to relevant literature and related standard operating procedures.

4.3 Data Processing of Source Data

Aerosol data processing and validation requires: (1) assignment of ID codes to substrates; (2) field data recording of the IDs and their corresponding sampling sites and times, sample flow rates, sampling dates, and deviations from normal sampling procedures; (3) laboratory instrument recording of analytical outputs; (4) Level I validation, flagging, and editing of these individual data files; (5) merging field and laboratory data for sample sets; (6) Level II validation, editing, flagging, and re-analysis; (7) calculation of concentrations and precision; and (8) formatting and reporting of concentration, precision, and data validation activities. A data management system which performs these functions is implemented in the dBase III Plus relational data base.

Field data sheets are entered into computerized data forms. These forms have limits which do not allow entry of values which lie outside a certain range. Every data item which is entered is verified by the data processing supervisor against the original data sheet.

A structure which contains fields for all chemical concentrations and their uncertainties is formed and the IDs, sample volumes, sampling times, sampling sites, and sampling dates are integrated into this structure from the field file. All other fields contain the missing data default value. These defaults are replaced by laboratory analysis data as they become available. In this way, it is always possible to determine which analyses have been completed and which have not.

The laboratory chain-of-custody data base records the disposition of each sample, and this data base can be consulted to determine the fate of missing values in the master data base. This independent tracking prevents sample IDs from being mixed up.

Most laboratory analysis instruments are linked to IBM-PC compatible computers and data are recorded in dBase III Plus or ASCII text files. All data are keyed to sample ID codes, and data base programs associate records in the laboratory files with data in the master file. These programs also replace the defaults in the master data file with the laboratory values. Separate flags are entered at the time of analysis to indicate that a sample is an ambient sample, a source sample, a field blank, a laboratory blank, a replicate, a re-run, a performance test standard, or an audit standard. These flags are used to separate these quality control values from the individual data bases to generate quality control charts and precision estimates.

When all data for a record have been assembled, dBase III Plus programs perform the Level II data validation comparisons. These include: (1) comparing sum of species with particle mass; (2) comparing sulfur by XRF with sulfate by IC; and (3) comparing soluble potassium by IC with total potassium by XRF. Statistical summaries, scatter plots, and time series plots of selected species concentrations are produced to identify

outliers for investigation and potential re-run. A data validation summary is maintained in the memo field associated with each record to provide a traceability trail for all data adjustments, replacements, or deletions.

When all sample concentration data have been assembled, a data base program creates another data base of source concentrations. Propagated precisions and blank subtraction calculations are made at this stage. The data validation flags and summaries accompany this final data base.

Both collocated and propagated precision are calculated following the methods of Mathai et al. (1985) and Watson et al. (1893), respectively. The propagated precision are derived from replicate measurements and performance tests. Table 4.3-1 summarizes the blank subtract values and uncertainties applied to the data base for non-XRF data.

Blank and precision levels are calculated differently for x-ray fluorescence than for the other measurement methods. Representative laboratory blank filters are analyzed, and spectra from those analyses are averaged and used directly for spectral background subtraction. Trace element blank filter impurities are automatically subtracted from sample analysis results by this procedure, even though laboratory blank concentrations are not determined directly. Field blanks are analyzed and subtracted in the usual method. However, field blank elemental concentrations were generally below the measurement uncertainty, so field blank subtraction was not required.

The XRF analysis procedure provides an estimate of precision directly from the analysis result based on counting statistics. This uncertainty is the best estimate of measurement precision, as it is based on elemental concentration of not only analyte, but other elements in the sample as well. Replicate samples are analyzed and their concentrations are verified to be within the counting statistics derived precision limits of the original analyses. Typical precision values based on replicate analyses results are shown in Table 4.3-2.

4.4 Data Validation Summary

During the process of Level II data validation of the source profiles, decisions were made concerning data validity and outliers based on the following: (1) the soluble potassium and XRF potassium should be close to one another in wood smoke samples, with the soluble potassium being less than the XRF (total) potassium; (2) the soluble sulfate should be less than three times the XRF sulfur measurement; and (3) measurements, including total deposit mass, should be consistent across both the different size fractions of one sample set and across all replicates of a source type. Table 4.4-1 gives the structure of the source profile data base. Table 4.4-2 lists the analyses and data validation flags used to identify individual datum points which require custom evaluation after routine analyses (Level I validation) were conducted. Level II data validation summaries are

Table 4.3-1
Source Profile Blanks and Uncertainties for Non-XRF Data

Filter Category[a]	Parameter	Applicable Filters on Threshold Value (μg)	Blank Subtract (μg)	Blank Uncertainty (μg)	Replicate Precision (μg or %)	Number of Replicates
RST	Mass	all	0	0	> of 8 or 2% of net mass	274
RSTX	Mass	all	0	0	7 μg	123
PST	Mass	all except AT070976-987	0	0	9 μg	111
PST	Mass	AT070976	0	0	536 μg	3
PST	Mass	AT070977	0	0	586 μg	3
PST	Mass	AT070978	0	0	585 μg	3
PST	Mass	AT070979	0	0	549 μg	3
PST	Mass	AT070980	0	0	412 μg	3
PST	Mass	AT070981	0	0	512 μg	3
PST	Mass	AT070982	0	0	508 μg	3
PST	Mass	AT070983	0	0	476 μg	3
PST	Mass	AT070984	0	0	348 μg	3
PST	Mass	AT070985	0	0	379 μg	3
PST	Mass	AT070986	0	0	377 μg	3
PST	Mass	AT070987	0	0	410 μg	3
RSQ	Volume	all	----	----	5%	---
PSQ	Volume	all	----	----	5%	---
RSQ	OC	≤130	29.94	5.37	10.47 μg	18
RSQ	OC	>130	29.94	5.37	17.91 μg	9
PSQ	OC	≤100	50.81	14.97	7.42 μg	3
PSQ	OC	>100, ≤1500	50.81	14.97	28.78 μg	16
PSQ	OC	>1500	50.81	14.97	186.20 μg	3
RSQ	EC	≤20	3.60	1.70	2.31 μg	21
RSQ	EC	>20	3.60	1.70	18.75 μg	6
PSQ	EC	≤140	4.55	3.65	9.47 μg	14
PSQ	EC	>140, ≤1500	4.55	3.65	18.58 μg	7
PSQ	EC	>1500	4.55	3.65	6.5%	1
RSQ	CO_3	≤20	1.45	1.74	3.66 μg	24
RSQ	CO_3	>20	1.45	1.74	13.98 μg	3
PSQ	CO_3	≤1	0.57	1.26	0.30 μg	20
PSQ	CO_3	>1	0.57	1.26	3.26 μg	2
RSQ	NO_3	all	0.0000	0.0000	6.1739 μg	51
PSQ	NO_3	≤15	0.0000	0.0000	0.2470 μg	28
PSQ	NO_3	>15	0.0000	0.0000	0.8037 μg	7

(continues)

Table 4.3-1 (continued)

Filter Category[a]	Parameter	Applicable Filters on Threshold Value (μg)	Blank Subtract (μg)	Blank Uncertainty (μg)	Replicate Precision (μg or %)	Number of Replicates
RSQ	SO_4	≤ 10	0.0000	0.8384	2.0663 μg	19
RSQ	SO_4	$>10, \leq 100$	0.0000	0.8384	21.5930 μg	27
RSQ	SO_4	>100	0.0000	0.8384	42%	5
PSQ	SO_4	≤ 15	0.1311	0.2354	0.2639 μg	15
PSQ	SO_4	$>15, \leq 35$	0.1311	0.2354	0.7473 μg	11
PSQ	SO_4	>35	0.1311	0.2354	5.2%	9
RSQ	K	≤ 5	0.0000	0.3488	0.4136 μg	22
RSQ	K	>5	0.0000	0.3488	2.1113 μg	13
PSQ	K	≤ 10	0.0609	0.1099	0.3018 μg	15
PSQ	K	$>10, \leq 50$	0.0609	0.1099	0.9042 μg	5
PSQ	K	$>50, \leq 100$	0.0609	0.1099	3.2202 μg	7
PSQ	K	>100	0.0609	0.1099	5.0163 μg	6
RSQ	Na	≤ 10	0.0934	0.0611	0.7028 μg	25
RSQ	Na	$>10, \leq 20$	0.0934	0.0611	1.9683 μg	5
RSQ	Na	>20	0.0934	0.0611	1.4830 μg	5
PSQ	Na	≤ 1	0.5825	0.1939	0.2444 μg	6
PSQ	Na	$>1, \leq 30$	0.5825	0.1939	0.3266 μg	18
PSQ	Na	>30	0.5825	0.1939	6.25%	1
RSQ	NH_4	all	0.0000	0.0000	0.1018 μg	35
PSQ	NH_4	≤ 1	0.3842	0.2058	0.0639 μg	4
PSQ	NH_4	$>1, \leq 40$	0.3842	0.2058	0.1202 μg	31
PSQ	NH_4	>40	0.3842	0.2058	0.5744 μg	8

a. RS = resuspended soil and road dust samples
PS = all other sources
T = Teflon filters
TX = Teflon coated glass fiber filters
Q = quartz filters

Table 4.3-2
Typical X-Ray Fluorescence Uncertainties for Source Samples

Species[a]	Threshold Value (μg)	Replicate Precision (μg)
RST Al	≤ 50 > 50	0.46 1.56
PST Al	all	0.30
RST Si	≤ 150 > 150	1.08 1.72
PST Si	all	0.39
RST S	≤ 1.0 $> 1, \leq 10$ > 10	0.057 0.38 1.12
PST S	≤ 1.0 $> 1, \leq 100$ > 100	0.048 0.40 11%
RST K	≤ 12 $> 12, \leq 100$ > 100	0.18 0.52 3.77
PST K	≤ 1.0 $> 1.0, \leq 50$ > 50	0.019 0.60 6.30
RST Ca	≤ 50 $> 50, \leq 200$ > 200	0.39 0.92 4.49
PST Ca	≤ 0.50 $> 0.50, \leq 5.0$ > 5.0	0.025 0.20 0.57
RST Fe	≤ 20 $> 20, \leq 150$ > 150	0.31 1.18 4.18
PST Fe	≤ 5.0 > 5.0	0.029 0.26
RST Pb	≤ 0.10 > 0.10	0.016 0.039
PST Pb	≤ 0.10 > 0.10	0.013 0.037

a. RST = Resuspended soil and road dust samples on Teflon filters.
PST = All other sources on Teflon filters.

Table 4.4-1
Structure of Source Profile Data Base

Field	Field Name	Type	Width	Description
1	DATE	Date	8	Sample date
2	SID	Character	6	Sample ID mnemonic (See Appendix A, Sections A-2 and A-3)
3	SIZE	Character	3	Size fraction (see Appendix A, Section A-4)
4	GROUP	Character	2	XRF size correction group (see Section 3.5)
5	TID	Character	10	Teflon ID[b]
6	QID	Character	10	Quartz ID[b]
7	TFFLG	Character	10	Teflon flag (see Table 4.4-2)
8	QFFLG	Character	10	Quartz flag (see Table 4.4-2)
9	MFLG	Character	5	Mass flag (see Table 4.4-2)
10	XFLG	Character	2	XRF flag (see Table 4.4-2)
11	AFLG	Character	10	Anion flag (see Table 4.4-2)
12	CAFLG	Character	10	Calcium flag (see Table 4.4-2)
13	N4FLG	Character	10	NH_4 flag (see Table 4.4-2)
14	KPFLG	Character	10	Potassium flag (see Table 4.4-2)
15	NAFLG	Character	10	Sodium flag (see Table 4.4-2)
16	S2FLG	Character	10	not used
17	QVOC	Numeric	10:4	Quartz sample volume (m^3)[b]
18	QVOU	Numeric	10:4	Quartz sample volume uncert. (nominally 5% of value in m^3)[b]
19	TVOC	Numeric	10:4	Teflon sample volume (m^3)[b]
20	TVOU	Numeric	10:4	Teflon sample volume uncert. (nominally 5% of value in m^3)[b]
21	TMAC	Numeric	11:4	Average total mass concentration of replicate samples ($\mu g/m^3$)[c]
22	TMAU	Numeric	10:4	Average total mass conc. uncert. of replicate samples ($\mu g/m^3$)[c]
23	AMAC	Numeric	11:4	Average analyzed mass concentration of rep. samples ($\mu g/m^3$)[c]
24	AMAU	Numeric	10:4	Average analyzed mass conc. uncert. of rep. samples ($\mu g/m^3$)[c]
25	N3IC	Numeric	10:4	NO_3 measurement (average mass % of replicate samples)
26	N3IU	Numeric	10:4	NO_3 uncertainty[a]
27	S4IC	Numeric	10:4	SO_4 measurement (average mass % of replicate samples)
28	S4IU	Numeric	10:4	SO_4 uncertainty[a]
29	N4TC	Numeric	10:4	NH_4 measurement (average mass % of replicate samples)
30	N4TU	Numeric	10:4	NH_4 uncertainty[a]
31	KPAC	Numeric	10:4	Soluble K measurement (average mass % of replicate samples)
32	KPAU	Numeric	10:4	Soluble K uncertainty[a]
33	NAAC	Numeric	10:4	Soluble Na measurement (average mass % of replicate samples)
34	NAAU	Numeric	10:4	Soluble Na uncertainty[a]
35	ECTC	Numeric	10:4	Elemental carbon measurement (avg. mass % of rep. samples)
36	ECTU	Numeric	10:4	Elemental carbon uncertainty[a]
37	OCTC	Numeric	10:4	Organic carbon measurement (avg. mass % of rep. samples)
38	OCTU	Numeric	10:4	Organic carbon uncertainty[a]
39	COTC	Numeric	10:4	Carbonate carbon measurement (avg. mass % of rep. samples)
40	COTU	Numeric	10:4	Carbonate carbon uncertainty[a]

(continues)

Table 4.4-1 (continued)

Field	Field Name	Type	Width	Description
41	ALXC	Numeric	10:4	Al measurement (average mass % of replicate samples)
42	ALXU	Numeric	10:4	Al uncertainty
43	SIXC	Numeric	10:4	Si measurement (average mass % of replicate samples)
44	SIXU	Numeric	10:4	Si uncertainty
45	PHXC	Numeric	10:4	P measurement (average mass % of replicate samples)
46	PHXU	Numeric	10:4	P uncertainty
47	SUXC	Numeric	10:4	S measurement (average mass % of replicate samples)
48	SUXU	Numeric	10:4	S uncertainty
49	CLXC	Numeric	10:4	Cl measurement (average mass % of replicate samples)
50	CLXU	Numeric	10:4	Cl uncertainty
51	KTXC	Numeric	10:4	Total K measurement (average mass % of replicate samples)
52	KTXU	Numeric	10:4	Total K uncertainty
53	CAXC	Numeric	10:4	Ca measurement (average mass % of replicate samples)
54	CAXU	Numeric	10:4	Ca uncertainty
55	TIXC	Numeric	10:4	Ti measurement (average mass % of replicate samples)
56	TIXU	Numeric	10:4	Ti uncertainty
57	VAXC	Numeric	10:4	V measurement (average mass % of replicate samples)
58	VAXU	Numeric	10:4	V uncertainty
59	CRXC	Numeric	10:4	Cr measurement (average mass % of replicate samples)
60	CRXU	Numeric	10:4	Cr uncertainty
61	MNXC	Numeric	10:4	Mn measurement (average mass % of replicate samples)
62	MNXU	Numeric	10:4	Mn uncertainty
63	FEXC	Numeric	10:4	Fe measurement (average mass % of replicate samples)
64	FEXU	Numeric	10:4	Fe uncertainty
65	COXC	Numeric	10:4	Co measurement (average mass % of replicate samples)
66	COXU	Numeric	10:4	Co uncertainty
67	NIXC	Numeric	10:4	Ni measurement (average mass % of replicate samples)
68	NIXU	Numeric	10:4	Ni uncertainty
69	CUXC	Numeric	10:4	Cu measurement (average mass % of replicate samples)
70	CUXU	Numeric	10:4	Cu uncertainty
71	ZNXC	Numeric	10:4	Zn measurement (average mass % of replicate samples)
72	ZNXU	Numeric	10:4	Zn uncertainty
73	GAXC	Numeric	10:4	Ga measurement (average mass % of replicate samples)
74	GAXU	Numeric	10:4	Ga uncertainty
75	ASXC	Numeric	10:4	As measurement (average mass % of replicate samples)
76	ASXU	Numeric	10:4	As uncertainty
77	SEXC	Numeric	10:4	Se measurement (average mass % of replicate samples)
78	SEXU	Numeric	10:4	Se uncertainty
79	BRXC	Numeric	10:4	Br measurement (average mass % of replicate samples)
80	BRXU	Numeric	10:4	Br uncertainty
81	RBXC	Numeric	10:4	Rb measurement (average mass % of replicate samples)
82	RBXU	Numeric	10:4	Rb uncertainty
83	SRXC	Numeric	10:4	Sr measurement (average mass % of replicate samples)
84	SRXU	Numeric	10:4	Sr uncertainty

(continues)

Table 4.4-1 (continued)

Field	Field Name	Type	Width	Description
85	YTXC	Numeric	10:4	Y measurement (average mass % of replicate samples)
86	YTXU	Numeric	10:4	Y uncertainty
87	ZRXC	Numeric	10:4	Zr measurement (average mass % of replicate samples)
88	ZRXU	Numeric	10:4	Zr uncertainty
89	MOXC	Numeric	10:4	Mo measurement (average mass % of replicate samples)
90	MOXU	Numeric	10:4	Mo uncertainty
91	PDXC	Numeric	10:4	Pd measurement (average mass % of replicate samples)
92	PDXU	Numeric	10:4	Pd uncertainty
93	AGXC	Numeric	10:4	Ag measurement (average mass % of replicate samples)
94	AGXU	Numeric	10:4	Ag uncertainty
95	CDXC	Numeric	10:4	Cd measurement (average mass % of replicate samples)
96	CDXU	Numeric	10:4	Cd uncertainty
97	INXC	Numeric	10:4	In measurement (average mass % of replicate samples)
98	INXU	Numeric	10:4	In uncertainty
99	SNXC	Numeric	10:4	Sn measurement (average mass % of replicate samples)
100	SNXU	Numeric	10:4	Sn uncertainty
101	SBXC	Numeric	10:4	Sb measurement (average mass % of replicate samples)
102	SBXU	Numeric	10:4	Sb uncertainty
103	BAXC	Numeric	10:4	Ba measurement (average mass % of replicate samples)
104	BAXU	Numeric	10:4	Ba uncertainty
105	LAXC	Numeric	10:4	La measurement (average mass % of replicate .amples)
106	LAXU	Numeric	10:4	La uncertainty
107	HGXC	Numeric	10:4	Hg measurement (average mass % of replicate samples)
108	HGXU	Numeric	10:4	Hg uncertainty
109	PBXC	Numeric	10:4	Pb measurement (average mass % of replicate samples)
110	PBXU	Numeric	10:4	Pb uncertainty
111	S2IC	Numeric	10:4	not used
112	S2IU	Numeric	10:4	not used
113	PERSUMC	Numeric	10:4	Mass percent sum of all species except SO_4 and Soluble K
114	PERSUMU	Numeric	10:4	Mass percent sum propagated uncertainty
115	NOTE	Character	60	Analysis and data validation notes

a. Each uncertainty is either the standard deviation among the replicates or the root-mean-square propagated analytical uncertainty, whichever is greater.

b. The Teflon and quartz filter ID is the ID of one of the Teflon/quartz filter sets that make up the composite. The quartz sample volume, the quartz sample volume uncertainty, the Teflon sample volume, and the Teflon sample volume uncertainty are for the same filter for which the ID is listed. The ID and volume data are included as place holders only.

c. The total mass and the analyzed mass are the same for non-resuspended samples. For resuspended samples, the analyzed mass is the mass deposited on the filter which was analyszed. The resuspension process requires a number of filters in the coarser sizes to be loaded before the finer filters are adequately loaded for analysis. The sum of the individual coarser filters for a given size category is the total mass. The mass uncertainty is either the standard deviation around mean of the replicates or the root-mean-square propagated uncertainty, whichever is larger.

Table 4.4-2
Analysis and Data Validation Flags

Analysis Flag Type	Description
TFFLG	Teflon field data validation flag
QFFLG	Quartz field data validation flag
MFLG	Gravimetric analysis flag
XFLG	X-ray fluorescence analysis flag
AFLG	Anion (ion chromatography) analysis flag
CAFLG	Carbon analysis flag
N4FLG	Soluble ammonium (colorimetric) analysis flag
KPFLG	Soluble potassium (atomic absorption) analysis flag
NAFLG	Sodium (atomic absorption) analysis flag

Analysis Flag	Description
f1	Filter damaged outside of deposit area
i1	Inhomogeneous filter deposit
i2	Deposit smeared or scraped after deposit
i3	Deposit appears to have fallen off
i4	Foreign object(s) on deposit
i5	Non-white filter punch after carbon analysis
i8	Deposit on back of filter
n0	1:10 dilution of sample extract during analysis

provided as Appendix H. As a whole, the resuspended soil profiles presented no unusual characteristics. Table 4.4-3 provides the composite mnemonics and the individual sample mnemonics for resuspended samples. The soil sample designated OMNI Soil #2 was not resuspended, as not enough material ($<38\mu$) was collected during sieving to make resuspension feasible on any of the three replicates. Even though a profile was not developed for this soil type, the evident lack of fine material indicates that this material will not have a significant impact on PM_{10}, $PM_{2.5}$, or PM_1 air quality.

In general, 45 to 60% of the mass was explained by the species measured. The remainder of the unexplained material is oxygen as mineral oxides. The percent masses explained on these samples are comparable to other studies.

The non-resuspended source profiles required more custom analysis and data interpretation primarily for two reasons: (1) the more complex the physio-chemical processes which generate the particles and (2) the more complex and frequently custom sampling procedures needed for the collection of sample material. The source profiles which were obtained were state-of-the-art in all cases. Table 4.4-4 provides the composite mnemonics and the individual mnemonics for the non-resuspended source samples. A number of procedures have been used to evaluate the source profile data for non-resuspended samples and are discussed here.

The woodstove profiles were all generally reasonable. Interestingly, the sample from the fireplace burning Mammoth Lakes fuel had large particles of soot or condensed carbon matter on the filters. These particles make analysis more difficult in two ways: they tend to fall off as the filters are handled, making accurate weights more difficult; and they essentially create an inhomogeneous deposit, making scaling of analytical result to the entire filter less certain. On all the woodstove samples, the soluble potassium was 5 to 30% higher than the total potassium as measured by XRF. No apparent analytical or sampling explanation for this phenomenon could be found and it has been seen in other smaller work (Pritchett, 1989). In most cases the quartz filter data was normalized to the XRF total potassium to correct the discrepancy. These normalized profiles typically explain 70 to 80% of the mass, in good agreement with profiles obtained in other studies. The remaining 20 to 30% of the mass is likely due to unmeasured hydrogen and oxygen associated with organic compounds.

The Mammoth Lakes diesel bus samples were somewhat inconsistent across the different size fractions and in terms of percent explained mass. These variations might be partly explained by the difficulty of getting all eight inlets of two PISD samplers into the directed plumes uniformly during sampling. Quartz species were ratioed to explain the mass remaining after the XRF species were summed. In reality, we would not expect to explain 100% of the mass due to unmeasured hydrogen and oxygen; however, the propagated uncertainties on

Table 4.4-3
Composite and Individual Sample Set Mnemonics, Resuspended Samples

Composite Mnemonic	Individual Sample Set Menmonic	Sample Description
SOIL01	S0125	OMNI Soil #1, replicate #1, Stockton agricultural soil, "peat"
	S0126	OMNI Soil #1, replicate #2, Stockton agricultural soil, "peat"
	S0127	OMNI Soil #1, replicate #3, Stockton agricultural soil, "peat"
SOIL02	S0128	OMNI Soil #2, replicate #1, Stockton agricultural soil, "mineral"
	S0129	OMNI Soil #2, replicate #2, Stockton agricultural soil, "mineral"
	S0130	OMNI Soil #2, replicate #3, Stockton agricultural soil, "mineral"
SOIL03	S0131	OMNI Soil #3, replicate #1, Fresno paved road
	S0132	OMNI Soil #3, replicate #2, Fresno paved road
	S0133	OMNI Soil #3, replicate #3, Fresno paved road
SOIL04	S0134	OMNI Soil #4, replicate #1, Visalia agricultural soil, cotton/walnut
	S0135	OMNI Soil #4, replicate #2, Visalia agricultural soil, cotton/walnut
	S0136	OMNI Soil #4, replicate #3, Visalia agricultural soil, cotton/walnut
SOIL05	S0137	OMNI Soil #5, replicate #1, Visalia agricultural soil, raisin
	S0138	OMNI Soil #5, replicate #2, Visalia agricultural soil, raisin
	S0139	OMNI Soil #5, replicate #3, Visalia agricultural soil, raisin
SOIL06	S0140	OMNI Soil #6, replicate #1, Visalia sand and gravel
	S0141	OMNI Soil #6, replicate #2, Visalia sand and gravel
	S0142	OMNI Soil #6, replicate #3, Visalia sand and gravel
SOIL07	S0143	OMNI Soil #7, replicate #1, Visalia urban unpaved
	S0144	OMNI Soil #7, replicate #2, Visalia urban unpaved
	S0145	OMNI Soil #7, replicate #3, Visalia urban unpaved
SOIL08	S0146	OMNI Soil #8, replicate #1, Visalia paved road
	S0147	OMNI Soil #8, replicate #2, Visalia paved road
	S0148	OMNI Soil #8, replicate #3, Visalia paved road
SOIL09	S0149	OMNI Soil #9, replicate #1, Bakersfield agricultural soil, alkaline
	S0150	OMNI Soil #9, replicate #2, Bakersfield agricultural soil, alkaline
	S0151	OMNI Soil #9, replicate #3, Bakersfield agricultural soil, alkaline
SOIL10	S0152	OMNI Soil #10, replicate #1, Bakersfield agricultural soil, sandy loam
	S0153	OMNI Soil #10, replicate #2, Bakersfield agricultural soil, sandy loam
	S0154	OMNI Soil #10, replicate #3, Bakersfield agricultural soil, sandy loam
SOIL11	S0155	OMNI Soil #11, replicate #1, Bakersfield unpaved road
	S0156	OMNI Soil #11, replicate #2, Bakersfield unpaved road
	S0157	OMNI Soil #11, replicate #3, Bakersfield unpaved road

(continues)

Table 4.4-3 (continued)

Composite Mnemonic	Individual Sample Set Menmonic	Sample Description
SOIL12	S0158	OMNI Soil #12, replicate #1, Bakersfield paved road
	S0159	OMNI Soil #12, replicate #2, Bakersfield paved road
	S0160	OMNI Soil #12, replicate #3, Bakersfield paved road
SOIL13	S0161	OMNI Soil #13, replicate #1, Bakersfield windblown urban unpaved
	S0162	OMNI Soil #13, replicate #2, Bakersfield windblown urban unpaved
	S0163	OMNI Soil #13, replicate #3, Bakersfield windblown urban unpaved
SOIL14	S0164	OMNI Soil #14, replicate #1, Bakersfield agricultural soil, Wasco sandy loam
	S0165	OMNI Soil #14, replicate #2, Bakersfield agricultural soil, Wasco sandy loam
	S0166	OMNI Soil #14, replicate #3, Bakersfield agricultural soil, Wasco sandy loam
SOIL15	S0167	OMNI Soil #15, replicate #1, Bakersfield agricultural soil, Cajon sandy loam
	S0168	OMNI Soil #15, replicate #2, Bakersfield agricultural soil, Cajon sandy loam
	S0169	OMNI Soil #15, replicate #3, Bakersfield agricultural soil, Cajon sandy loam
SOIL16	S0170	OMNI Soil #16, replicate #1, Bakersfield unpaved road
	S0171	OMNI Soil #16, replicate #2, Bakersfield unpaved road
	S0172	OMNI Soil #16, replicate #3, Bakersfield unpaved road
SOIL17	S0173	OMNI Soil #17, replicate #1, Taft unpaved road
	S0174	OMNI Soil #17, replicate #2, Taft unpaved road
	S0175	OMNI Soil #17, replicate #3, Taft unpaved road
SOIL18	S0176	OMNI Soil #18, replicate #1, Brawley urban unpaved
	S0177	OMNI Soil #18, replicate #2, Brawley urban unpaved
	S0178	OMNI Soil #18, replicate #3, Brawley urban unpaved
SOIL19	S0179	OMNI Soil #19, replicate #1, Brawley paved road
	S0180	OMNI Soil #19, replicate #2, Brawley paved road
	S0181	OMNI Soil #19, replicate #3, Brawley paved road
SOIL20	S0182	OMNI Soil #20, replicate #1, El Centro paved road
	S0183	OMNI Soil #20, replicate #2, El Centro paved road
	S0184	OMNI Soil #20, replicate #3, El Centro paved road
SOIL21	S0185	OMNI Soil #21, replicate #1, El Centro agricultural soil
	S0186	OMNI Soil #21, replicate #2, El Centro agricultural soil
	S0187	OMNI Soil #21, replicate #3, El Centro agricultural soil
SOIL22	S0188	OMNI Soil #22, replicate #1, Trona desert soil
	S0189	OMNI Soil #22, replicate #2, Trona desert soil
	S0190	OMNI Soil #22, replicate #3, Trona desert soil

(continues)

Table 4.4-3 (continued)

Composite Mnemonic	Individual Sample Set Menmonic	Sample Description
SOIL23	S0191	OMNI Soil #23, replicate #1, Owens Lake desert soil
	S0192	OMNI Soil #23, replicate #2, Owens Lake desert soil
	S0193	OMNI Soil #23, replicate #3, Owens Lake desert soil
SOIL24	S0194	OMNI Soil #24, replicate #1, Owens Lake desert soil
	S0195	OMNI Soil #24, replicate #2, Owens Lake desert soil
	S0196	OMNI Soil #24, replicate #3, Owens Lake desert soil
SOIL25	S0197	OMNI Soil #25, replicate #1, Owens Valley desert soil composite
	S0198	OMNI Soil #25, replicate #2, Owens Valley desert soil composite
	S0199	OMNI Soil #25, replicate #3, Owens Valley desert soil composite
SOIL26	S0200	OMNI Soil #26, replicate #1, Mammoth Lakes cinder
	S0201	OMNI Soil #26, replicate #2, Mammoth Lakes cinder
	S0202	OMNI Soil #26, replicate #3, Mammoth Lakes cinder
SOIL27	S0203	OMNI Soil #27, replicate #1, Mammoth Lakes paved road
	S0204	OMNI Soil #27, replicate #2, Mammoth Lakes paved road
	S0205	OMNI Soil #27, replicate #3, Mammoth Lakes paved road

Table 4.4-4
Composite and Individual Sample Set Mnemonics, Non-Resuspended Source Samples

Composite Mnemonic	Individual Sample Set Menmonic	Sample Description
WHDIEC	WhDie1	Wheeler weigh station diesel truck emissions, run 1
	WhDie2	Wheeler weigh station diesel truck emissions, run 2
	WhDie3	Wheeler weigh station diesel truck emissions, run 3
	WhDie4	Wheeler weigh station diesel truck emissions, run 4
	WhDie5	Wheeler weigh station diesel truck emissions, run 5
	WhDie6	Wheeler weigh station diesel truck emissions, run 6
	WhBkg1	Wheeler weigh station background, for runs 1-3
	WhBkg2	Wheeler weigh station background, for runs 4-6
SFCRUC	SFCru1	Santa Fe Energy crude oil boiler emissions, run 1
	SFCru2	Santa Fe Energy crude oil boiler emissions, run 2
	SFCru3	Santa Fe Energy crude oil boiler emissions, run 3
	SFCru4	Santa Fe Energy crude oil boiler emissions, run 4
CHCRUC	CHCru1	Chevron crude oil boiler emission, run 1
	CHCru2	Chevron crude oil boiler emission, run 2
	CHCru3	Chevron crude oil boiler emission, run 3
BAAGBC	BaAgB1	Bakersfield ag burn, wheat and barley, run 1
	BaAgB2	Bakersfield ag burn, wheat and barley, run 2
	BaAgB3	Bakersfield ag burn, wheat and barley, run 3
ELAGBC	ElAgB1	El Centro ag burn, wheat stubble, run 1
	ElAgB2	El Centro ag burn, wheat stubble, run 2
	ElAgB3	El Centro ag burn, wheat stubble, run 3
STAGBC	StAgB1	Stockton ag burn, wheat stubble, run 1
	StAgB2	Stockton ag burn, wheat stubble, run 2
	StAgB3	Stockton ag burn, wheat stubble, run 3
VIAGBC	ViAgB1	Visalia ag burn, wheat stubble, run 1
	ViAgB2	Visalia ag burn, wheat stubble, run 2
	ViAgB3	Visalia ag burn, wheat stubble, run 3
	ViAgB4	Visalia ag burn, wheat stubble, run 4
VIDAIC	ViDai1	Visalia dairy, run 1
	ViDai2	Visalia dairy, run 2
	ViDai3	Visalia dairy, run 3
FRCONC	FrCon1	Fresno construction dust, run 1
	FrCon2	Fresno construction dust, run 2
	FrCon3	Fresno construction dust, run 3

(continues)

Table 4.4-4 (continued)

Composite Mnemonic	Individual Sample Set Menmonic	Sample Description
MADIEC	MaDie1	Mammoth Lakes bus diesel emissions, run 1
	MaDie2	Mammoth Lakes bus diesel emissions, run 2
	MaDie3	Mammoth Lakes bus diesel emissions, run 3
BAMAJC	OmMa1A	OMNI woodstove test, Majestic fireplace, Bakersfield, run 1
	OmMa1A	OMNI background for Majestic fireplace test, Bakersfield, run 1
	OmMa2	OMNI woodstove test, Majestic fireplace, Bakersfield, run 2
	OmMa2A	OMNI background for Majestic fireplace test, Bakersfield, run 2
	OmMa3	OMNI woodstove test, Majestic fireplace, Bakersfield, run 3
	OmMa3A	OMNI background for Majestic fireplace test, Bakersfield, run 3
MAMAJC	OmMa4	OMNI woodstove test, Majestic fireplace, Mammoth Lakes, run 1
	OmMa4A	OMNI background for Majestic fireplace test, Mammoth Lakes, run 1
	OmMa5	OMNI woodstove test, Majestic fireplace, Mammoth Lakes, run 2
	OmMa5A	OMNI background for Majestic fireplace test, Mammoth Lakes, run 2
	OmMa6	OMNI woodstove test, Majestic fireplace, Mammoth Lakes, run 3
	OmMa6A	OMNI background for Majestic fireplace test, Mammoth Lakes, run 3
MAFISC	OmF71	OMNI woodstove test, Fisher Mama Bear, Mammoth Lakes, run 1, set 1
	OmF72	OMNI woodstove test, Fisher Mama Bear, Mammoth Lakes, run 1, set 2
	OmF71A	OMNI background for Fisher Mama Bear, Mammoth Lakes, run 1, sets 1 and 2
	OmF81	OMNI woodstove test, Fisher Mama Bear, Mammoth Lakes, run 2
	OmF81A	OMNI background for Fisher Mama Bear test, Mammoth Lakes, run 2
	OmF91	OMNI woodstove test, Fisher Mama Bear, Mammoth Lakes, run 3
	OmF91A	OMNI background for Fisher Mama Bear test, Mammoth Lakes, run 3

the composites for this source are on the order of 20% and the profiles are certainly acceptable within that range.

The deposit on the 30μ fraction of the Fresno construction dust samples did not stick well to the Teflon filters, causing mass determination and XRF analysis to be more difficult than usual. In addition, the amount of material on the fine fraction filters, as would be expected from a predominantly physically-generated particle source, were quite low. The resulting detection limits and propagated uncertainties are somewhat higher for this sample because of these considerations.

The Wheeler diesel truck emissions and agricultural burn samples generally exhibited few anomalies.

Both the Santa Fe Energy and the Chevron samples exhibited a number of unusual features. Quartz filter punches from both sources were dark orange after carbon analysis, indicating that some non-volatile material was being chemically transformed by the high temperatures of the carbon analyzers. Normally this residual color is only seen on samples containing large amounts of crustal material, such as the resuspended soil samples. Nearly all of the filters contained small droplets on the deposits even after conditioning in a low humidity environment, apparently due to the hydroscopic nature of the source particles. These small droplets may have some attenuating effect on the low energy XRF results, particularly for sulfur; some evidence of this possible attenuation may be seen in the inter-condition comparisons of condition 4 and 5 XRF results for sulfur, potassium and calcium. The samples from the Chevron facility drifted in gross mass by nearly 10% over time, despite being equilibrated in a temperature- and humidity-controlled room. These samples were placed in sealed Mylar bags before XRF analysis to prevent possible damage to the detector window and analyzed under a helium atmosphere. The Santa Fe Energy samples were analyzed in the normal fashion.

Some variability was noted in the SO_4^{2-} results across the size fractions for the Chevron samples. Because the SO_4^{2-} analysis is performed on a water extract of the quartz filters and because the Chevron samples were obviously oily, the variable results may be due to incomplete penetration of the water into the filters. Three outlier SO_4^{2-} results are presumed to be due to this problem and were removed from the data base.

The percent mass explained for the Santa Fe Energy samples ranged from 8 to 10 percent. These low explained masses are due to: (1) the SO_4^{2-} results are not included in the percent sums to avoid duplication of the XRF sulfur results; this normally does not cause a significant difference except in those samples where the SO_4^{2-} levels are high; (2) reweights of several Teflon filters after XRF analysis revealed a consistent 56% to 57% drop in deposit mass; this is apparently due to tightly bound water which was not released except under the extreme conditions of the XRF vacuum; and (3) unmeasured oxygen and hydrogen (viz, water of hydration, and oxygen and hydrogen in organic compounds) chemical species are not included in the sums.

The percent mass explained for the Chevron samples ranged from 24 to 26%. The same considerations described for the Santa Fe samples should be taken into account.

It should be further noted that the normalization to mass and potassium applied to a very few samples mentioned above is not resulting in artificial source profiles. The use of inter-method measurements of potassium and sulfur allows credible relationships between Teflon and quartz results to be made. In all cases, an uncertainty is calculated for the normalizing ratio and is propagated in the normal fashion; the final source profiles include the uncertainties of these ratios, and as long as the certainties in the source profiles are recognized, the results are valid. It should be further noted that the few inconsistencies in the individual profiles are neither unexpected nor unusual and represent a very small fraction of the overall data set which is comprised of 593 filters, each analyzed for 43 chemical species and mass.

4.5 Data Base Format

Source profile data have been prepared on IBM-compatible $5^1/_4$ inch floppy disks in the following formats:

(1) dBase III data base file. The structure of this file is summarized in Table 4.4-1. This data base file is compatible with the U.S. EPA source composition library (Core et al., 1984). A recent revision of the U.S. EPA source composition library has been proposed (Shareef and Bravo, 1988).

(2) ASCII data file. This is compatible with the EPA Chemical Element Balance Receptor Model program, version 7.0 (Watson, 1989) and ARB's PCA and CMB Level I PM_{10} Assessment package (Freeman et al., 1987; Watson et al., 1987). This file is ready for direct input into these programs and uses the same species codes as depicted in Table 4.4-1.

(3) Data file for ARB RAMIS emission inventory system. This ASCII data file contains sources and chemical species listed vertically, with $<1.0\mu$, $>1.0\mu$ but $<2.5\mu$, $<2.5\mu$, $>2.5\mu$ but $<10\mu$, $<10\mu$, $>10\mu$ but $<30\mu$ (or simply $<10\mu$), and $<30\mu$ (or TSP) measurements listed horizontally.

5.0 Results and Discussions

5.1 Overview

The chemical compositions of particulate material from all sources in the seven size categories are provided in Appendix A. A summary of these source profiles, tabulated to permit comparisons of given chemical species among sources, is included as Appendix G. The data have also been provided on floppy disks (Section 4.5). The mass distribution with size for each source is given in Tables 3.5-2 and 3.5-3. The results of the interlaboratory carbon comparison study are presented in Section 3.11.

A discussion of each of the source types is provided in this section. The major and minor measured chemical constituents for each source type are given. Notable chemical species which were not measured, and hence not discussed, include total sodium (versus water-soluble sodium which was measured), magnesium, oxygen, hydrogen, and nitrogen. Oxygen and hydrogen are associated with waters of hydration; oxygen, hydrogen, and nitrogen are associated with organic compounds; and oxygen can be in the form of oxides. It should also be noted that while the individual concentration of a given element is important in defining a source profile, the overall pattern or "fingerprint," as illustrated by the histograms included in this section, is in essence what distinguishes a given source profile.

The primary intent of this study was the compilation of source profiles and it was not intended to be interpretative in nature. To this end, the discussions on each source profile are brief and designed to familiarize the receptor or dispersion modeler with key factors characteristic of each source type.

5.2 Size Distribution

The percentages of mass in each size range for each source are tabulated in Tables 3.5-2 and 3.5-3. Particles generated from physical processes tend to be larger in size and those generated from combustion sources tend to be smaller in size. The trend was evident in the data generated from this study. Figure 5.2-1 illustrates the mean size distribution for particles from the soil, road, and miscellaneous bulk material dusts, from the four agricultural burning composites, and from three residential wood combustion (RWC) composites. As can be seen from the figure, the various dust particles are predominantly larger than 2.5μ, whereas the particles from RWC are predominantly smaller than 1μ. The particle distributions from the agricultural burns are most like the RWC distribution but fall between the distributions for dust and RWC. This was expected, due to the highly turbulent conditions during field burning that can resuspend soil and other debris.

It is well known that vehicular emissions and most industrial combustion emissions are in the respirable size fraction ($< 2.5\mu$). The data generated in this study for diesel truck emissions and crude oil combustion illustrate both this fact and the fact that the majority of the particulate mass is in particles less than 1μ (Figure 5.2-2). Like the diesel truck emissions, the Mammoth Lakes ski tour bus emissions are also predominantly in the $< 1\mu$ size fraction (Table 3.5-3).

While sampling at a highway construction site in Fresno, it was observed that the emissions impacting the sampler were a combination of soil dust and diesel exhaust from heavy equipment. Analysis of the mass distribution data reveals that the soil dust dominated the sample mass (Figure 5.2-2). Similarly, dairy and feedlot emissions were speculated as being a combination of primary dust particulate and secondary organic and nitrogen-containing particles. Analysis of the mass distribution of data clearly illustrates that primary dust particles make up the majority of the particulate sample mass. (Secondary particles are generally less than 2.5μ.)

No size distribution data are available for one soil composite (SOIL02). This was an agricultural soil composite collected in the Stockton area (see Table 2.7-2 for description). The material was composed of such coarse material that insufficient sample passed through the 38μ sieve for analysis during the pre-resuspension sieving process. While no analyses were conducted on this material, it can be concluded that it does not represent a significant PM_{10}, $PM_{2.5}$, or PM_1 source.

For each source, the data for size categories corresponding to directly sampled material (i.e., $< 1\mu$, $< 2.5\mu$, $< 10\mu$, and $< 30\mu$ [TSP]) have a high degree of accuracy, precision, and state-of-the-art detection limits. The data for size categories determined by subtraction (i.e., 1μ - 2.5μ, 2.5μ - 10μ, and 10μ - 30μ [or $> 10\mu$]) are inherently poorer due to the propagation of error associated with the subtraction of one data set from another. More significant, however, for these "subtraction categories" is the difficulty associated with subtracting values of nearly equivalent magnitude from one another. Frequently the $< 1\mu$ and $< 2.5\mu$ or the 2.5μ and $< 10\mu$ are nearly equivalent for combustion sources (Figures 5.2-1 and 5.2-2). When, for example, the 1μ - 2.5μ size category is calculated from the subtraction of the $< 1\mu$ data set from the $< 2.5\mu$ data set, and the $< 1\mu$ and $< 2.5\mu$ particulate mass for a given source are nearly equivalent, the calculated values for the 1μ - 2.5μ size category have very high uncertainties associated with them, and in same cases even have negative values. The physical basis for this problem is, of course, that most of the particles in this example would be less than 1μ and very few particles would fall into the 1μ to 2.5μ size range. It should again be emphasized that there should be no difficulties in using the directly measured source profiles in any modeling effort; however, if the "subtraction" size categories are to be used, the size distribution data for a given source should first be reviewed.

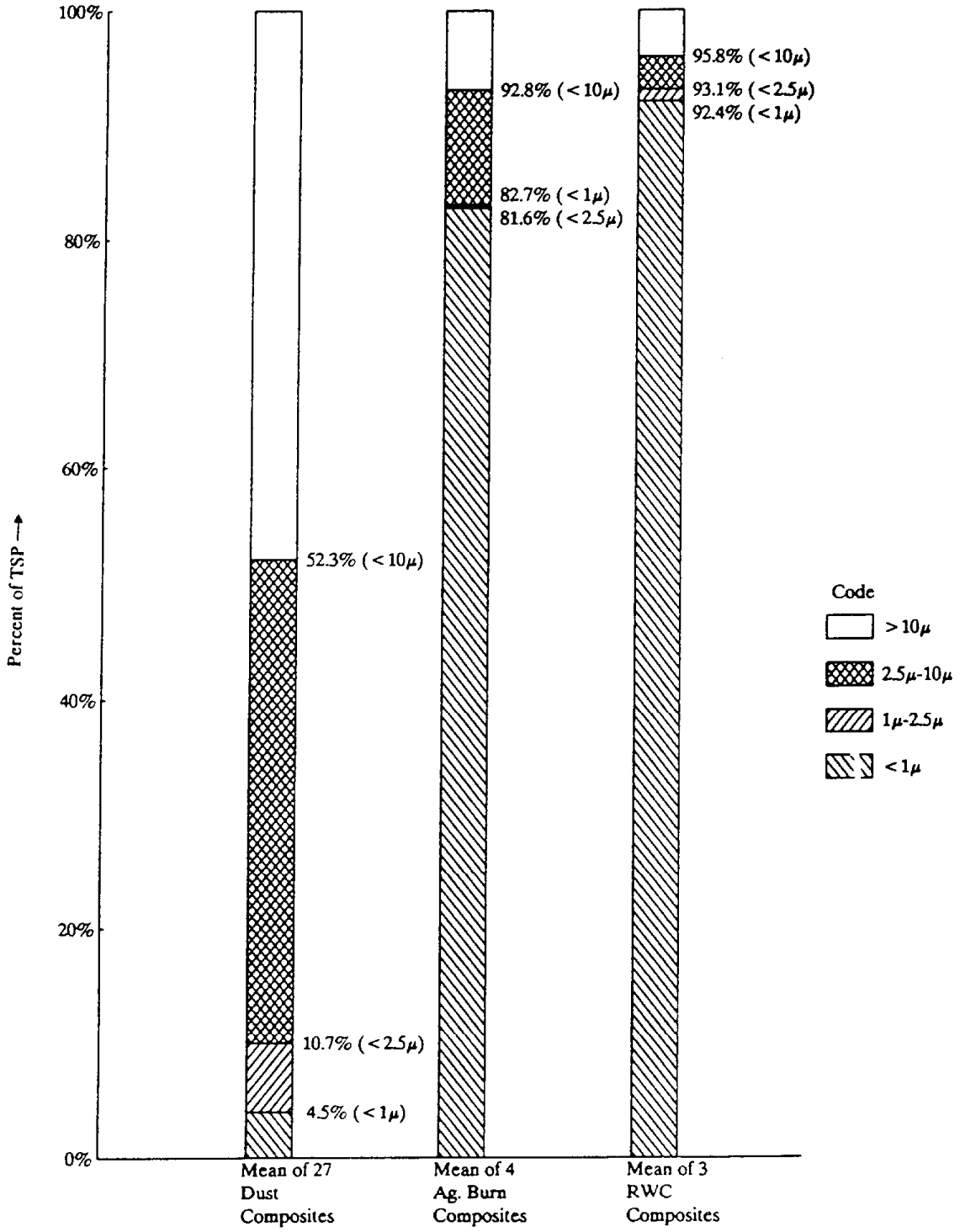

Figure 5.2-1. Size distribution comparison of particles from dust, agricultural burning, and residential wood combustion. (The mean percentage of the $<1\mu$ particles for the 4 agricultural burning composites is slightly higher than the mean percentage of the $<2.5\mu$ particles. The uncertainties around the means overlap. These data demonstrate that there is very little particulate mass in the 1μ to 2.5μ range for that source category.)

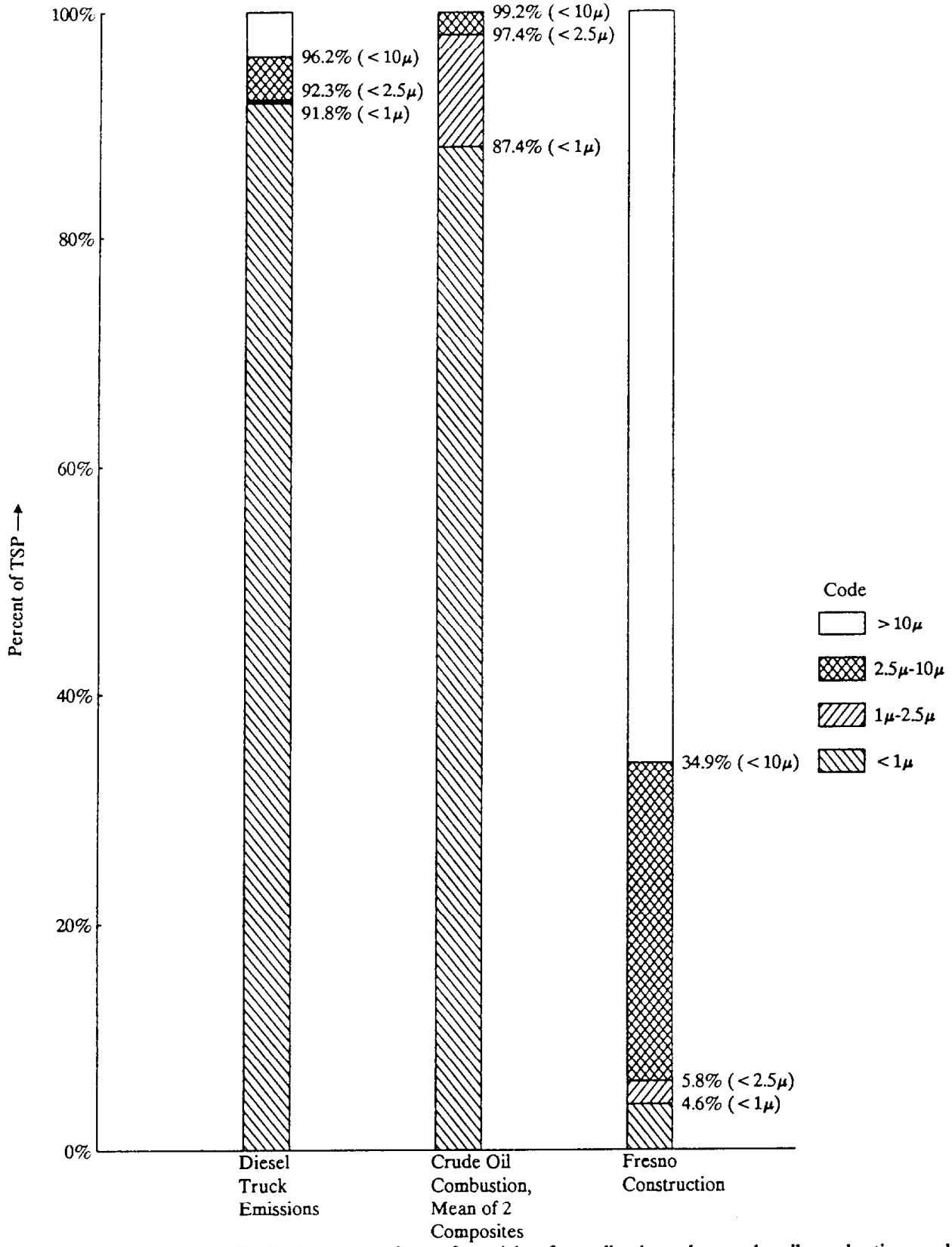

Figure 5.2-2. Size distribution comparison of particles from diesel trucks, crude oil combustion, and construction activities.

5.3 Agricultural Soil and Unpaved Road Dust

The major (>1%) measured chemical species common to all agricultural soil and unpaved road dust samples are aluminum, silicon, total potassium (K_X in printouts and histograms), calcium, iron, and organic carbon. The principal minor (>0.1%) chemical species are water-soluble sodium (Na^+, simply listed as Na on printouts and histograms), phosphorus, sulfur, sulfate, chlorine, water-soluble potassium (K^+, listed as $K_{\_a}$ on printouts and histograms), titanium, nitrate, elemental carbon, and carbonate carbon (listed as either CO_3 or CC on printouts and histograms). The organic carbon and most of the minor elements are quite variable from composite to composite, apparently dependent on soil alkalinity, soil amendments, vehicular impact, and the geological source of the soil. In a portion of the soil samples, some of the chemical species listed as minor chemical species reach the percent level and in others some fall below the tenth-of-a-percent level. Figure 5.3-1 illustrates logarithmic histograms for $<10\mu$ chemical source profiles for an agricultural soil composite collected near Bakersfield and for an agricultural soil composite collected near El Centro.

5.4 Sand and Cinder Storage Dust

The major measured chemical species in the sand and cinder storage dust are aluminum, silicon, total potassium, calcium, and iron. The key minor chemical species are water-soluble sodium, phosphorus, sulfur, chlorine, water-soluble potassium, titanium, strontium, barium, organic carbon, and carbonate carbon. The concentration of the minor elements varies between the two composite types. Figure 5.4-1 illustrates logarithmic histograms for $<10\mu$ chemical source profiles for a sand storage area composite collected near Visalia and for a road cinder storage area composite collected near Mammoth Lakes.

5.5 Alkaline Desert Soil and Playa Sediment Dusts

The major measured chemical species in the alkaline desert soil and playa sediment dusts are water-soluble potassium, aluminum, silicon, total potassium, calcium, iron, sulfur, sulfate, chlorine, carbonate carbon, and organic carbon. Minor chemical species are water-soluble potassium, titanium, nitrate, and strontium. Trace levels of arsenic and selenium are detectable in some of the samples. Figure 5.5-1 illustrates logarithmic histograms for $<10\mu$ chemical source profiles for alkaline desert soil and playa sediment composites collected from the Searles Lake area and from the Owens Lake area. It should be noted that one alkaline playa sample from composite SOIL24 (Owens Lake sediments) was included in the interlaboratory carbon comparison study. The carbonate carbon value reported by Sunset Laboratory was 2.8 times higher than the value reported by DRI.

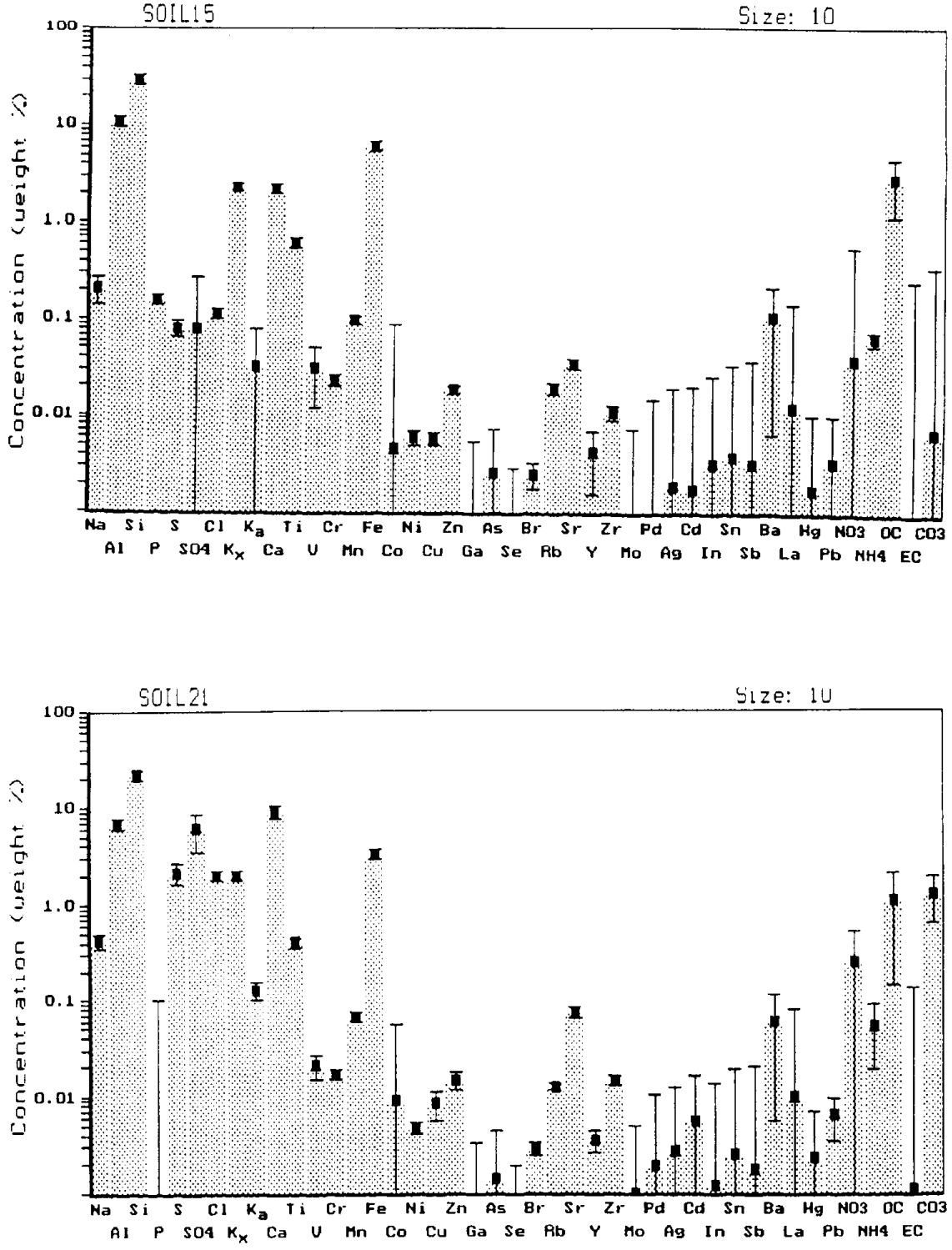

Figure 5.3-1. Chemical source profiles, $< 10\mu$ particles, agricultural soils. Top figure, composite collected near Bakersfield; bottom figure, composite collected near El Centro. Logarithmic scale; uncertainty bars shown.

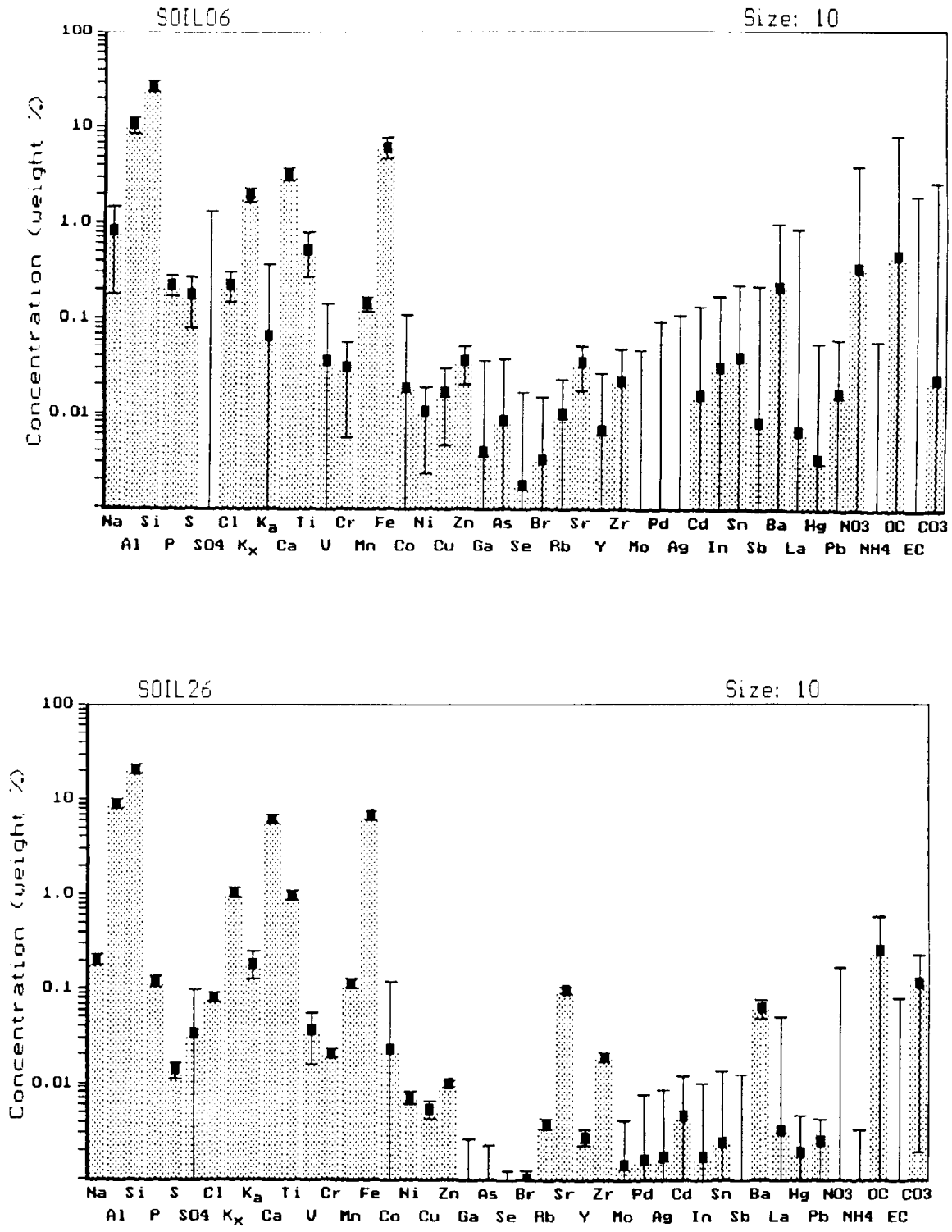

Figure 5.4-1. Chemical source profiles, $< 10\mu$ particles, sand and cinder storage dust. Top figure, sand composite collected in Visalia; bottom figure, cinder composite collected near Mammoth Lakes. Logarithmic scale, uncertainty bars shown.

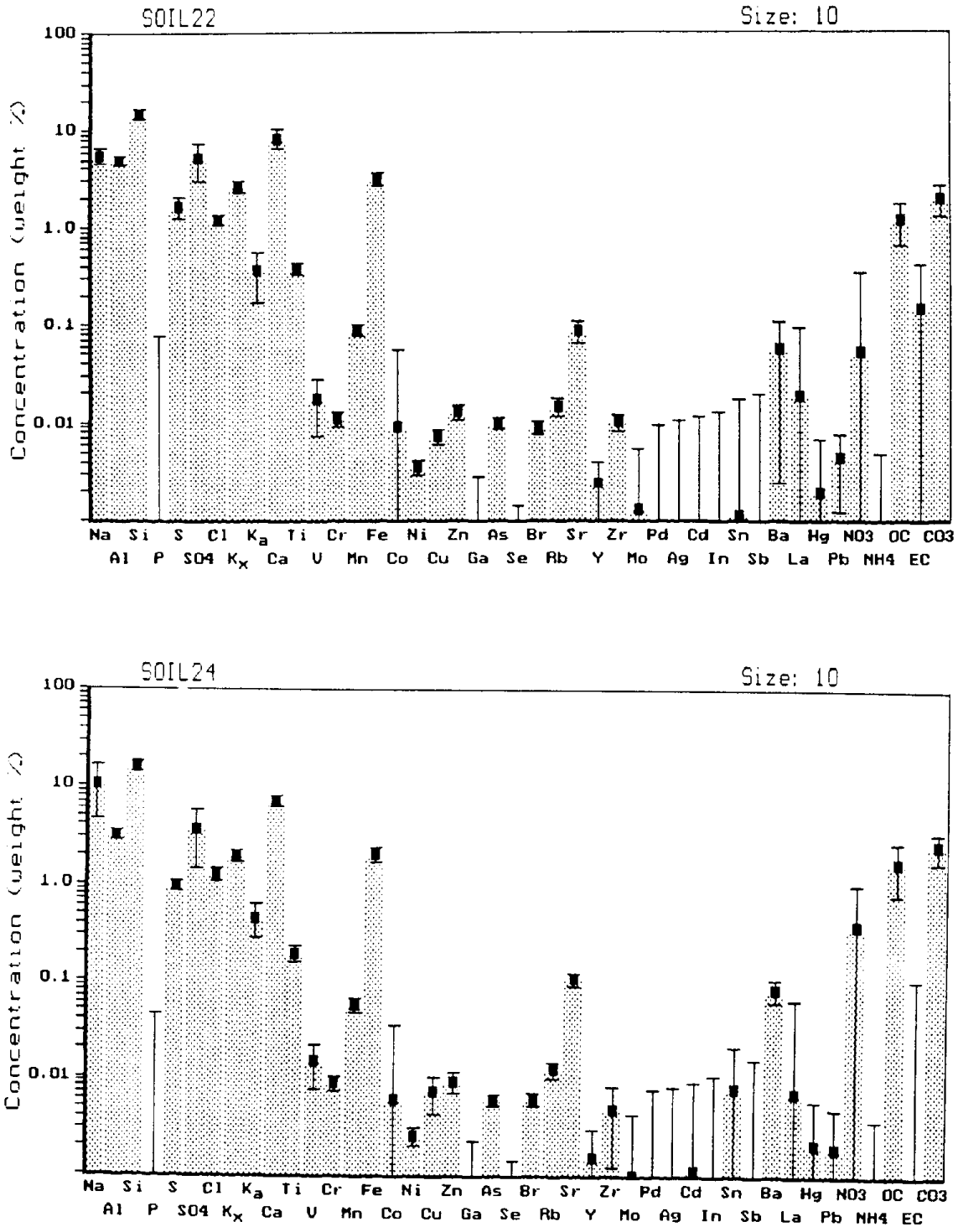

Figure 5.5-1. Chemical source profiles, $< 10\mu$ particles, alkaline desert soil and playa sediment dust composites. Top figure, composite collected from Searles Lake area. Bottom figure, composite collected from Owens Lake area. Logarithmic scale, uncertainty bars are shown.

5.6 Unpaved Urban Areas and Paved Road Dust

The major measured chemical species in unpaved urban areas and paved road dusts are aluminum, silicon, total potassium, calcium, iron, organic carbon, and elemental carbon. The minor chemical species are water-soluble sodium, phosphorous, sulfur, sulfate, chlorine, water-soluble potassium, titanium, nitrite, and lead. The most notable features about unpaved urban area and paved road dust profiles as compared to soil dust profiles are the elevated organic carbon, elemental carbon, lead, and, in some cases, zinc content. The degree of elevation is, of course, dependent on the level of vehicular impact and is generally seen in the finer size fractions. Table 5.6-1 provides a size distribution and concentration comparisons of anthropogenic chemical species in paved road and agricultural soil dusts. Figure 5.6-1 illustrates the logarithmic histograms for $< 10\mu$ chemical source profiles for unpaved urban areas (parking lots and alleys), dust composites in Bakersfield, and a paved road (city street) composite in Fresno.

5.7 Diesel Emissions

The major measured chemical species in diesel emissions are organic carbon, elemental carbon, sulfur, and sulfate. In addition, silicon at the tenth-of-a-percent level and ammonium at the percent level were measured in the Wheeler Ridge diesel truck exhaust samples. Figure 5.7-1 illustrates the logarithmic histograms for $< 1\mu$ chemical source profile for the diesel truck composite collected at the Wheeler Ridge Weigh Station and the ski tour bus diesel composite collected in Mammoth Lakes. The $< 1\mu$ profiles were selected for illustration since nearly all diesel emission particles are in that size range (Figure 5.2-2).

5.8 Crude Oil Emissions

The key factors of the crude oil combustion emissions at both the Chevron (Kern River Oilfield) and Santa Fe (Westside Kern County Oilfield) units are the relatively high sulfur, sulfate, nickel, and vanadium concentrations. Other minor chemical species significant to one or both of the sources are water-soluble sodium, iron, zinc, organic carbon, and elemental carbon. Figure 5.8-1 illustrates the logarithmic histograms for $< 1\mu$ chemical source profiles for the Chevron crude oil combustion boiler located in the Kern River Oilfield and the Santa Fe Energy crude oil combustion boiler located in the Westside Kern County Oilfield.

5.9 Agricultural Burning

The major measured chemical species common to all four field-burning composites (Stockton, Bakersfield, Visalia, and El Centro areas) are water-soluble sodium, sulfate, chlorine, total potassium, water-soluble potassium, ammonium, organic carbon, and elemental carbon. Minor chemical species include sulfur,

Table 5.6-1
Size Distribution and Concentration Comparisons of
Anthropogenic Chemical Species in Paved Road and Agricultural Soil Dusts[a]

Size (μ)	Organic Carbon (wt %)		Elemental Carbon (wt %)		Lead (wt %)		Zinc (wt %)	
	Urban Street	Agri. Soil	Urban Street	Agri. Soil	Urban Street	Agri. Soil	Urban Street	Agri. Soil
< 1	31±4	12±1	7.1±0.9	< 0.1	0.41±0.04	0.01	0.27±0.02	0.032±0.003
< 2.5	25±3	6.0±0.8	3.9±0.5	< 0.05	0.38±0.03	0.011±0.002	0.27±0.02	0.033±0.003
< 10	22±3	4.6±0.6	3.9±0.5	< 0.04	0.26±0.02	< 0.01	0.18±0.02	0.026±0.002
< 30 (TSP)	8±1	3.6±0.5	1.3±0.2	< 0.03	0.21±0.02	< 0.01	0.14±0.02	0.020±0.002

a. Urban Street = Olive Street near ARB monitoring site in Fresno, California (SOIL03).
Agri. Soil = Composite agricultural soil sample collected in cotton fields and walnut orchards 5 to 10 km northwest of Visalia ARB monitoring site (SOIL04).

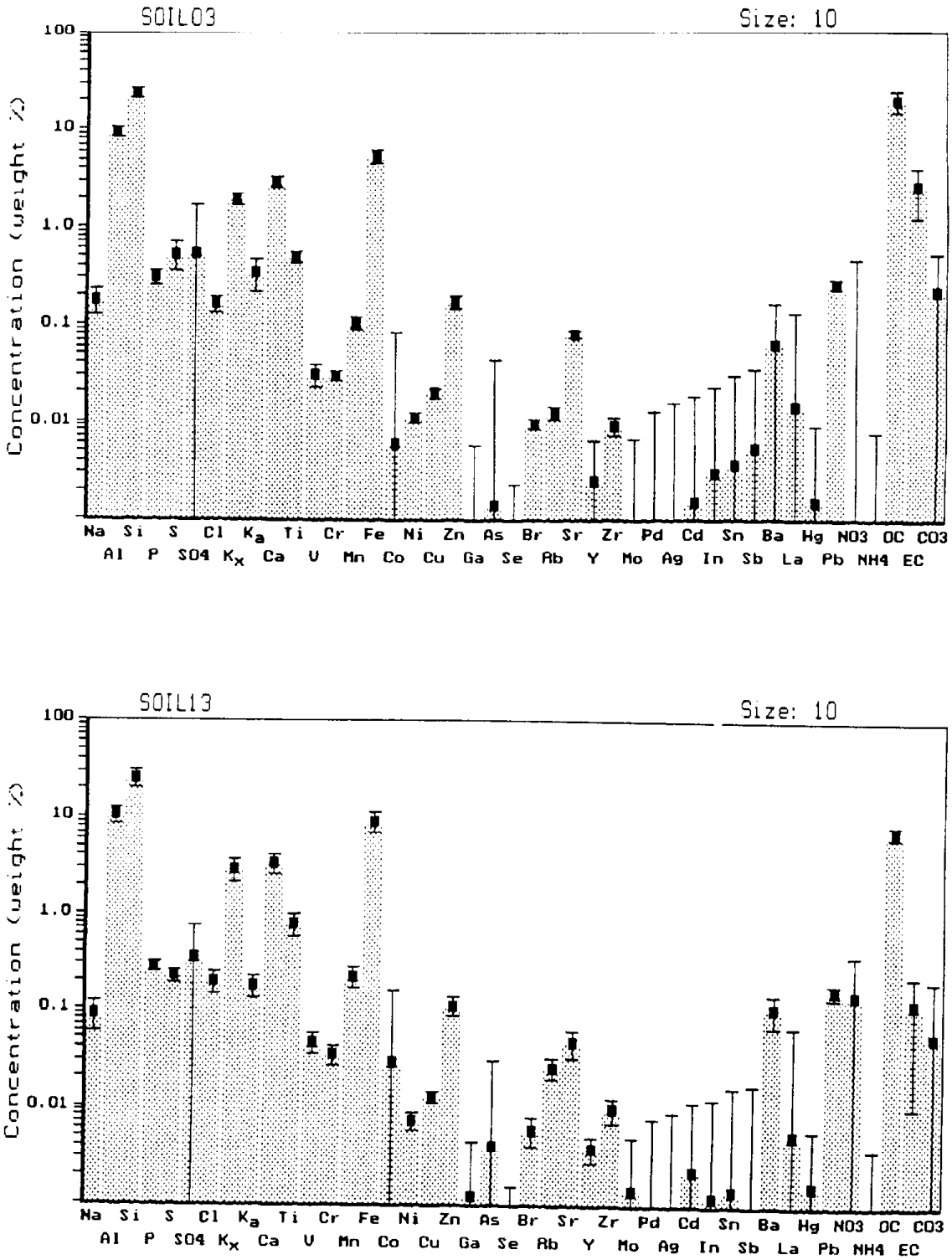

Figure 5.6-1. Chemical source profile, $< 10\mu$ particles, unpaved urban areas and paved road dust. Top figure, composite, road dust collected in Fresno. Bottom figure, composite, unpaved urban areas collected in Bakersfield. Logarithmic scale, uncertainty bars shown.

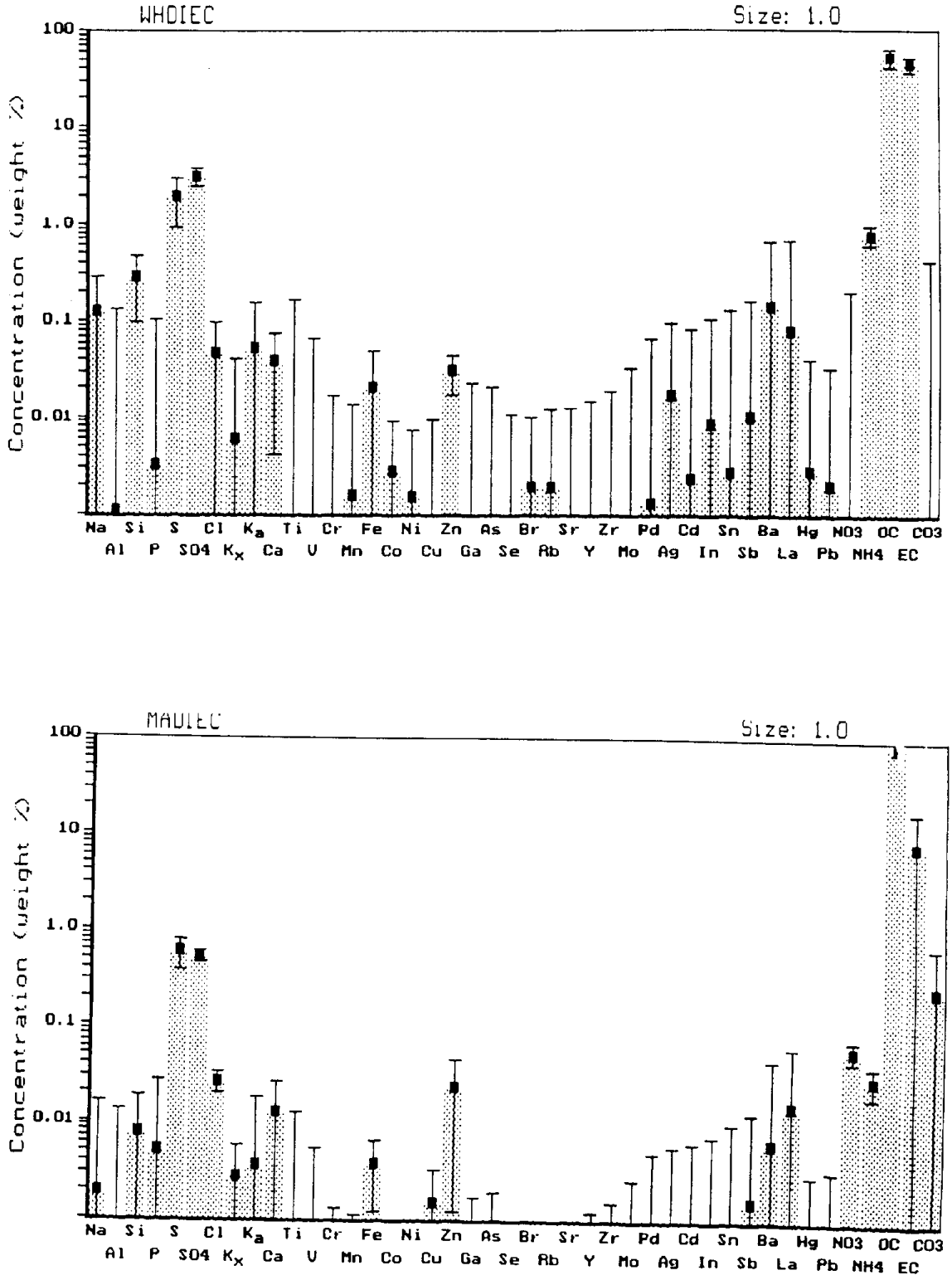

Figure 5.7-1. Chemical source profiles, $< 1\mu$, diesel emissions. Top figure diesel truck emissions, collected at Wheeler Ridge Weigh Station. Bottom figure, ski tour bus emissions, collected at Mammoth Lakes. Logarithmic scale, uncertainty bars are shown.

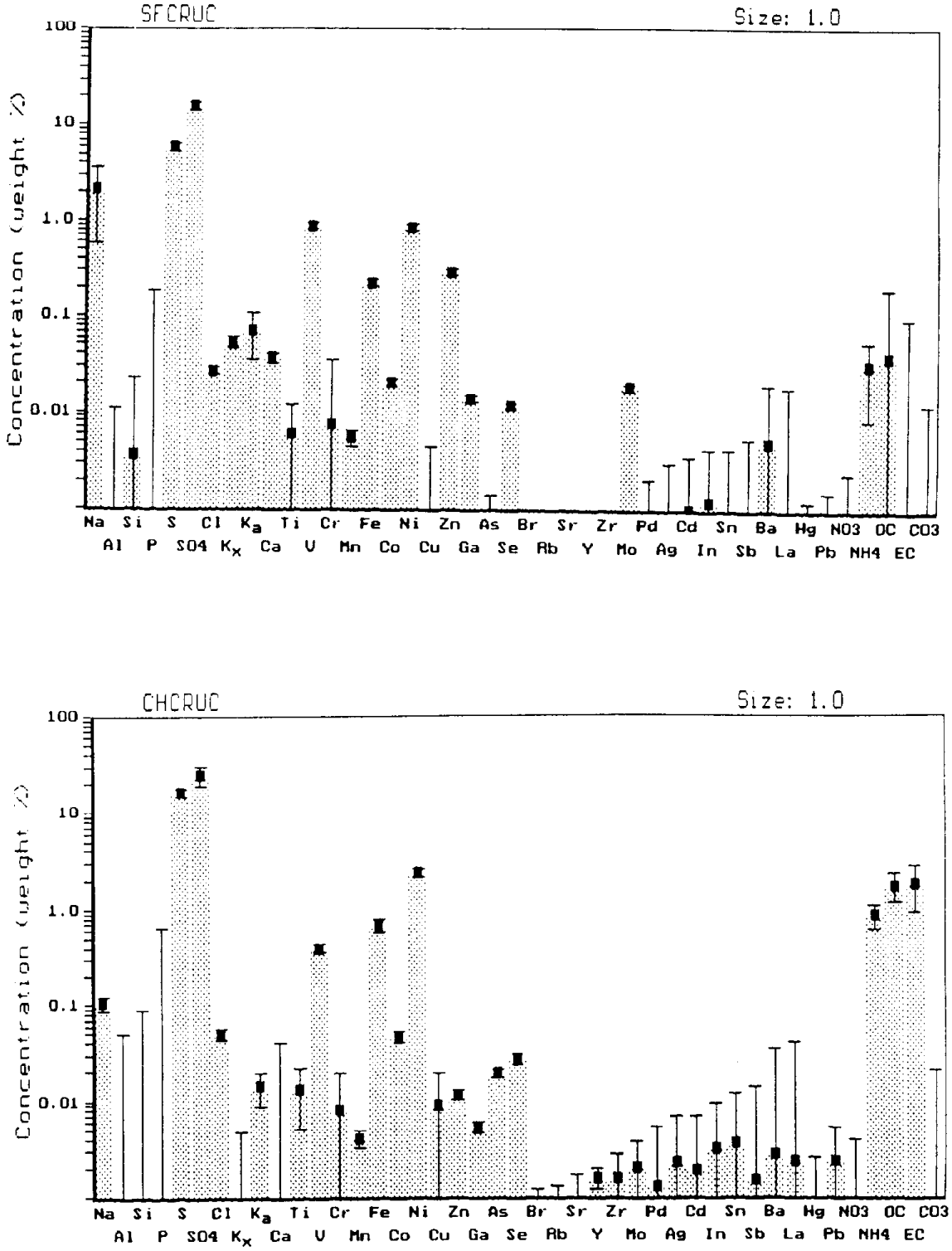

Figure 5.8-1. Chemical source profile, $<1\mu$, crude oil combustion. Top figure, Santa Fe Energy unit in West County Oilfield. Bottom figure, Chevron unit in Kern River Oilfield. Logarithmic scale, uncertainty bars are shown.

calcium, iron, and nitrate. The relatively high chlorine and potassium concentrations make the agricultural burn profiles unique among the sources. Most of the potassium appears to be in the water-soluble form. Figure 5.9-1 illustrates logarithmic histograms for $<10\mu$ chemical source profiles for composite agricultural burn samples collected near Visalia and El Centro. The $<10\mu$ size categories were selected for review, even though the majority of the particulate mass for this source category is in the $<1\mu$ size range, since approximately 10% of the total TSP mass does fall into the size range between 1μ and 10μ (Figure 5.2-1).

5.10 Dairy/Feedlot Emissions

One sample set of dairy emissions was collected at a dairy in the Visalia area. It was assumed that dairy and feedlot emissions would be similar in nature. The size distribution of the composite was very similar to the other dust sources (Tables 3.5-2 and 3.5-3), suggesting that most of the emissions are simply entrained dust. However, not surprisingly, the organic carbon, nitrate, and ammonium content were significantly increased in the emissions from the dairy as compared to typical agricultural soil collected within a few kilometers of the dairy. Other chemical species also appeared elevated (Na^+, Cl, P, and K^+). The higher content of organic compounds and other waste-derived chemical species in the emissions had the effect of depressing the concentration of the "geological" chemical species (Al, Si, Ti, Mn, Fe, and non-water-soluble K) in the dairy emissions in contrast to the non-impacted nearby agricultural soil. Table 5.10-1 compares the organic carbon content and the geological chemical species concentrations in the $<10\mu$ size fraction of dairy emissions and agricultural soil data. While the majority of the dairy emissions are in the coarser size fractions (2.5μ–10μ and $>10\mu$)(Table 3.5-3), measurable mass was also collected on the $<1\mu$ and $<2.5\mu$ filters. The percent composition of organic carbon, nitrate, and ammonium in the finer size ranges is higher than in the coarser size ranges (Table 5.10-2). This finding is consistent with secondary organic and nitrogen-containing compounds originating from dairies and feedlots.

5.11 Construction Emissions

A sample set of highway construction emissions was collected in Fresno. It was observed that both dust and emissions from heavy equipment exhaust impeded the samplers. The size distribution of the construction composites was essentially the same as would be expected from a dust source alone (Figure 5.2-2). The major chemical species in the $<10\mu$ size fraction were also the same as those characteristic of soil dusts (i.e., Al, Si, K, Ca, Fe, and OC). Ammonium and nitrate, however, were higher than that which is seen with typical soil dusts. The elevated ammonium and nitrate may be an artifact of the ground-based sampler collecting background aerosol in the San Joaquin Valley airshed. (The other dust profiles were based on laboratory resuspensions.) The most interesting feature of the construction profiles is that while the $<1\mu$ and $<2.5\mu$ size fractions make up only a small portion of the overall TSP mass, the organic carbon, elemental carbon, and

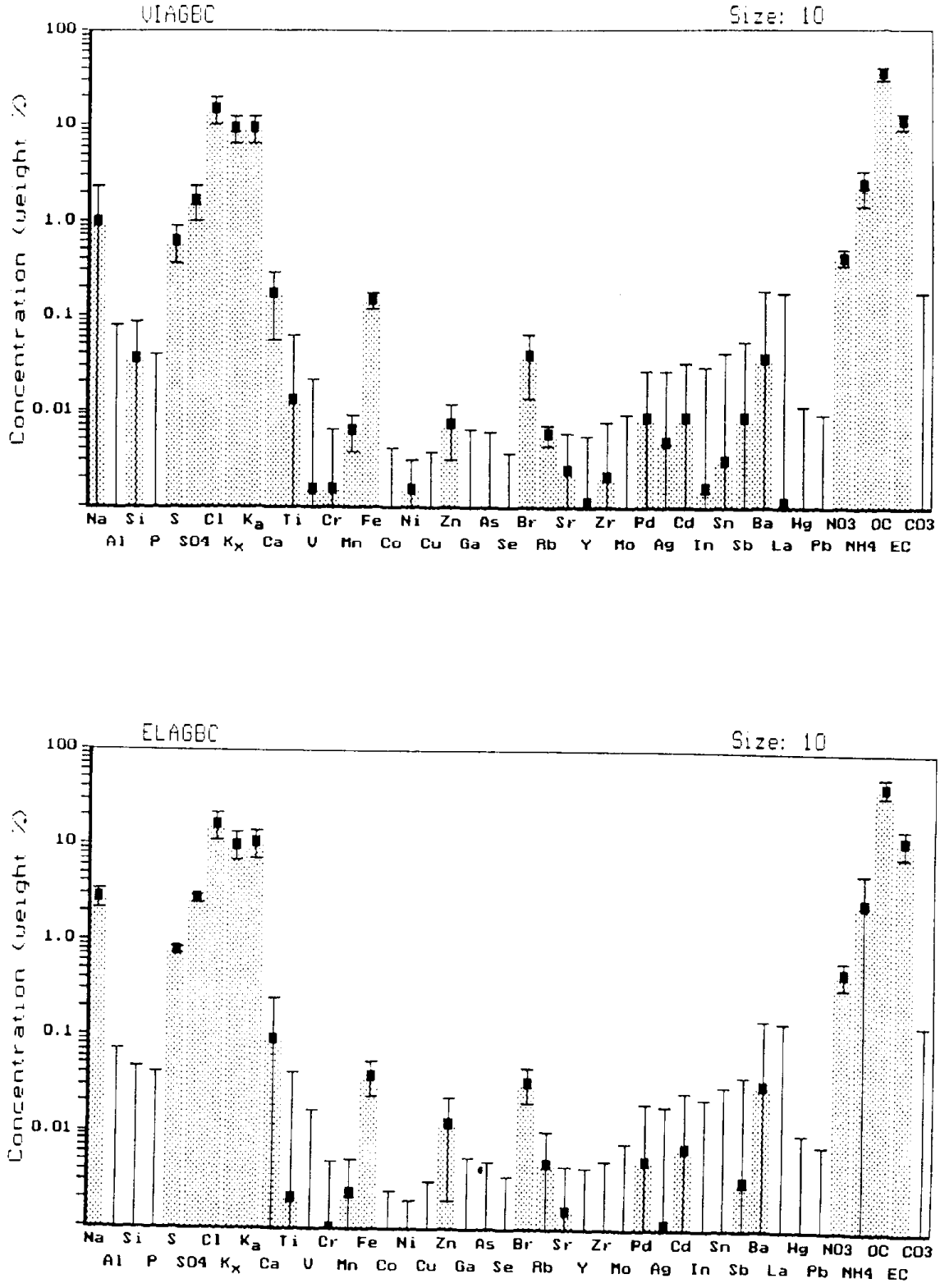

Figure 5.9-1. Chemical source profiles, $< 10\mu$, agricultural burning emissions. Top figure, composite of samples collected near Visalia; bottom figure, composite of samples collected near El Centro. Logarithmic scale, uncertainty bars are shown.

Table 5.10-1
Comparison of Organic Carbon and Geological Chemical Species
in $< 10\mu$ Dairy Emissions with Agricultural Dust

Source	OC (%)	Al (%)	Si (%)	Ti (%)	Mn (%)	Fe (%)	Non-H_2O Soluble K (%)
Dairy	21.7 ± 2.6	2.2 ± 0.6	7.0 ± 1.7	0.21 ± 0.02	0.060 ± 0.007	2.16 ± 0.24	1.0 ± 0.4
Ag. Dust[a]	2.5 ± 0.6	9.9 ± 1.6	24.6 ± 3.9	0.80 ± 0.09	0.13 ± 0.01	8.1 ± 0.9	3.0 ± 0.4

a. Agricultural composite collected near Visalia (SOIL04).

Table 5.10-2
Size Distribution and Concentration Comparisons
of Waste-Derived Chemical Species

	OC (%)		NO_3^- (%)		NH_4^+ (%)	
Size (μ)	Dairy	Ag. Soil[a]	Dairy	Ag. Soil[a]	Dairy	Ag. Soil[a]
< 1	34.5 ± 8.4	3.1 ± 2.9	10.2 ± 4.8	< 0.8	4.0 ± 2.5	< 0.01
< 2.5	32 ± 13	2.5 ± 1.1	9.2 ± 3.9	< 0.3	3.3 ± 2.1	< 0.005
< 10	21.7 ± 2.6	2.5 ± 0.6	1.8 ± 1.6	< 0.2	0.45 ± 0.40	< 0.003
< 30 (TSP)	23.0 ± 2.5	2.7 ± 0.4	1.0 ± 0.9	< 0.1	0.24 ± 0.17	< 0.003

a. Agricultural composite collected near Visalia (SOIL04).

sulfate concentration in these fractions are much higher than in the coarser fractions (Table 5.11-1). These data are consistent with the observation that heavy equipment exhaust as well as dust impacted the samples.

5.12 Residential Wood Combustion

The two major chemical species associated with residential wood combustion are organic carbon and elemental carbon. The linear histogram provided in Figure 5.12-1 of a woodstove emission composite (woodstove burning Mammoth Lakes cordwood) illustrates this point. Water-soluble sodium, sulfur, sulfate, chlorine, total potassium, water-soluble potassium, zinc, nitrate, and ammonium are typically at the tenth-of-a-percent level. Virtually all the potassium present in RWC particles is in the water-soluble form. The non-carbon portions of RWC profiles are generally slightly higher for fireplace emissions than for woodstove emissions. It is thought that the higher, more turbulent air flow through a fireplace, as compared to a woodstove, may entrain more ash, which has a high mineral content. The data in this study is consistent with this supposition (Table 5.12-1). The emissions from a fireplace burning Mammoth Lakes cordwood and from a fireplace burning Bakersfield cordwood do appear to be slightly different (Table 5.12-1). Figure 5.12-1 contains both linear and logarithmic histograms for the $<1\mu$ size fraction of an emission composite from a woodstove burning Mammoth Lakes cordwood. The $<1\mu$ size fraction was selected for review since the overwhelming preponderance of particulate mass is in that size range (Figure 5.2-1).

Table 5.11-1
Size Distribution of Sulfate, Organic Carbon, and Elemental Carbon
in Road Construction Emissions

Size (μ)	SO_4^{2-} (%)	OC (%)	EC (%)
< 1	6.7 ± 0.9	67 ± 35	55 ± 13
< 2.5	5.4 ± 0.6	40 ± 15	29 ± 9
< 10	1.2 ± 0.1	9 ± 4	7 ± 2
< 30 (TSP)	0.73 ± 0.07	3 ± 1	4 ± 2

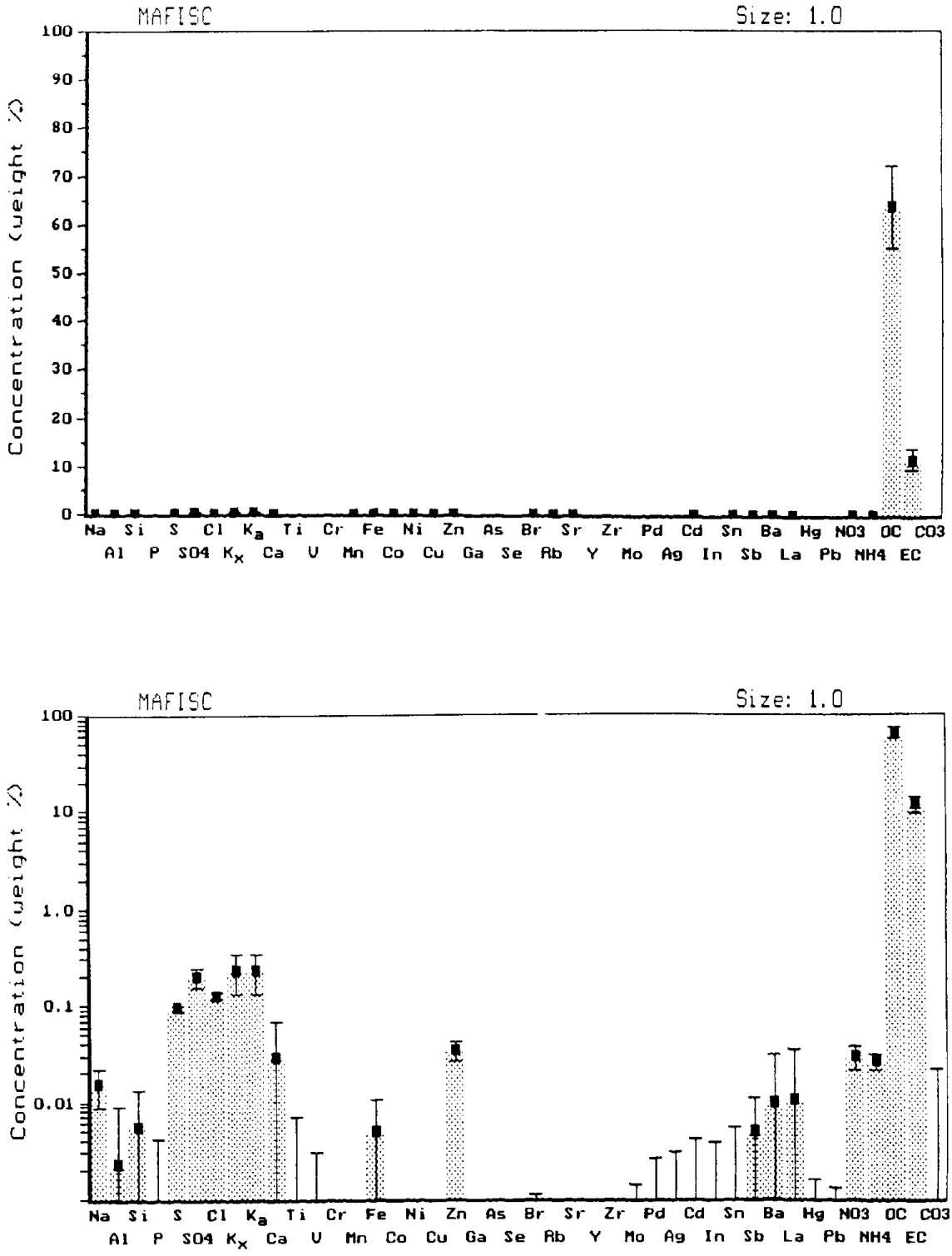

Figure 5.12-1. Chemical source profile histograms of woodstove emissions, $<1\mu$, Mammoth Lakes cordwood. Top figure has linear scale. Bottom figure has logarithmic scale. Uncertainty bars are shown.

Table 5.12-1
Major and Minor Constituents of Residential Wood Combustion Emissions
$< 1\mu$ Size Fraction

Composite Description[a]	Na^+ (%)	S (%)	SO_4^{2-} (%)	Cl (%)	K (%)	Zn (%)	NO_3^- (%)	NH_4^+ (%)	OC (%)	EC (%)
Fireplace, B	0.14 ±0.06	0.52 ±0.20	1.37±0.43	1.8 ±0.7	3.9±0.2	0.085±0.035	0.46 ±0.14	0.08±0.06	45.8±8.4	16.0±5.8
Fireplace, ML	0.025±0.007	0.19 ±0.04	0.58±0.06	0.42±0.07	0.9±0.5	0.80 ±0.026	0.17 ±0.02	0.05±0.03	43.2±7.1	29.2±3.3
Woodstove, ML	0.015±0.007	0.096±0.007	0.20±0.04	0.13±0.01	0.2±0.1	0.344±0.007	0.029±0.008	0.26±0.005	63.8±8.4	11.7±2.2

a. B = Bakersfield cordwood
ML = Mammoth Lakes cordwood

6.0 Summary

Source sampling was conducted on forty particulate sources in the Great Basin Valleys, San Joaquin Valley, and Southeast Desert Air Basins. Chemical source profiles were developed for each of the sources in seven size categories. The seven size categories were $<1\mu$, 1μ to 2.5μ, $<2.5\mu$, 2.5μ to 10μ, $<10\mu$, 10μ to 30μ (or $>10\mu$), and $<30\mu$ (or TSP). Chemical analyses were conducted for forty-three chemical species and mass. The chemical profile data have been reported in hard copy (Appendices A and G) and on floppy disks in formats compatible with standard receptor and dispersion model input requirements.

The source sampling was conducted using several specialized sampling approaches and instruments. These included: (1) a ground-based parallel impactor sampling device (PISD); (2) an industrial dilution source sampler (DSS); (3) paved road dust sample collection with a high-volume road dust sampler or handbroom followed by laboratory resuspension in a custom resuspension system; (4) soil, unpaved road, and bulk material dust grab sampling followed by laboratory resuspension in a custom resuspension system; and (5) a modified Method 5G-type dilution tunnel for residential wood combustion (RWC) sampling. The RWC sampling was conducted in the laboratory under simulated burning conditions characteristic of the geographical area of interest. Impactors with cut-points of 1μ, 2.5μ, and 10μ were used for size characterization in the PISD, DSS, resuspension chamber, and modified Method 5G-type sampler. One channel in each device had no impactor in place, in order to collect the total suspended particle fraction (TSP). The impactors' performances were evaluated using an aerosol generator and particle counter and with comparisons with a commercial PM_{10} sampler. The 1μ and 2.5μ impactors were protected from overloading when deployed in dusty environments with a pre-separator cyclone with a cut-point of approximately 4μ. To assess source variability, three to six individual replicates were collected for each source and a composite profile was calculated. In addition, each individual soil, road, and bulk material dust sample was a composite from a number of sub-samples collected from selected locations (e.g., various fields in an agricultural region). Field blanks and background samples were taken where appropriate. Samples on Teflon and quartz filters for each size fraction were collected simultaneously.

Analyses were conducted for forty-three chemical species and mass on each of the 593 filters. X-ray fluorescence spectrometric analysis was conducted on the Teflon filters for thirty-six elements. The particulate deposit mass was also determined from the Teflon filters with an electrobalance. Sections were removed from the quartz filters for ion chromatographic analysis, thermal/optical analysis, and automated colorimetric analysis. Water-soluble sodium and potassium were determined by atomic absorption spectrophotometry. Elemental carbon, carbonate carbon, and organic carbon were determined by the thermal/optical reflectance technique. Sulfate and nitrate were determined by ion chromatography. Ammonium was determined by automated colorimetry. The chemical data from each of the analytical procedures were merged to produce a

single tabulation or profile for each size category of each source. The uncertainties associated with the values were either the propagated root mean squares of the analytical uncertainties of the individual samples which made up the components, or the standard deviation of the individual values, whichever was greater.

Comprehensive standard operating procedures were developed and followed throughout the sampling, analysis, and data reduction portion of this study. A quality assurance plan was prepared and a detailed data validation process was followed.

A blind interlaboratory comparison for organic carbon, elemental carbon, and carbonate carbon was conducted. Three laboratories were involved. The agreement among the laboratory results for organic and elemental carbon was reasonable. The agreement for total carbon was good. The agreement for carbonate carbon was poor (only two laboratories conducted carbonate carbon analysis). The agreement for total carbon was better than for organic, elemental, and carbonate carbon since it is the sum of three fractions and the variability in the analytical results appears to be in partitioning the carbon into a given fraction.

Table 6.0-1 summarizes the key features of the chemical source profiles. It should be noted that while it is useful to review the individual concentrations of chemical species, the overall pattern of concentration or "fingerprint" is what in essence distinguishes a given source profile. Based on these fingerprints, sources sampled in this study can be divided into ten categories. These are:

1. Agricultural soil and unpaved road dust. This source category is characterized by predominantly coarser particles ($>2.5\mu$), geological elements (Al, Si, K, Ca, and Fe), and organic carbon. The organic carbon content and the content of minor chemical constituents vary due to differences in soil alkalinity, soil amendments, the geological origins of the soil, and the degree of vehicular impact.

2. Sand and cinder storage dust. Dust from this source category is characterized by predominantly coarse particles and geological elements.

3. Alkaline desert soil and playa sediment dusts. This source category is characterized by predominantly coarser particles, the geological elements (Al, Si, K, Ca, and Fe), those species associated with alkaline environments (Na^+, S, SO_4^{2-}, Cl, and carbonate carbon) and some organic carbon. Trace levels of arsenic and selenium also are somewhat higher in some of these samples as compared to the soils.

Table 6.0-1
Summary of Source Profile Features[a]

Source Type	Major Chemical Species[b] (>1%)	Minor Chemical Species[b] (>0.1%)	Comments
Agricultural Soil, Unpaved Road	Al, Si, K, Ca, Fe, OC	Na^+, P, S, SO_4^{2-}, Cl, K^+, Ti, NO_3^-, EC, CC	OC and minor elements variable. Soil alkalinity, soil amendments, vehicular impact, and geological source affect chemical composition.
Sand and Cinder Storage	Al, Si, K, Ca, Fe	OC, Na^+, P, S, Cl, K^+, Ti, Sr, Ba, OC, CC	
Alkaline Desert Soil, Playa Sediments	Na^+, Al, Si, K, Ca, Fe, S, SO_4^{2-}, Cl, CC, OC	K^+, Ti, NO_3^-, Sr	Se and As at trace level.
Unpaved Urban Areas, Paved Roads	Al, Si, K, Ca, Fe, OC, EC	Na^+, P, S, SO_4^{2-}, Cl, K^+, Ti, NO_3^-, Pb	Anthropogenic impact (OC, EC, Pb) higher in $<2.5\mu$ and $<1\mu$ sizes.
Diesel Emissions	OC, EC, S, SO_4^{2-}	Si, NH_4^+ in Wheeler Ridge Truck Samples	
Crude Oil Combustion	S, SO_4^{2-}, Fe, Ni	Na^+, V, NH_4^+, OC, EC in Chevron boiler emissions; Zn in Santa Fe boiler emissions	Ni and V very unique.
Agricultural Burning	Na^+, SO_4^{2-}, Cl, K^+, K, NH_4^+, OC, EC	S, Ca, Fe, NO_3^-	Relatively high K, K^+, and Cl.
Dairy/Feedlot	Al, Si, P, K^+, K, Ca, Fe, NO_3^-, OC, EC	Na^+, S, SO_4^{2-}, Cl, Ti, NH_4^+, CC	OC, NH_4^+, and NO_3^- higher in $<2.5\mu$ and $<1\mu$ size fractions.
Construction	Al, Si, K, Ca, Fe, OC, EC, SO_4^{2-}, NO_3^-	Na^+, P, S, Cl, K^+, Ti, NH_4^+	SO_4^{2-}, NH_4^+, NO_3^-, OC, and EC higher in $<2.5\mu$ and $<1\mu$ sizes.
Residential Wood Combustion	OC, EC	S, SO_4^{2-}, NO_3^-, Cl, K^+, K	Stove emissions lower than fireplace emissions in S, SO_4^{2-}, Cl, K^+, K, and NO_3^-.

a. $<10\mu$ size category.
b. OC = organic carbon
EC = elemental carbon
CC = carbonate carbon

4. Unpaved urban area and paved road dust. This source category is characterized by predominantly coarse particles, the geological elements, organic and elemental carbon, and lead, which is present at the tenth-of-a-percent level. The anthropogenic impact causes elevated organic carbon, elemental carbon, lead, nitrate, and zinc, as compared to nearby soils. The concentration of these anthropogenic chemical species is highest in the finer size fractions ($< 1\mu$ and $< 2.5\mu$).

5. Diesel emissions. Diesel emission particles are predominantly in the fine size fraction ($< 1\mu$). Organic carbon, elemental carbon, sulfur, and sulfate are the key chemical species.

6. Crude oil combustion. The emissions from crude oil combustion are predominantly in the fine size fraction. Sulfur, sulfate, iron, nickel, and vanadium are the key components of this source profile. Nickel and vanadium are nearly unique to this source category.

7. Agricultural burning. The particles from the emissions of agricultural burning are predominantly in the fine size fraction. There is slightly more coarse material than for a "pure" vegetative combustion process such as residential wood combustion, suggesting that some soil and other debris are entrained in the turbulent burning conditions characteristic of this activity. Sulfate, sulfur, water-soluble sodium, chlorine, potassium, water-soluble potassium, calcium, iron, nitrate, organic carbon and elemental carbon are the major chemical species present. The relatively high potassium and chlorine content makes this source category unique among the sources examined in the study. Most of the potassium appears to be in the water-soluble form.

8. Dairy/feedlot emissions. Dairy emissions are composed primarily of dust (coarser particles) and of a small amount of secondary particles in the fine size fractions. This dust contains the typical geological elements as well as nitrate, organic carbon, and elemental carbon. The concentrations of the geological elements are lower than those typical of agricultural soils due to the "diluting" effect of the higher organic carbon concentration. The concentrations of organic carbon, nitrate, and ammonium are higher in the finer size fractions, which is consistent with the suspected secondary origin of the fine particles.

9. Construction. The source profile of highway construction had both a dust component and a heavy equipment exhaust component. The predominant size of the particles was in the coarser fractions and these fractions contained the geological elements and organic compound concentrations typical of soils. In the finer size fraction, however, the organic carbon, elemental carbon, and sulfate concentrations were much higher, consistent with the observation that heavy equipment exhaust was a component of the source.

10. Residential wood combustion. Residential wood combustion particles are predominantly in the fine size fraction, and are comprised almost solely of organic compounds and elemental carbon. Water-soluble sodium, sulfur, sulfate, chlorine, total potassium, water-soluble potassium, zinc, nitrate, and ammonium are frequently at or near the tenth of a percent level. All potassium appears to be in the water-soluble form. Fireplace emissions have a slightly higher concentration of non-carbon species than woodstoves. The higher flow and more turbulent conditions associated with fireplaces in contrast to woodstoves are thought to cause more ash (which is high in inorganic species) to be entrained.

In summary, source profiles for all of the sources in all size categories have been compiled. Each source profile contains the percent composition and associated uncertainty for forty-three chemical species. These profiles will provide state-of-the-art input data for modeling efforts in the Great Basin Valleys, San Joaquin Valley, and Southeast Desert Air Basins.

7.0 Acknowledgements

The authors wish to acknowledge the assistance of John Rau in the design and calibration of the impactor systems, the assistance of Robert Cary in the interpretation of the interlaboratory carbon analysis data, and Ellen Hardebeck and Mike Horn for their help in sampling ski tour bus emissions. Personnel with OMNI received assistance from a number of individuals during the source sampling portion of this program. The following is an alphabetical list of those individuals whom the authors would like to acknowledge for their help, cooperation, and comments:

Raul S. Alvarado, Soil Conservation Service, El Centro
Kim Anderson, Caltrans
Lee Beilu, Sequoia National Forest
Steve Birdsall, Deputy Agricultural Commissioner, Imperial County
Steve Cameron, Soil Conservation Service, Visalia
Bill G. Cox, Great Basin Unified, A.P.C.D.
Harry S. Dillon, Air Pollution Control District, Imperial County
Erwin B. Eby, Agricultural Commissioner, San Joaquin County
Robert Edwards, Agricultural Commissioner, Kern County
Dave Fishel, Air Pollution Control District, Tulare County
Fred Fischer, Soil Conservation Service, Bishop
Charles L. Fryxell, Air Pollution Control District, San Bernardino County
Dave Gilreath, Mammoth Mountain Ski Area
Lakhmir S. Grewal, San Joaquin County, Air Pollution Control District
Daryl Gunderson, WOGA
Kater D. Hake, University of California Cooperative Extension, Kern County
Tom Hastin, Econo Air, Bakersfield
Oscar P. Hellrich, Air Pollution Control District, San Bernardino County
David Houck, field contractor, Rio Vista
Franz R. Kegel, University of California Cooperative Extension, San Joaquin County
Martin Keith, Air Pollution Control District, Tulare County
J.E. Kemp, Caltrans
Dave Kohut, Sierra National Forest
Frank Laemmlen, University of California Extension Service, Imperial County
Pauline Larwood, Supervisor, Third Supervisorial District, Bakersfield
Chris Leithiser, Kern County Board of Trade
Evan Long, Tulare County Fire Department
M.D. Lundy, Chevron USA, Inc.
Carlos Martinez, Pablo Bunyan Firewood, Mammoth Lakes
Henry Mayrsohn, Air Pollution Control District, Bakersfield
Michael A. McElhiney, Soil Conservation Service, Stockton
Robert F. Miller, University of California Cooperative Extension, San Joaquin County
Gary Patton, California Highway Patrol
William L. Peacock, University of California Cooperative Extension, San Joaquin County
Mike Petty, Chevron USA, Inc.
Ralph L. Phillips, University of California Cooperative Extension, Kern County
T.R. Porter III, Chevron USA, Inc.
James F. Regal, Soil Conservation Service, Bakersfield
Don Richards, Chevron USA, Inc.
Jack Ringer, Kern County Fire Department
Jim Robinson, Santa Fe Energy Company
Ralph I. Robles, Air Resources Board, Bakersfield
William Roddy, Air Pollution Control District, Fresno County (currently with the Kern County APCD)
John Schrodder, Air Pollution Control District, Fresno County
Philip R. Shafer, Air Pollution Control District, Imperial County

Bill Taylor, Mammoth Lakes Planning Department
C. Lynn Thomas, Deputy Agricultural Commissioner, Tulare County
Michael Tomko, Chevron USA,Inc.
Paul Torez, Air Pollution Control District, Imperial County
Arlene J. Tugel, Soil Conservation Service, Stockton
Bob Wattington, Caltrans
Steve Whittenburg, City of Fresno
Dale Wierman, California Forestry Department
Personnel with Boesch Firewood, Bakersfield
Personnel with Sierra Nevada Inn, Mammoth Lakes
Personnel with the Terra Bolla Fire Station
Personnel with the Tipton Fire Station
Personnel with the Visalia Fire Station 19
Personnel with the Woodville Fire Station

8.0 References

Arinc, F.; Wielopolski, L.; and Gardner, R.P.; The Linear Least-Squares Analysis of X-Ray Fluorescence Spectra of Aerosol Samples Using Pure Element Library Standards and Photon Excitation; In *X-Ray Fluorescence Analysis of Environmental Samples*; T.G. Dzubay, ed.; Ann Arbor Science, Ann Arbor, MI; p. 277; 1977.

Armstrong, J.A.; Russel, P.A.; Sparks, L.E.; Drehmel, D.C.; Tethered Balloon Sampling Systems for Monitoring Air Pollution; *JAPCA*; 31, 735; 1981.

Ashton-Tate; dBase III Plus Version 1.0; User's Manual, Ashton-Tate, CA; 1985.

Azevedo, J.; Farm Animal Manures: An Overview of Their Role in the Agricultural Environment; University of California, Division of Agricultural Sciences, Manual 44; 1974.

Barone, J.B.; Kusko, P.H.; Ashbaugh, L.L.; and Chahill, T.A.; A Study of Ambient Aerosols in the Owens Valley Area; University of California, Davis, CA; 37 pp. plus appendices, (ARB Contract A7-178-30); 1979.

Burnet, P.G.; Edmisten, N.G.; Tiegs, P.E.; Houck, J.E.; and Yoder, R.A.; Particulate, Carbon Monoxide, and Acid Emission Factors for Residential Wood Burning Stoves; *JAPCA*, vol. 36, p. 1012--1018; 1986.

California Cattle Feeders Association; How to Control Feedlot Pollution—Measurement and Control of Feedlot Particulate Matter; Bulletin C., Bakersfield, CA; 1971.

Chan, T.; and Lippman, M.; Particle Collection Efficiencies of Air Sampling Cyclones: An Empirical Theory; *Environmental Science and Technology*, vol. 11, n. 4, p. 377–382; 1974.

Chemical Rubber Company, The; Handbook of Chemistry and Physics, 59th ed.; CRC Press, Inc.; West Palm Beach, Florida; 1978.

Cheng, Y.S.; Yeh, H.C.; Particle Bounce in Cascade Impactors; Environmental Science and Technology, 13, 1392–1396; 1979.

Chow, J.C.; Test of Filter Extraction Efficiency; Documented in *Sulfate Regional Experiment (SURE) Program* File, Electric Power Research Institute, Palo Alto, CA; 1981.

Chow, J.C.; Development of a Composite Modeling Approach to Assess Air Pollution Source/Receptor Relationships; Doctor of Science Dissertation; Harvard University, Cambridge, MA; 1985.

Chow, J.C.; Watson, J.G.; Frazier, C.A.; A Survey of Existing Fugitive/Area Source Characterization Methods for Receptor Modeling; In *Proceedings, Particulate Matter/Fugitive Dusts: Measurement and Control in Western Arid Regions*; Air Pollution Control Association, Pittsburgh, PA; 1988.

Cooke, W.M.; Piispanen, W.H.; Wensky, A.K.; Lutz, G.A.; Cole, T.F.; Ogden, J.S.; Levy, A.; Barnes, R.H.; Cornaby, B.W.; and Degner, K.B.; Candidate Sampling and Analysis Methods for 21 Suspect Carcinogens in Combustion Emissions; EPA-600/57-84-078; U.S. Environmental Protection Agency, Research Triangle Park, NC; 1984.

Core, J.; and Houck, J.E. (eds.); Pacific Northwest Source Profile Library, Sampling and Analytical Protocls, final report; Oregon Department of Environmental Quality; Portland, OR; 1987.

Core, J.E.; Shah, J.J.; and Cooper, J.A.; Receptor Model Source Composition Library; U.S. EPA-450/4-85-002; 1984.

Countess, R.J.; Interlaboratory Analyses of Carbonaceous Aerosol Samples, Proceedings Third International Carbon Conference; Berkely, CA, October 1987.

Criss, J.W.; Particle Size and Composite Effects in X-Ray Fluorescence Analysis of Pollution Samples; *Anal. Chem.*, 48(1), 1976.

Drane, E.A.; Branton, D.G.; Tysinger, S.H.; and Courtney, W.J.; Data Processing Procedures for Elemental Analysis of Atmospheric Aerosols by X-Ray Fluorescence; Report TR-83-01, Northrop Services, Inc., Research Triangle Park, NC; 1983.

Dzubay, T.G.; Analysis of Aerosol Samples by X-Ray Fluorescence; Report dated April 30, 1986; U.S. Environmental Protection Agency, Research Triangle Park, NC; 1986.

Dzubay, T.G.; Personnel communication; U.S. Environmental Protection Agency, 1988.

Dzubay, T.G.; Morosoff, N.; Whitaker, G.L.; and Yasuda, H.; Evaluation of Polymer Films as Standards for X-Ray Fluorescence Spectrometers; Submitted for Publication in Electron Microscopy and X-Ray Applications to Environmental and Occupational Health Analysis, 3; Ann Arbor Science Publishers, Inc.; Ann Arbor, MI; 1981.

Dzubay, T.G.; Nelson, R.O.; Self Absorption Corrections for X-Ray Fluorescence Analysis of Aerosols; *Advances in X-Ray Analysis*, 18, 619; 1975.

Engineering Science, Analysis of Carbon Monoxide and Inhalable Particulate Emissions From Woodburning Devices in Fresno, California; report to U.S.EPA Region 9; Contract 68-02-3509, working assignment 21; 1982.

Esmen, N.A.; Zieg.er, P.; and Whitfield, R.; The Adhesion of Particles Upon Impaction; J. Aerosol Science, 9, 547–556; 1978.

Finnel, C.; Imperial County Agriculture - 1986; Office of Imperial County Agricultural Commissioner, El Centro, CA; 6 pp.; 1987.

Freeman, D.L.; Robinson, N.F.; Watson, J.G.; Chow, J.C.; Egami, R.T.; Level I PM_{10} Assessment Package User's Guide; final report to California Air Resources Board; ARB Contract A4-155-32; 1987.

Gonzalez, R.A.; Guidelines to Production Costs and Practices, 1984-1986, Imperial County Crops; University of California Cooperative Extension, El Centro, CA; 55 p (circular 104); 1985.

Gordon, G.E.; Pierson, W.R.; Daisey, J.M.; Lioy, P.J.; Cooper, J.A.; Watson, J.G.; and Cass, G.E.; Considerations for Design of Source Apportionment Studies; *Atmos. Environ.*, 18, 1567; 1984.

Groblicki, P.J.; Cadle, S.H.; Ang, C.C.; and Mulowa, P.A.; Interlaboratory Comparison of Methods for the Analysis of Organic and Elemental Carbon in Atmospheric Particulate Matter, GMR Report 4054, General Motors Research Laboratories; Warren, MI; 1983.

Harris, D.B.; Source Sampling Systems Used to Develop Source Signatures; In *Transactions, Receptor Methods for Source Apportionment: Real World Issues and Applications*, T.G. Pace, ed. Air Pollution Control Association, Pittsburgh, PA, p. 46; 1986.

Heinsohn, R.J.; Davis, J.W.; and Knapp, K.T.; Dilution Source Sampling Systems; *Environ. Sci. Technol.*, 14, 1205; 1980.

Hering, S.V.; Friedlander, S.K.; Collins, J.J.; and Richards, W.L.; Design and Evaluation of New Low-pressure Impactor; *Environmental Science Technology*; 13, 184; 1979.

Hidy, G.M.; Jekyll Island Meeting Report; *Environ. Sci. Technol.*, 19, 1032; 1985.

Hinds, C.; Aerosol Technology: Properties, Behavior, and Measurement of Airborne Particles; John Wiley & Sons, New York, NY; 1982.

Houck, J.E.; Cooper, J.A.; Frazier, C.A.; and DeCesar, R.T.; East Helena Source Apportionment Study; Report to Montana Department of Health and Environmental Sciences; 1982.

Houck, J.E.; Cooper, J.A.; Frazier, C.A.; Larsen, E.R.; Mohan, J.F.; and Bradeen, A.S.; Application of Chemical Mass Balance Methods to the Determination of the Contribution of Potlatch Corporation's Air Particulate Emissions to the Lewiston-Clarkston Airshed; 1981.

Houck, J.E.; Cooper, J.A.; and Larson, E.R.; Dilution Sampling for Chemical Receptor Source Fingerprinting; Presented at 75th Annual Meeting, New Orleans, LA; Air Pollution Control Association, Pittsburgh, PA; 1982.

Huynh, C.F.; Vuduc, T.; Schwab, C.; and Rollier, H.; In-Stack Dilution Techniques for the Sampling of Polycyclic Organic Compounds; Applications to Effluents of a Domestic Waste Incineration Plant; *Atmos. Environ.*, 18, 255; 1984.

Inouye, D.; Estimates of Carbon Monoxide and Particulate Emissions From Woodburning Devices in the Fresno/Clovis Metropolitan Area; report to Fresno Air Pollution Control District; 1985.

Ipps, D.T.; Nature and Causes of the PM_{10} Problem in California; California Air Resources Board Report; ARB/TS-87-002; 1987.

Javitz, H.S.; Watson, J.G.; Guertin, J.P.; and Mueller, P.K.; Results of a Receptor Modeling Feasibitility Study; *JAPCA*, 38, 661; 1988.

Johnson, R.L.; Shah, J.J.; Cary, R.A., and J.J. Huntzicker, J.J.; An Automated Thermal/Optical Metho for the Analysis of Carbonaceous Aerosol; ACS Symposium Series, No. 169; *Atmospheric Aerosol, Source/Air Quality Relationships*; E.S. Macias and P.K. Hopke, eds., American Chemical Society, Plenum Press, New York, NY; 1981.

Karlik, J.; Kern Crops - Planting and Harvesting Calendar; University of California Farm and Home Advisor's Office; Bakersfield, CA; 9 pp (Pub. No. 8436); undated.

Kemp, J.E.; Comparative Study of Sand Versus Cinders Used as Wintertime Abrasive Agents on Roadways Within the Mammoth Lakes Area of Mono County, Department of Transportation, Caltrans District 9, Bishop, CA; 17 pp. plus appendices; 1986.

Kerr-McGee Chemical Corporation, Trona Soda Ash and the Argus Facility; Corporation Bulletin 1400, Olkahoma City, OK; 23 pp; undated.

Kunkel, G.; Tulare County Agricultural Crop Report 1986; Office of Tulare County Agricultural Commissioner, Visalia, CA; 15 pp.; 1987.

Kusko, B.H.; Barone, J.B.; and Cahill, T.A.; The Effect of Mono Lake on the Air Quality in the Mono Lake Region; Final Report to California Air Resource Board; University of California, Davis, CA; Contract No. A9-147-31; 1981.

Kusko, B.H.; and Cahill, T.A.; Study of Particle Episodes at Mono Lake; Final Report to California Resources Board; University of California, Davis, CA; Contract No. A1-144-32; 1984.

Marple, V.A.; A Fundamental Study of Inertial Impactors; Ph.D. Dissertation; University of Minnesota; 1970.

Marple, V.A.; Liu, B.Y.H.; and Whitby, K.T.; "Fluid Mechanics of the Laminar Flow Aerosol Impactor;" *Aerosol Science*; 5, 1–16; 1974.

Marple, V.A.; Rubow, K.L.; Turner, W.; and Spengler, J.; Low Flow Rate Sharp Cut Impactors for Indoor Air Sampling: Design and Calibration; *JAPCA*, vol. 37, p. 1303–1307; 1987.

Mathai, C.V.; Tombach, I.H.; Watson, J.G.; and Rogers, C.R.; Intercomparison of Ambient Aerosol Samples Used in Western Visibility and Air Quality Studies; Presented at 78th Annual Meeting, Detroit, MI; Air Pollution Control Association, Pittsburgh, PA; 1985.

McCain, J.D. and Williamson, A.D.; Development and Evaluation of Dilution Probes Used for Sampling to Determine Source Signatures; EPA 600/3-84-045, U.S. Environmental Protection Agency, Research Triangle Park, NC; 1984.

Miller, R.F.; Space Requirements and Dust Control for Feedlot Cattle; California Agriculture, December issue, p 14–15; 1962.

Miller, R.F.; Clawson, W.J.; Fairbank, W.C.; and Deal, A.S.; Feedlot Sanitation in the San Joaquin Valley, Agricultural Sanitation and Waste Management Series; University of California, Cooperative Extension; 1974.

Mueller, P.K.; Hidy, G.M.; and Tong, E.Y.; Implementation and Coordination of the Sulfate Regional Experiment (SURE) and Related Research Programs; Report EA-1066; Electric Power Research Institute, Palo Alto, CA; 1979.

Mueller, P.K.; Hidy, G.M.; Watson, J.G.; Baskett, R.L.; Fung, K.K.; Henry, R.C.; Lavery, T.F.; and Warren,K.K.; The Sulfate Regional Experiment: Report of Findings, Volumes 1, 2, 3; Report EA-1901; Electric Power Research Institute, Palo Alto, CA; 1983.

Mueller, P.K.; and Watson, J.G.; The SURE Measurements; Presented at 74th Annual Meeting, Philadelphia, PA; Air Pollution Control Association, Pittsburgh, PA; 1981.

Pan, Y.S.; Review Summary of Stack Sampling of Fine Particulates; U.S. Department of Energy Report DOE/PETC/TR-87/2; Pittsburgh Energy Technology Center; Pittsburgh, PA; 1986.

Parkes, J.; Rabbit, L.G.; Hamshire, M.J.; Live Peak-Stripping During X-Ray Energy-Dispersive Analysis, *Analy. Chem.*, 46; 1830.

Perrier, E.R.; Mackenzie, A.J.; and Zimmerman, R.P.; Physical and Chemical Properties of Major Imperial Valley Soils; U.S. Department of Agricultural, Agricultural Research Service and Soil Conservation Service, Berkeley, CA, 31 pp (ARS W-17); 1974.

Pierson, W.R.; and Bracchaczek, W.W.; Particulate Matter Associated with Vehicles on the Road II; *Aerosol Science Technology*, 2, 1; 1983.

Pritchett, L.C.; personal communication; 1989.

Rau, J.A.; Residential Wood Combustion Aerosol Characterization as a Function of Size and Source Apportionment Using Chemical Mass Balance Modeling; Ph.D. Dissertation, Oregon Graduate Center; 1986.

Rheingrover, S.W.; and Gordon, G.E.; Identifying Locations of Dominant Point Sources of Elements in Urban Atmospheres from Large Multi-element Data Sets; Fourth International Conference on Nuclear Methods in Environmental and Energy Research; University of Missouri, Columbia, MO; 1980.

Richards, L.W.; Anderson, J.A.; Blumenthal, D.L.; McDonald, J.A.; Macias, E.S.; Hering, S.V.; and Wilson, W.E.; Chemical Aerosol and Optical Measurements in the Plumes of Three Midwestern Coal-Fired Power Plants; *Atmos. Environ.*, 19, 1685; 1985.

Richards, L.W.; Markowski, G.R.; and Waters, N.; Comparison of Nephelometer Telephotometer and Aerosol Data in the Southwest; Presented at 74th Annual Meeting, Philadelphia, PA; Air Pollution Control Association; Pittsburgh, PA; 1981.

Russ, J.C.; Processing of Energy-Dispersive X-Ray Spectra; In *X-Ray Spectrometry*, 6, 37; 1977.

Saint-Armand, P.; Mathews, L.A.; Gaines, C.; and Reinking, R.; Dust Storms from Owens and Mono Valleys, California; Naval Weapons Center, China Lake, CA, 17 pp. plus appendices; 1986.

Schultz, H.B.; and Carlton, A.B.; Field Windbreaks for Row Crops; California Agriculture, November Issue: 5 (1959); 1959.

Shah, J.J.; Johnson, R.; and Houck, J.E.; Source Characterization Using Tethered Balloons; in *Transactions, Receptor Models in Air Resources Management*; J.G. Watson, ed., Air Pollution Control Association, Pittsburgh, PA; 1988.

Shareef, G.S.; and Bravo, L.A.; Air Emissions Species Manual, Volume II, Particulate Matter Species Profiles; U.S. EPA 450/2-88-003b; 1988.

Shelton, J.W.; and Gay, L.W.; Evaluation of Low-Emission Woodstoves; Shelton Research, Inc.; Report 1086 to California Air Resource Board, Sacramento, CA; Contract A3-122-32; 1986.

Shelton, J.W.; and Gay, L.W.; Colorado Fireplace Report; Shelton Research, Inc., report to Colorado Air Pollution Control Division; Contract no. C375322; 1987.

Small, M.; Germani, M.S.; Small, A.M.; Zoller, W.W.; and Moyers, J.L.; Airborne Plume Study of Emissions From the Processing of Copper Ores in Southeastern Arizona; *Environ. Sci. Technol.*, 15, 293; 1981.

Stiles, D.C.; Evaluation of an S^2 Sampler for Receptor Modeling of Woodsmoke Emissions; Presented at 76th Annual Meeting, Atlanta, GA; Air Pollution Control Association, Pittsburgh, PA; 1983.

Taback, H.J.; Brienza, A.R.; Macko, J.; and Burnetz, N.; "Fine Particle Emissions from Stationary and Miscellnaeous Sources in the South Coast Air Basin," final report, ARB-R-A6-191-30-79-94; Sacramento, CA, NTIS PB-293-923/2; 1979.

Tuchman, D.P.; Nurtan, A.E.; and Dietrich, A.W.; Design and Calibration of a Low Flow Parallel State Impactor; *Am. Ind. Hyg. Assoc. J.*, vol. 47, n. 1, p. 55–58; 1986.

U.S. Environmental Protection Agency, Method 5G–Determination of Particulate to Emissions from Wood Heaters from a Dilution Tunnel Sampling Location, Federal Register, vol. 52, p. 5024-5033; February 18, 1987a.

U.S. Department of Agriculture, Soil Conservation Service, Soil Survey of Imperial County California, Imperial Valley Area; U.S. Government Printing Office, 112 pp plus maps (1675/15); 1980.

U.S. Department of Agriculture, Soil Conservation Service, unpublished soil survey maps and soil series descriptions, Stockton, Visalia, Bakersfield, and Bishop field offices; undated.

U.S. Environmental Protection Agency; Revisions to National Ambient Air Quality Standards for Particulate Matter; Federal Register, vol. 52, n. 126, p. 24634–24750; July 1, 1987b.

Watkins, T.; San Joaquin County Agricultural Report 1986; Office of San Joaquin County Agricultural Commissioner, Stockton, CA; 6 pp.; 1987.

Watson, J.G.; personal communication, 1989.

Watson, J.G.; Chow, J.C.; Freeman, D.L.; Egami, R.T.; Roberts, P.T.; and Countess, R.J.; Model and Data Base Description for California's Level I PM_{10} Assessment Package; final report to California Air Resources Board; ARB Contract A4-155-32; 1987.

Watson, J.G.; Chow, J.C.; Richards, L.W.; Neff, W.D.; Andersen, S.R.; Dietrich, D.L.; Houck, J.E.; and Olmez, I.; The 1987-1988 Metro Denver Brown Cloud Study, Final Report; 1987-1988 Metro Denver Brown Cloud Study, Inc.; Denver, CO.; 1988.

Watson, J.G.; Lioy, P.J.; and Mueller, P.K.; The Measurement Process: Precision, Accuracy, and Validity; in *Air Sampling Instruments for Evaluation of Atmospheric Contaminants*, 6th ed.; Paul J. Lioy and Mary Jean Y. Lioy, eds. American Conference of Governmental Industrial Hygienist, Cincinnati, OH, p. L-2; 1983.

Wilbur, S.; Kern County Agricultural Crop Report 1986; Office of Kern County Agricultural Commissioner, Bakersfield, CA; 14 pp.; 1987.